

wiscobolt

A free, open-source, deterministic photon-electron Boltzmann transport solver

Note: This document is a work-in-progress

Muhsin H. Younis

First published 10-21-2023

Latest version: 0.1, published 10-21-2023

Document updated 6-4-2024

Disclosures

wiscobolt was created with the support of the National Cancer Institute of the National Institutes of Health under Award Number T32CA009206, administered through the Radiological Sciences Training Program of the University of Wisconsin – Madison. The content in this document is solely the responsibility of the author and does not necessarily represent the official views of the National Institutes of Health.

License

Copyright (C) 2023. Muhsin H. Younis.

wiscobolt is free software: you can redistribute it and/or modify it under the terms of the GNU General Public License as published by the Free Software Foundation, either version 3 of the License, or (at your option) any later version. wiscobolt is distributed in the hope that it will be useful, but without any warranty; without even the implied warranty of merchantability or fitness for a particular purpose. See the GNU General Public License, located at `LICENSE/gpl-3.0.txt` in the main wiscobolt directory or <https://www.gnu.org/licenses/> for more details.

Acknowledgements

There are several people and entities the author would like to thank for their contribution and assistance.

- Dan Younis, for providing advice with Fortran, numerical methods, and physics more generally, at a critical stage in this program's development.
- The authors of ELSEPA (ELastic Scattering of Electrons and Positrons by neutral Atoms, molecules, and positive ions) – Francesc Salvat, Aleksander Jablonski and Cedric J. Powell. Cedric J. Powell brought ELSEPA to the author's attention. Aleksander Jablonski provided a helpful description of how to operate ELSEPA. Francesc Salvat provided answers to questions the author had relating to ongoing research in electron scattering cross sections. Francesc Salvat also created PENELOPE, a Monte Carlo Boltzmann transport solver. Documentation relating to PENELOPE's 2018 release has been useful in the creation of wiscobolt's cross section generating code.
- The authors of Sandia National Labs' CEPXS program, a photon-electron-positron cross-section generating code, in particular for their 'physics guide,' which has been useful in the creation of wiscobolt's cross section generating code.
- The authors of Sandia National Labs' SCEPTR program, as well as Los Alamos National Labs' Attila program, and finally Varian's Acuros XB program. Publications relating to these solvers and their algorithms have been tremendously influential on wiscobolt.

- The authors of the Geant4DNA project, whose documentation was very informative in relation to low energy electron scattering cross sections.
- Bryan Bednarz of the medical physics department at the University of Wisconsin – Madison.
- All institutions from which physics data used by wiscobolt has been obtained: The National Institute of Standards and Technology (NIST), the International Atomic Energy Agency (IAEA), and Lawrence Livermore National Laboratories (LLNL).

Foreword

The purpose of this document is to describe wiscobolt, a free and open-source deterministic Boltzmann transport solver, written in the language Fortran. At the moment, wiscobolt is specialized for photon and/or electron transport, with the ability to handle external beams and coupled photon-electron transport. The Boltzmann transport equation provides essentially the density of radiation particles at some location (3 coordinates) and with some momentum (3 coordinates), or equivalently some direction (2 coordinates) and energy (1 coordinate). It is essentially an equation which underlies radiological physics, much like Newton's second law, or the Euler-Lagrange equations of motion, or Hamilton's equations of motion dictate mechanics, and Maxwell's equations dictate electrodynamics. Such a thorough description of a system of radiation particles is very useful across a range of fields, most notably for us, in radiology, wherein it can be used to calculate a number of interesting quantities, including energy deposition following radiation therapy and transmission factors used for radiation safety. However, this is a six-dimensional problem, and as such it is computationally demanding. In the early days of computing, solutions were most feasibly obtained using so-called 'infinite slab geometry,' wherein one assumes that there is no variation in the source and medium except in one dimension, that being the exact representation of an infinitely wide planar beam incident upon an infinitely wide slab. For practical purposes, this is a great representation of the behavior of the radiation particle density along the central axis in a beam and medium that is laterally much bigger than the range of the particles being transported. Nevertheless, this reduces the problem to one dimension in space and two dimensions in momentum (one dimension in angle, and one dimension in energy), making solution much more feasible. This method of solution was popular in the neutron transport community. On the other hand, the Monte Carlo method of radiation transport, developed by physicists at Los Alamos National Labs, rapidly became the method of choice for research in transport of high energy (\sim MeV) photons and electrons. This method involves random sampling of scattering probability distributions in order to simulate the interaction of radiation particles with a medium. Due to the simplicity of this method, and the wealth of research dedicated to its optimization over the last \sim fifty years, Monte Carlo remains the method of choice in medical physics.

In the last twenty or so years, with the development of faster computers, larger storage availability, and more efficient numerical methods, the study of deterministic, fully six-dimensional Boltzmann transport has grown. Most notably, treatment of the three spatial dimensions with the versatile and efficient 'finite element' method has become a cornerstone of modern deterministic Boltzmann transport calculations. At the moment, however, the author is not aware of any free, open-source, 3D finite element photon-electron Boltzmann transport solvers. Such is the motivation for wiscobolt. However, it must be noted that there are a handful that are not open-source and not generally available to one such as the author. These include Sandia National Labs' SCEPTR, a very efficient, extremely versatile research program which has been used extensively not only in medical physics, but also the study of the effects of radiation in electronics. Additionally, there is the clinically-oriented Varian Acuros XB, and its progenitor Attila. Notably, Varian Acuros XB is one example of an ongoing shift in radiation therapy treatment planning, from approximate

forms of dose calculation such as convolution-superposition, to more sophisticated forms, such as Monte Carlo and deterministic Boltzmann transport, which more appropriately treat material inhomogeneities as well as transport in a magnetic field (useful for magnetic resonance-guided radiotherapy) and ion therapy (proton therapy for instance).

The typical user will likely find the **wiscobolt implementation** document much more useful, in which we describe primarily: 1) the user input, 2) the output of the program, and 3) the exhaustive details of each module and each subroutine contained within the program. There also exists the **wiscobolt physics** document, which describes the physics data and models used to determine, essentially, the interaction probabilities for a given material that are involved in the Boltzmann transport equation. Then, the **wiscobolt verification** document describes a number of numerical studies that have been performed to demonstrate the mathematical *and* physical integrity of the solver. That is, in that document, we verify that we are capable of numerically performing the mathematical operations that we claim here to construct, as well as quantify how well our solver works under some kinds of stress tests, such as a problem whose (known) solution has sharp spatial/energy gradients, or one with particular boundary conditions. The document also demonstrates that we can reproduce experimental results relating to the physics data and models we use, materials, etc., which is important in demonstrating that the solver is using reliable physics data and models that have also been implemented correctly.

In all, wiscobolt is intended to be used by researchers in any field to which MeV photon and/or electron Boltzmann transport can be applied. We hope that wiscobolt, due to its accessibility, will satisfy a need in the research community. We intend to generalize it eventually to more particle types (first up: positrons and protons), as well as allow for more generality in the problem geometry. A big drawback of our solver is that it currently can not treat any non-convex geometries, including objects with cavities. While this is not necessarily a fundamental feature of the program, we are not sure when we will have the time to implement this capability (requests will go a long way). Another feature with an undecided ETA is the ability to use elements other than tetrahedra. For this, hexahedra will likely be the first to be included.

The author invites all questions, feedback, comments, or problems, and can be reached most easily at: myounis@wisc.edu. It is inevitable that errors will arise during day-to-day use. Therefore, contacting the author about these errors will tremendously benefit wiscobolt. Additionally, this document has not yet been peer-reviewed, and so if any erroneous statements have been made, we will appreciate corrections. Our confidence in this document is derived from the research from which it was created, as well as the results in the **wiscobolt verification** document.

Table of Contents

1	Introduction	1
1.1	Purpose	1
1.2	Radiation transport	2
1.3	The Boltzmann transport equation	3
1.4	Sources, uncollided fluences, and the first collision method	5
1.5	Coupling particle types	7
1.6	Continuous slowing down	8
2	Discretization	10
2.1	The multi-group formalism	11
2.1.1	Energy iteration and the monoenergetic BTE	14
2.1.2	Deposition cross sections	16
2.2	The spatial finite element method	16
2.2.1	The finite element method	17
2.2.2	The weak form	17
2.2.3	Applying the FEM	19
2.2.4	Evaluation of spatial integrals for tetrahedra	24
2.3	PN scattering	30
2.4	SN angular discretization	33
2.4.1	Angular quadrature	34
2.4.2	Sweep	37
2.4.3	Summary	41
3	Solution	41
3.1	Iterative methods	42
3.1.1	Source iteration	42
3.1.2	Acceleration of SI	43
3.1.3	Generalized minimal residual method	44
3.1.4	Acceleration of GMRES	45
3.1.5	Approximate systems for acceleration	45
3.2	Further useful numerical approximations	47
3.2.1	The extended transport correction	47
3.2.2	Integration of uncollided fluence	49
3.3	Workflow of wiscobolt	50
A	Angular inner products	50

A.1	Analytical solution	58
A.1.1	Summary	63
A.2	Quadrature solution	64
References		66

1 Introduction

1.1 Purpose

This is an in-depth dissection of deterministic Boltzmann transport in the context of radiation therapy. The Boltzmann transport equation (BTE) provides essentially the density of radiation particles at some location (three coordinates) and with some momentum (three coordinates), or equivalently some direction (two coordinates) and energy (one coordinate), making it a six-dimensional problem. Such a thorough description of a system of radiation particles is very useful across a range of fields, most notably for this document, in radiology [1], wherein it can be used to calculate a number of interesting quantities, particularly in the context of radiotherapy treatment planning [1–3] and health physics [4].

However, being a six-dimensional mathematical problem, numerical solutions of the Boltzmann transport can be computationally demanding. In the early days of computing, solutions were most feasibly obtained using so-called ‘infinite slab geometry,’ [5–9] wherein one assumes that there is no variation in the source and medium except in one dimension, that being the exact representation of an infinitely wide planar beam incident upon an infinitely wide slab. For practical purposes, this is a great representation of the behavior of the radiation particle density along the central axis in a beam and medium that is laterally much bigger than the range of the particles being transported [5, 10]. Nevertheless, this reduces the problem to one dimension in space and two dimensions in momentum (equivalently one dimension in angle, and one dimension in energy), making solution much more feasible. On the other hand, the Monte Carlo method of radiation transport [11–13], developed by physicists at Los Alamos National Laboratory [13], has rapidly become a popular method for research in transport of high energy (\sim keV-MeV) photons and electrons [12, 14]. This method involves random sampling of scattering probability distributions in order to simulate the interaction of radiation particles with a medium.

Recently, deterministic Boltzmann transport (or, typically just ‘Boltzmann transport’) has emerged as an interesting alternative to Monte Carlo both in clinical and research contexts [14–16], with Boltzmann transport often demonstrating a speed advantage that can be crucial in the clinic, among other advantages as well as drawbacks for both methods. Within the last twenty or so years in particular, deterministic solution methods have developed to the point where full six-dimensional solutions to the radiotherapy Boltzmann transport problem can feasibly be performed. Perhaps most notably, these developments include treatment of the three spatial dimensions with the versatile and efficient ‘finite element method,’ [14, 16–19]. However, as of writing this document there are, to the authors’ knowledge, three popular programs capable of performing deterministic Boltzmann transport for photons and electrons using the finite element method: Sandia National Labs’ SCEPTRÉ [20], a research program limited to use by government and government contractors only, and the clinically-oriented Varian Acuros XB [16], which was built upon Attila, originally developed at Los Alamos National Laboratory [14–16]. None of these programs is available free and/or open-source. Conversely, the solver wiscobolt is a free and open-source program with the aforementioned capabilities, written in the language Fortran.

We will first introduce the basic physics of Boltzmann transport. Then, we will de-

scribe discretization on an operator-by-operator, coordinate-by-coordinate, basis. Notably, space is discretized exclusively using the finite element method, which gives the problem unique complexities, especially when coupled with different angular discretization methods. Also, we only discuss one method of angular and one method of energy discretization: respectively, discrete ordinates and the multigroup method. However, the treatment of spatial discretization is adequately general and systematic such that different angular and energy discretization methods can be readily applied. Afterwards, we will describe practical solution of the Boltzmann transport equation, from its iterative methods to some other numerical methods which are commonly employed that alleviate significant difficulties faced, particularly in massive particle transport. Refer to **wiscobolt validation** for validation of the discretization and solution methods, in addition to (as yet not fully validated) solves of real-life physical problems.

1.2 Radiation transport

Radiation transport is the study of the behavior and dynamics of free or ‘radiation’ particles and their interaction with a target of interest. Any information relating to a radiation field in a certain volume is fully specified if one is able to know, at a given location \mathbf{r} , and for a given particle momentum \mathbf{p} (or equivalently, direction $\hat{\mathbf{k}}$ and energy E); what is the density of radiation particles? Thus, one can quantify a radiation field as a ‘number density’ $n(\mathbf{r}, \hat{\mathbf{k}}, E)$, which lives in a six-dimensional ‘phase space,’ where three dimensions correspond to the position at which an evaluation is made, and three correspond to the momentum at which an evaluation is made. A useful surrogate for the number density is the so-called ‘angular fluence’ $\psi(\mathbf{r}, \hat{\mathbf{k}}, E)$, which is most intuitively described in the language of calculus: the quantity $\Delta N = \psi(\mathbf{r}, \hat{\mathbf{k}}, E) \Delta A \Delta E \Delta \Omega$ is roughly the ‘total’ (in + out) number of particles crossing a surface at \mathbf{r} with area ΔA , with energy within ΔE of E , and within solid angle $\Delta \Omega$ of $\hat{\mathbf{k}}$, provided that ΔA , ΔE , and $\Delta \Omega$ are small. An alternative way to define ψ is to consider it the magnitude of the so-called current density distribution, $\mathbf{j} = \mathbf{v}n$, where \mathbf{v} is the velocity of a particle with direction $\hat{\mathbf{k}}$ and energy E . That is, $\psi = |\mathbf{v}|n$.

The angular fluence is a quantity which is directly implicated in one of the most important metrics in radiology: the ‘dose’ [3, 21]. Dose is a spatial distribution of energy deposition per unit mass of a target volume, due to exposure to ionizing radiation. Its use in clinical radiology is ubiquitous and extends beyond just radiotherapy. In radiotherapy, it is used to plan and predict therapeutic outcomes during radiation therapy, with models existing that map from a dose value or distribution to a cell-survival fraction for various cell types [22–26]. However, it is also used in imaging, among other reasons to quantify the level of safety of a given imaging procedure [27, 28], as well as in health physics [4], to study and limit occupational and/or non-occupational exposures to radiation.

Determination of dose is thus a major motivation of radiation transport. In a given target volume, one could identify discrete sub-volumes of known mass and tally ionization events (and therefore energy deposition) in each. In fact, this is a common method of dose calculation provided that one is capable of simulating the interaction of the radiation beam with the target on the basis of individual ionization events, such as in Monte Carlo [12].

However, the continuous generalization of this procedure is actually:

$$D(\mathbf{r}) = \int dE \int d\Omega S_{\text{col}}(\mathbf{r}, E) \psi_c(\mathbf{r}, \hat{\mathbf{k}}, E) \quad (1.2.1)$$

where D is the dose, ψ_c is the angular fluence of charged ‘secondary’ radiation particles, i.e., radiation particles other than those that have not scattered since creation by the source of the radiation field, and then $S_{\text{col}}(\mathbf{r}, E)$ is the collisional stopping power of the material at \mathbf{r} for charged particles of energy E . In general, the secondary radiation particles are electrons that are ionized by whatever source, be it an X-ray beam, an electron beam, and ion beam, etc.

1.3 The Boltzmann transport equation

The Boltzmann transport equation (BTE) describes the motion of the angular fluence $\psi(\mathbf{r}, \hat{\mathbf{k}}, E)$, asking only for a description of a source $s(\mathbf{r}, \hat{\mathbf{k}}, E)$ as well as the composition of the medium: specifically, the ‘linear attenuation coefficient of scattering’ $\Sigma_s(\mathbf{r}, \hat{\mathbf{k}}' \rightarrow \hat{\mathbf{k}}, E' \rightarrow E)$ and the ‘linear attenuation coefficient of absorption,’ $\Sigma_a(\mathbf{r}, E)$. The quantity $\Sigma_s(\mathbf{r}, \hat{\mathbf{k}}' \rightarrow \hat{\mathbf{k}}, E' \rightarrow E) \Delta E \Delta \Omega$ is the fraction of particles which map from an incident momentum $(\hat{\mathbf{k}}', E')$ to within ΔE and $\Delta \Omega$ of an outgoing momentum $(\hat{\mathbf{k}}, E)$, per unit path length of travel in the medium. Similarly, the quantity $\Sigma_a(\mathbf{r}, E)$ alone is the fraction of particles of energy E which are absorbed by the medium per unit path length of particle travel. We will only discuss these in some detail; they are precisely the typical particle-particle interaction (differential) cross sections, which we will briefly discuss soon, multiplied by a scattering center density factor. The document [29] describes in very satisfying detail the basic physics of these attenuation coefficients, while [30] provides most of what one would need to apply these to the Boltzmann transport equation. Once these coefficients are defined, the Boltzmann transport equation used in radiation transport is:

$$\hat{\mathbf{k}} \cdot \nabla \psi(\mathbf{r}, \hat{\mathbf{k}}, E) + \Sigma_t(\mathbf{r}, E) \psi(\mathbf{r}, \hat{\mathbf{k}}, E) = \int_E^{E_{\text{max}}} dE' \int d\Omega' \Sigma_s(\mathbf{r}, \hat{\mathbf{k}}' \rightarrow \hat{\mathbf{k}}, E' \rightarrow E) \psi(\mathbf{r}, \hat{\mathbf{k}}', E') + s(\mathbf{r}, \hat{\mathbf{k}}, E) \quad (1.3.1)$$

which we recognize is a first-order, linear, integro-differential equation in six dimensions. Note that we have used the definition of the ‘total linear attenuation coefficient’:

$$\Sigma_t(\mathbf{r}, E) \equiv \Sigma_a(\mathbf{r}, E) + \int_{E_{\text{min}}}^E dE' \int d\Omega' \Sigma_s(\mathbf{r}, \hat{\mathbf{k}} \rightarrow \hat{\mathbf{k}}', E \rightarrow E') \quad (1.3.2)$$

Also note that the quantity E_{max} is the maximum energy found in our system, and E_{min} is a cutoff energy below which transport is not interesting. Also, when polarization of the radiation particles is neglected, the angular dependence of $\Sigma_s(\mathbf{r}, \hat{\mathbf{k}} \rightarrow \hat{\mathbf{k}}', E \rightarrow E')$ is only upon the ‘scattering angle cosine’ $\mu_s = \hat{\mathbf{k}} \cdot \hat{\mathbf{k}}'$, or:

$$\Sigma_s(\mathbf{r}, \hat{\mathbf{k}} \rightarrow \hat{\mathbf{k}}', E \rightarrow E') = \Sigma_s(\mathbf{r}, \mu_s, E \rightarrow E') \quad (1.3.3)$$

Derivation of (1.3.1) is found in a number of texts, and the sixth chapter of [2] is particularly recommended for its first-principles description of each term. More precisely, (1.3.1)

is the time-independent Boltzmann transport equation, because during its derivation it is assumed that both the source and medium are not changing with time, resulting in a time-independent fluence. The other assumptions made by this transport equation are that our radiation particles do not interact with one another, and that no external forces are present. The latter assumption may be violated if transport is being performed in the context of, say, a magnetic resonance (MR)-field, such as with MR-guided radiotherapy [2, 31, 32]. Principally, this affects charged particle travel inbetween scattering events, where trajectories now form helices about magnetic field lines rather than straight rays in direction $\hat{\mathbf{k}}$. However, modifications are readily made to the Boltzmann transport equation which appropriately describe such behavior [2], or external forces more generally [33], which is a frequent starting point for many plasma physics extensions of Boltzmann transport.

Nevertheless, the BTE is fundamentally a balance equation which describes, at any phase space point $(\mathbf{r}, \hat{\mathbf{k}}, E)$, the removal (LHS) and creation (RHS) of particles. The term $\hat{\mathbf{k}} \cdot \nabla \psi$ is sometimes called the ‘streaming term,’ because it describes particle travel in straight lines or rays in the direction $\hat{\mathbf{k}}$, which occurs inbetween scattering events that serve only to change the direction and energy of the particles. The attenuation term $\Sigma_t \psi$ describes the aggregate removal of particles due to scattering and absorption. The scattering term $\int dE' d\Omega' \Sigma_s \psi$ describes creation of particles at a point due to scattering from all other points. The source by definition describes creation of particles.

We also note that the Boltzmann transport equation requires a boundary condition. In the context of external beam radiation therapy problems in a convex volume, which are the primary focus of this document, one frequently finds the so-called ‘non re-entrant boundary condition’. This condition says that we know the fluence of particles entering the volume but not leaving, and so equivalently, that no particles can return to the volume after leaving (otherwise we’d need to know the history of these re-entering particles to know the boundary condition). More formally, if V is the spatial domain of our volume, Γ is its surface, and $\hat{\mathbf{n}}(\mathbf{r})$ is the normal vector of the surface position \mathbf{r} (meaningful only when $\mathbf{r} \in \Gamma$), then the non-reentrant boundary condition is:

$$\psi(\mathbf{r}, \hat{\mathbf{k}}, E) = \bar{\psi}(\mathbf{r}, \hat{\mathbf{k}}, E), \quad \hat{\mathbf{k}} \cdot \hat{\mathbf{n}}(\mathbf{r}) < 0 \text{ & } \mathbf{r} \in \Gamma \quad (1.3.4)$$

where $\bar{\psi}$ is assumed to be known. Other boundary conditions include ‘reflective boundary conditions’ [34]. Also, an important case of the non re-entrant boundary condition for this document is the vacuum boundary condition, $\bar{\psi} = 0$.

Lastly, we will rewrite the Boltzmann transport equation in terms of the following operators:

$$\hat{L}\psi = s \quad (1.3.5)$$

$$\hat{L} \equiv \hat{T} - \hat{K} \quad (1.3.6)$$

$$\hat{T} \equiv \hat{\mathbf{k}} \cdot \nabla + \Sigma_t \quad (1.3.7)$$

$$(\hat{K}\psi)(\mathbf{r}, \hat{\mathbf{k}}, E) \equiv \int dE' d\Omega' \Sigma_s(\mathbf{r}, \hat{\mathbf{k}}' \rightarrow \hat{\mathbf{k}}, E' \rightarrow E) \psi(\mathbf{r}, \hat{\mathbf{k}}', E') \quad (1.3.8)$$

where \hat{L} is called the ‘Boltzmann transport operator’ (or, much more loosely, the ‘BTE operator’), while \hat{T} is the ‘transport operator,’ and \hat{K} is the ‘scattering operator.’

1.4 Sources, uncollided fluences, and the first collision method

The next important matter to discuss is the sources with which we are interested in radiotherapy. The source function $s(\mathbf{r}, \hat{\mathbf{k}}, E)$ can come in many forms, if not a simple function of $(\mathbf{r}, \hat{\mathbf{k}}, E)$ that represents a continuous distribution of sources within our volume of interest. The most simple is a spherical, isotropic point source. That is, a point which emits particles in all directions in equal proportion. This source can be defined as localized at some point \mathbf{r}_0 , with an energy spectrum $f(E)$ (the number of particles created per unit energy). To be fully consistent with the integral behavior of such a description, this source is:

$$s(\mathbf{r}, \hat{\mathbf{k}}, E) = \frac{1}{4\pi} s_0 \delta^3(\mathbf{r} - \mathbf{r}_0) f(E) \quad (1.4.1)$$

where s_0 is the total number of particles created by the source, often written as $\dot{s}_0 \Delta t$, where \dot{s}_0 is the (assumedly constant) rate of particle creation and Δt is the time interval over which particles are being created (i.e., a sort of beam ‘on-time’). Then, $\delta^3(\mathbf{r})$ is the 3D Dirac delta function, and $f(E)$ is some function of energy which is normalized over a relevant energy interval. By construction:

$$\int d^3\mathbf{r} d\Omega dE s(\mathbf{r}, \hat{\mathbf{k}}, E) = s_0 \quad (1.4.2)$$

Alternatively, one could suggest a spherical but not isotropic point source. If, for instance, one were to block some of the source, or the source is the idealization of a process which does not create particles equally in every direction (both of which are relevant in the context of radiation therapy), then one can give an arbitrary (spherically normalized) angular distribution $g(\hat{\mathbf{k}})$ instead of $1/4\pi$, so that:

$$s(\mathbf{r}, \hat{\mathbf{k}}, E) = s_0 g(\hat{\mathbf{k}}) \delta^3(\mathbf{r} - \mathbf{r}_0) f(E) \quad (1.4.3)$$

Furthermore, planar sources can be created, however, they are best expressed with respect to the fluence that results from a planar source. We will briefly give the fluence at the end of the section using what is derived in the context of a spherical point source. Finally, one can create an arbitrarily-shaped source through the superposition of point sources, using a sum or an integral with a density function over the source location \mathbf{r}_0 .

We will find that we will never need to express the source alone in external beam problems, but we will always need to express the ‘uncollided’ angular fluence of particles due to the source, at least at the boundary of the volume, and in some cases throughout the entire volume. So, we must have a discussion on these quantities. A source creates particles in our system, which stream and get attenuated, but are re-populated at different points in phase space by scattering. We can therefore examine the angular fluence of ‘uncollided’ particles using the differential equation:

$$\hat{T} \tilde{\psi}^0 = s \quad (1.4.4)$$

where $\tilde{\psi}^0$ is the angular fluence of uncollided particles, sometimes called the primary angular fluence [1, 12]. This leads to the definition of particles which have scattered at least once:

$$\tilde{\psi} \equiv \psi - \tilde{\psi}^0 \quad (1.4.5)$$

For our immediate purposes, $\tilde{\psi}^0$ yields the most general boundary condition of $\hat{L}\tilde{\psi} = s$, which replaces the external beam sources that are zero throughout the whole volume, essentially turning the BTE into a boundary-value problem. However, we can also use these relationships to explicitly write a Boltzmann transport equation for $\tilde{\psi}$ which involves a continuous source constructed using $\tilde{\psi}^0$. That is, using the previous two equations, the Boltzmann transport equation can be written:

$$\hat{L}\tilde{\psi} = \hat{K}\tilde{\psi}^0 \equiv \tilde{s} \quad (1.4.6)$$

Now, $\hat{L}\tilde{\psi}^0 = s$ actually has an analytical solution [2]. It is most generally:

$$\tilde{\psi}^0(\mathbf{r}, \hat{\mathbf{k}}, E) = \int_V d^3\mathbf{r}' \frac{1}{|\mathbf{r} - \mathbf{r}'|^2} s(\mathbf{r}', \hat{\mathbf{k}}, E) e^{-\tau(\mathbf{r}, \mathbf{r}', E)} \delta^2\left(\hat{\mathbf{k}} - \frac{\mathbf{r} - \mathbf{r}'}{|\mathbf{r} - \mathbf{r}'|}\right) \quad (1.4.7)$$

where $\tau(\mathbf{r}, \mathbf{r}', E)$ is the ‘optical path length’ of a particle of energy E travelling from \mathbf{r}' to \mathbf{r} , that is:

$$\tau(\mathbf{r}, \mathbf{r}', E) = \int_0^{|\mathbf{r} - \mathbf{r}'|} d\ell \Sigma_t \left(\mathbf{r} - \ell \frac{\mathbf{r} - \mathbf{r}'}{|\mathbf{r} - \mathbf{r}'|} \right) \quad (1.4.8)$$

The quantity $e^{-\tau}$ is the fraction of particles that are attenuated during this trip. To see why the FCS method may be useful, we should consider the uncollided angular fluences which result from the sources of our interest. Consider the isotropic spherical point source:

$$\tilde{\psi}^0(\mathbf{r}, \hat{\mathbf{k}}, E) = \frac{1}{4\pi|\mathbf{r} - \mathbf{r}_0|^2} s_0 f(E) e^{-\tau(\mathbf{r}, \mathbf{r}_0, E)} \delta^2\left(\hat{\mathbf{k}} - \frac{\mathbf{r} - \mathbf{r}_0}{|\mathbf{r} - \mathbf{r}_0|}\right) \quad (1.4.9)$$

The corresponding fluence is:

$$\tilde{\varphi}^0(\mathbf{r}, E) = \frac{1}{4\pi|\mathbf{r} - \mathbf{r}_0|^2} s_0 f(E) e^{-\tau(\mathbf{r}, \mathbf{r}_0, E)} \quad (1.4.10)$$

which we recognize is the statement of the inverse square law ($1/|\mathbf{r} - \mathbf{r}_0|^2$) and Beer’s law ($e^{-\tau}$). But, $\tilde{\psi}^0$ only has particles with direction $\hat{\mathbf{k}}_0 \equiv (\mathbf{r} - \mathbf{r}_0)/|\mathbf{r} - \mathbf{r}_0|$, and is actually singular. So, in principle, the angular fluence ψ itself has a singular part in $\tilde{\psi}^0$, and an asingular part in $\tilde{\psi}$. This contributes to so-called ‘ray-effects’ in the total fluence φ , which are numerical (i.e., unphysical) buildups of fluence that radiate along particular ordinate directions from the location of a point source [14, 35, 36]. These problems can be mitigated by using more refined discretization parameters (and thus computation time and storage). Alternatively, one can reformulate the problem as $\hat{L}\tilde{\psi} = \tilde{s}$, with $\tilde{\varphi}^0$ produced more manually, in what is known as the ‘first collision source’ (FCS) method [36]. The FCS method is able to mitigate ray effects without refining the discretization parameters, with only a few caveats: first, we must be able to obtain the optical path length τ at a given point of the problem volume (which, pending discussion of energy discretization, is a problem that reduces to ray-tracing [14, 36, 37]). Second, we must take the vacuum boundary condition for $\hat{L}\tilde{\psi} = \tilde{s}$, i.e., $\tilde{\psi} = 0$. This follows directly from the fact that $\tilde{\psi} = \tilde{\psi}^0$, so the boundary condition of $\tilde{\psi}$ alone is zero. Throughout this document, we will discuss the treatment of the FCS method concurrently with discretization of the generic Boltzmann transport problem, $\hat{L}\psi = s$. That is, we will

be discretizing not only \hat{L} and the external beam source s , but we will also carry along the discretization of \tilde{s} , which is generally a continuous source of a particular form, i.e., $\hat{K}\tilde{\psi}^0$.

Now we can give the uncollided fluence due to a planar source. Let the normal vector of the source be $\hat{\mathbf{k}}_0$. Let the source have an areal density of particles, $\rho_A(x_s, y_s)$, in some 2D local coordinate system (x_s, y_s) which spans the plane. For a given point \mathbf{r} in the medium, the areal density of particles will be given by the source's areal density at the point (x_s, y_s) such that \mathbf{r} is along a ray travelling from (x_s, y_s) and perpendicular to the source plane, attenuated as per Beer's law. The energy distribution factor $f(E)$ is then applied. The coordinates (x_s, y_s) associated with \mathbf{r} can be obtained by defining an origin of the 2D system \mathbf{r}_0 and then two basis vectors in this system, $\hat{\mathbf{x}}_s$ and $\hat{\mathbf{y}}_s$, which form a mutually orthogonal coordinate system with $\hat{\mathbf{k}}_0$. If these are defined, then simple vector analysis shows:

$$\begin{aligned} x_s(\mathbf{r}) &= (\mathbf{r} - \mathbf{r}_0) \cdot \hat{\mathbf{x}}_s \\ y_s(\mathbf{r}) &= (\mathbf{r} - \mathbf{r}_0) \cdot \hat{\mathbf{y}}_s \end{aligned} \quad (1.4.11)$$

Thus:

$$\tilde{\varphi}^0(\mathbf{r}, E) = \rho_A[x_s(\mathbf{r}), y_s(\mathbf{r})] f(E) e^{-\tau[\mathbf{r}, \mathbf{r}_0 + x_s(\mathbf{r})\hat{\mathbf{x}}_s + y_s(\mathbf{r})\hat{\mathbf{y}}_s, E]} \quad (1.4.12)$$

where the optical path length took as the source for \mathbf{r} the point $\mathbf{r}_0 + x_s(\mathbf{r})\hat{\mathbf{x}}_s + y_s(\mathbf{r})\hat{\mathbf{y}}_s$, which lies on the source plane. Indeed, the expression above does result from a spherical point source when the point source is considered arbitrarily far away, but the number of particles dedicated to the arbitrarily small solid angle subtending the volume is increased in proportion to the inverse-square-law factor, up to a dimensionful factor which is essentially ρ_A .

1.5 Coupling particle types

Radiation therapy, whether external or internal, with photons, electrons, alpha particles, protons, neutrons, etc., is not a problem of one particle alone [3, 38]. It is therefore important to construct a set of BTE's wherein our particles all 'talk' to each other. For instance, in the case of external photon radiotherapy, the photons, electrons, and positrons are able to create one another, which must therefore be transported as a new source. This is implemented in the BTE by creating a scattering source from one particle to another. For instance, if some particle α sources some particle β following some scattering events, then we include in the source for β the term:

$$s^{\alpha\beta}(\mathbf{r}, \hat{\mathbf{k}}, E) = \int dE_\alpha d\Omega_\alpha \Sigma_s^{\alpha\beta}(\mathbf{r}, \hat{\mathbf{k}}_\alpha \rightarrow \hat{\mathbf{k}}, E_\alpha \rightarrow E) \psi^\alpha(\mathbf{r}, \hat{\mathbf{k}}_\alpha, E_\alpha) \quad (1.5.1)$$

where $\Sigma_s^{\alpha\beta} \Delta E_\alpha \Delta \Omega_\alpha$ is the number of the particles β created from a particle α within ΔE_α and $\Delta \Omega_\alpha$, per unit path length of its travel. One example of a scattering mechanism is Compton scattering of photons, which will ionize the medium, and thus there is a source of electrons due to photon scattering [1, 3]. Since the photons emerge from this event, this is also a typical scattering mechanism to be included in \hat{K} . Terms like the above will not be treated specially in this document, because they follow from discretization of \hat{K} , where the

basic distinction is in the attenuation coefficient used ($\Sigma_s \rightarrow \Sigma_s^{\alpha\beta}$) and, of course, the object to which it is applied ($\psi \rightarrow \psi^\alpha$).

In media composed of atoms and molecules, and in the MeV energy regime, one may take the set of interactions described by Table 1 [3, 29, 30]. Note that the Auger effect and fluorescence are considered to refer to all products of a cascade that occur following ionization, except for the initially ejected electron [39]. Thus, for instance, fluorescence via $\gamma \rightarrow \gamma$ describes the emission of any and all photons emitted in the cascade after the initial photoelectron is ejected, while Auger emission via $\gamma \rightarrow e^-$ describes the emission of any and all electrons in the cascade not including the initial photoelectron ejected. Similarly for the Auger effect and fluorescence as mechanisms of electron scattering, where the first ejected electron is ejected via inelastic scattering (ionization), a process also called impact ionization [40].

Thus, one can write three coupled BTE's which demand to be solved simultaneously. In X-ray or electron radiation therapy, however, one is able to simplify this picture dramatically. Positrons here are only created by pair production. In principle, positron transport is similar to electron transport except that a positron will annihilate at latest at the very end of its trajectory when it has lost all of its kinetic energy through inelastic scattering. Thus, except for in the context of charge deposition calculations, one can say that the photoelectric effect will essentially produce two electrons, and then positron transport can be neglected [30]. Effectively, this only neglects the annihilation photons created by the positron, which are most often 0.511 keV each, and so the effect is not significant in the result [2, 3]. Next, one can neglect the transport of Bremsstrahlung and fluorescence following impact ionization, which once again yields little effect on the accuracy of the calculation [2]. This means that the photon angular fluence is fully uncoupled, and the electron angular fluence depends only on the photon angular fluence, so that the problem is soluble sequentially. With these approximations, the new scheme is modified to Table 2. Importantly, note how Bremsstrahlung and fluorescence were previously listed as a process for $e^- \rightarrow \gamma, e^-$, but are now $e^- \rightarrow e^-$. This means that the processes of Bremsstrahlung and fluorescence are still used to account for energy loss and redirection of the parent electron, and we simply neglect the resulting photon.

This scheme leads to the coupled equations:

$$\hat{L}^\gamma \psi^\gamma = s^\gamma \quad (1.5.2)$$

$$\hat{L}^e \psi^e = s^e + \hat{K}^{\gamma e} \psi^\gamma \quad (1.5.3)$$

where 'e' refers to electrons.

1.6 Continuous slowing down

In electron transport, inelastic scattering cross sections in use today are highly inaccurate for $E' \approx E$, and singular for $E' = E$ [5, 30, 41]. Thus, it is necessary to use the so-called continuous slowing down approximation (CSDA), or more specifically, the restricted CSDA. In the restricted CSDA, inelastic (collisional) scattering events and Bremsstrahlung (radiative) scattering events are divided into 'soft' and 'hard,' with the former being when

Table 1: Processes of scattering (describing attenuation as well) relevant to MeV transport of external X-rays and electrons.

Parent	Scattering Mechanism	Outgoing
γ	Compton Effect	γ, e^-
	Photoelectric Effect	e^-
	Pair Production	e^-, e^+
	Auger Effect	e^-
	Fluorescence	γ
e^-	Bremsstrahlung	γ, e^-
	Elastic Scattering	e^-
	Inelastic Scattering (Slowing Down)	e^-
	Inelastic Scattering (Ionization)	e^- (x2)
	Auger Effect	e^- (x2)
e^+	Bremsstrahlung	γ, e^+
	Pair Annihilation	γ (x2)
	Bhabha Scattering (Slowing Down)	e^+
	Bhabha Scattering (Ionization)	e^-, e^+
	Elastic Scattering	e^+

Table 2: Modified diagram like Table 1, but with approximations specific to X-ray and electron radiotherapy applied.

Parent	Scattering Mechanism	Outgoing
γ	Compton Effect	γ, e^-
	Photoelectric Effect	e^-
	Pair Production	e^- (x2)
	Auger Effect	e^-
	Fluorescence	γ
e^-	Bremsstrahlung	e^-
	Elastic Scattering	e^-
	Inelastic Scattering (Slowing Down)	e^-
	Inelastic Scattering (Ionization)	e^- (x2)
	Auger Effect	e^- (x2)
	Fluorescence	e^-

the energy difference is less than some cutoff Δ and the latter being when the difference exceeds this cutoff. Thus, the scattering term can be written:

$$\hat{K}_{\text{inel}}\psi = \int_E^{E+\Delta} dE' \int d\Omega' \Sigma_{\text{inel}}(E' \rightarrow E)\psi(E') \quad (1.6.1)$$

$$+ \int_{E+\Delta}^{E_{\text{max}}} dE' \int d\Omega' \Sigma_{\text{inel}}(E' \rightarrow E)\psi(E') \quad (1.6.2)$$

The first integral is considered the soft scattering integral, and the second integral is the hard scattering integral. The second is used as-is, and is relegated to special treatment during construction of cross sections for a given energy discretization method. This term is not discussed further in this document, but is discussed in [30, 41] for two different energy discretization methods. Nevertheless, the first integral describes the inaccurate part of the calculation. Using the assumption that Σ_s will grow very large, an expansion can be made that results in the following term:

$$\int_E^{E+\Delta} dE' \int d\Omega' \Sigma_{\text{inel}}(E' \rightarrow E)\psi(E') \approx \frac{\partial}{\partial E} [L_\Delta(E)\psi(E)] \quad (1.6.3)$$

where:

$$L_\Delta(E) = \int_{E-\Delta}^E dE' \int d\Omega (E - E')\Sigma_{\text{inel}}(\mu, E \rightarrow E') \quad (1.6.4)$$

is the ‘restricted linear energy transfer.’ It is the energy deposited per unit path length due to soft scattering events, i.e., when the energy deposition is $E - E' \leq \Delta$. Derivation of (1.6.3) is described in [5]. Now, for future reference, we will define:

$$\hat{R}\psi \equiv \frac{\partial}{\partial E} [L_\Delta(E)\psi(E)] \quad (1.6.5)$$

which describes the action of the restricted CSDA operator on an angular fluence.

2 Discretization

There are a number of ways the BTE can be discretized, with each physically unique set of coordinates from phase space receiving its own treatment, and interaction between the different discretization methods yielding radically different problems. We will briefly touch upon some of these methods, however, in this document we will only discuss in detail one choice of discretization method for each set of coordinates.

First, the energy coordinate is often discretized with the multigroup approximation [2, 5, 16, 30], but it is also possible and in some cases interesting to use the 1D finite element method (FEM) for energy discretization, for which the reference [41] has a great introduction and discussion. In a later update of this document, we will discuss this method of discretization (abbreviated as FEXS, for ‘finite-element cross sections’). In either case, energy discretization is most intuitively discussed first because the energy coordinate can be removed from our problem quite simply. If the problem takes place in the rest frame of the medium, then the source particles can not gain energy, as scattering will always result in transfer of energy to the medium, the constituents of the medium being unable to lose energy

at rest. This is the reason for the bounds of the energy integral in (1.3.1), which were to take E' from E to E_{\max} . Thus, the highest energy particles in the system are not populated as a result of scattering, and this observation with any energy discretization method results in an iterative procedure that turns the polyenergetic BTE into a sequence of monoenergetic BTEs, as we will soon see.

Next, the spatial coordinates can be discretized by the finite element method (FEM) [2, 16, 17, 42], which are more complex but also more versatile than basic spatial differencing techniques [21]. In the solver wiscobolt, the FEM is used exclusively for spatial discretization. This method of discretization demands the most attention out of the discussed methods.

As for angular discretization, two popular methods are discrete ordinates (S_N , where we will consider N as the number of polar angles at which our result is evaluated) and real spherical harmonics expansions (P_N , where N is the order of real spherical harmonics up to which we assume the moments of ψ are other than zero) [19, 34]. The angular discretization method combines with the spatial FEM to produce some unique properties that must be taken into consideration when solving the problem. At the moment, this document only describes S_N discretization in angle. Note, however, that the angular dependence of the scattering terms is generally treated with a P_N discretization [2, 19, 30] regardless, which results immediately from a moment expansion of the scattering operator. These expansions will be made prior to the S_N discretization. Also note that, recently there has been interest in the use of angular finite elements [43, 44], which is indeed functional in the SCEPTR program [45], however we will not discuss these and the reader is referred to the aforementioned sources.

Following discretization, we need to use introduce iterative numerical methods that are used to arrive at a solution, and sometimes acceleration methods to act upon these methods. These will be the primary concern of the next section of this document, however. This section is divided into four subsections:

1. The multi-group formalism
2. The spatial finite element method
3. PN scattering
4. SN angular discretization

Our BTE will initially take the generic form:

$$(\hat{T} - \hat{K})\psi = s \quad (2.0.1)$$

and much of our focus will be discretization on an operator-to-operator basis, with special notes for sources of the form \tilde{s} and in energy discretization the operator \hat{R} , which has straightforward treatment in spatial and angular discretization.

2.1 The multi-group formalism

To discretize the energy coordinate of the phase space, a common method is the multi-group approximation. In this approximation, one considers ψ to be binned into various energy

‘groups,’ and assumes that it is constant in these groups, as well as that cross sections to map from one group to another are also constant.

First, a particle energy range that is relevant to the problem is chosen, and then divided into G (not necessarily uniform) intervals. Conventionally, E_1 is taken as the maximum energy and E_{G+1} is taken as the minimum energy, because we will soon see that particles are only going to map from higher energies to lower energies (thus, they progress from, for instance, group 1, to 2, to 3, and so on). Typically E_{G+1} is a cutoff energy after which we are not interested in the interactions of the particle in question. The particles in group g are those within interval $\Delta E_g = E_g - E_{g+1}$. Note that while ΔE_g is not generally constant, however, it should be chosen such that energy-dependent quantities, in particular cross sections, are relatively unchanging within. For example, with photons, and when the photoelectric effect is relevant, it is typically customary have an energy group split by the edge energy. It is also typical to have different energy groups for different particle types.

Now, $\psi(E)$ is ‘grouped’ by being integrated over group g :

$$\psi_g(\mathbf{r}, \hat{\mathbf{k}}) \equiv \int_{E_{g+1}}^{E_g} dE \psi(\mathbf{r}, \hat{\mathbf{k}}, E) \quad (2.1.1)$$

For brevity, we say:

$$\int_{E_{g+1}}^{E_g} dE f(E) \equiv \int_g dE f(E) \quad (2.1.2)$$

In terms of energy grouped quantities, we can say:

$$\int_0^\infty dE f(E) \approx \sum_{g=1}^G \int_g dE f(E) \quad (2.1.3)$$

Now, integrate the BTE term-by-term. Consider the total attenuation term first. Under the assumption that $\psi(E)$ is constant within an energy group, we can consider it to be $\psi_g/\Delta E_g$. Therefore, we can take:

$$\int_g dE \Sigma_t(E) \psi(E) = \Sigma_{t,g} \psi_g \quad (2.1.4)$$

where:

$$\Sigma_{t,g} = \frac{1}{\Delta E_g} \int_g dE \Sigma_t(E) \quad (2.1.5)$$

which we interpret as a constant attenuation coefficient for particles in group g . Effectively, this means we are ‘binning’ our particles into energy bins ranging from E_{g+1} to E_g . Now consider the scattering cross section. Under this approximation:

$$\int dE' \Sigma_s(E' \rightarrow E) \psi(E') \approx \sum_{g'=1}^G \int_g dE' \Sigma_{s,g'g} \psi_{g'} \quad (2.1.6)$$

where:

$$\Sigma_{s,g'g}(\mathbf{r}) = \frac{1}{\Delta E_{g'}} \int_g dE \int_{g'} dE' \Sigma_s(\mathbf{r}, E', E) \quad (2.1.7)$$

We emphasize the relative ordering of the summed index g' to the un-summed index g , because the element $\Sigma_{s,g'g}$ is written to describe transfer from g' to g . This amounts to the matrix holding the elements $\Sigma_{s,gg'}$ being transposed prior to application to any vector.

To perform physically meaningful BTE calculations, it is necessary to have the energy-grouped cross sections described above. This is a major task, and generally, it can be distinct from the BTE solver itself. For instance, popular solvers such as Sandia National Labs' SCEPTR and Varian's Acuros XB have in the past relied upon Sandia National Labs' Coupled Electron-Photon Cross Section (CEPXS) code [15, 16, 20, 30]. However, as CEPXS is similarly not openly available, other programs exist and/or are in development for the purpose of generating photon-electron cross sections for radiotherapy, including ELECTR [46] for the DRAGON-5 nuclear reactor solver (a lattice Boltzmann transport solver for photons and neutrons, [47]), as well as wiscobolt's built-in cross section generation modules. Typically, these programs rely not only on analytical expressions, but also numerical and (in limited cases) experimental data, valid for the first 100 or so elements of the periodic table [5, 30, 39]. Each mechanism also entails its own cut-off energies, below or above which the cross section is not accurate. Cross sections for molecules and mixtures can be approximately formulated using mass- or electron number-weighted sums [29, 30, 48] frequently referred to as the ‘additivity rule,’ however, these cross sections are generally not suitable when the wavelength of the radiation is at or greater than the interatomic distance [3, 29], i.e., for energies in the hundreds of electronvolts or less.

Now, the generic BTE with only energy grouping reads:

$$[\hat{\mathbf{k}} \cdot \nabla + \Sigma_{t,g}(\mathbf{r})] \psi_g = \sum_{g'=1}^g \int d\Omega' \Sigma_{s,g'g} \psi_{g'} + s_g \quad (2.1.8)$$

The prescription is, intuitively, to replace energy integrals of $f(E', E)h(E')$ with sums of $f_{g'g}h_{g'}$.

Finally, a note about the CSDA approximation for electron transport. Energy grouping of the CSDA operator leads to:

$$\int_g dE \frac{\partial}{\partial E} [L_\Delta(E) \psi(E)] = L_\Delta(E_g) \psi(E_g) - L_\Delta(E_{g+1}) \psi(E_{g+1}) \quad (2.1.9)$$

which, notably, is not clearly written in terms of integrals of $\psi(E)$ over g . However, under the assumptions of the CSDA, one can suggest that soft collisions should account for electron transport into a group g from the adjacent higher energy group $g - 1$ [30]. Thus, one can instead impose that the CSDA is accounted for by a term such as:

$$\int_g dE \frac{\partial}{\partial E} [L_\Delta(E) \psi(E)] \approx R_{g-1,g} \psi_{g-1} \quad (2.1.10)$$

which is to say, this is a source of particles in group g due to group $g - 1$. This is referred to as a ‘first-order’ CSDA [30]. There also exist second and higher order discretizations [30, 49, 50], which more generally come from the usual form:

$$\int_g dE \frac{\partial}{\partial E} [L_\Delta(E) \psi(E)] \approx \sum_{g'=1}^{g-1} R_{g'g} \psi_{g'} \quad (2.1.11)$$

with attenuation, absorption, and deposition coefficients also existing for the group g . The precise expressions for $R_{g'g}$ are what distinguish these different kinds of discretizations, however, we will not describe their derivations nor state their results, and the reader is referred to [30]. Two notes that should be made however: first, the CSDA's results always heavily depend upon the multigroup structure, and consequently, the transfer coefficients $R_{g'g}$ can be negative [30]. They are therefore frequently referred to as 'unreal.' Second, the transfer coefficients for hard inelastic scattering are therefore not taken to map from g' to g except when $g' \leq g - 2$, i.e., when the incident particle's group has a substantially larger energy than the outgoing particle's group. This is the case regardless of the use of first or second order discretization. Nevertheless, the reader is generally referred to [5, 30, 49] to learn more about the CSDA in the multigroup approximation.

2.1.1 Energy iteration and the monoenergetic BTE

Notably, our scattering mechanisms require that the outgoing energy E is less than the incident energy E' , because they occur in the rest frame of the target material. Therefore, $\Sigma_{s,g'g}$ is the g' th row and g th column of an upper triangular matrix, because the outgoing index g must be higher than the incoming index g' . That is to say, our BTE problem can be written as a matrix in the g index, like:

$$\begin{pmatrix} \hat{L}_{11} & \hat{L}_{21} & \dots & \hat{L}_{G1} \\ \hat{L}_{12} & \hat{L}_{22} & \dots & \hat{L}_{G2} \\ \vdots & \vdots & \ddots & \vdots \\ \hat{L}_{1G} & \hat{L}_{2G} & \dots & \hat{L}_{GG} \end{pmatrix} \begin{pmatrix} \psi_1 \\ \psi_2 \\ \vdots \\ \psi_G \end{pmatrix} = \begin{pmatrix} s_1 \\ s_2 \\ \vdots \\ s_G \end{pmatrix} \quad (2.1.12)$$

where we've kept the ordering of the summed index relative to the un-summed index. Now, eliminating transfer from higher energy to lower energy (i.e., lower g' to higher g), we have:

$$\begin{pmatrix} \hat{L}_{11} & 0 & \dots & 0 \\ \hat{L}_{12} & \hat{L}_{22} & \dots & 0 \\ \vdots & \vdots & \ddots & \vdots \\ \hat{L}_{1G} & \hat{L}_{2G} & \dots & \hat{L}_{GG} \end{pmatrix} \begin{pmatrix} \psi_1 \\ \psi_2 \\ \vdots \\ \psi_G \end{pmatrix} = \begin{pmatrix} s_1 \\ s_2 \\ \vdots \\ s_G \end{pmatrix} \quad (2.1.13)$$

and thus, our system is lower-triangular. This means that we can iteratively write our BTE like:

$$\hat{L}_{11}\psi_1 = s_1 \quad (2.1.14)$$

$$\hat{L}_{22}\psi_2 = s_2 - \hat{L}_{12}\psi_1 \quad (2.1.15)$$

$$\hat{L}_{33}\psi_3 = s_3 - \hat{L}_{13}\psi_1 - \hat{L}_{23}\psi_2 \quad (2.1.16)$$

$$\vdots \quad (2.1.17)$$

$$\hat{L}_{gg}\psi_g = s_g - \sum_{g'=1}^{g-1} \hat{L}_{g'g}\psi_{g'} \quad (2.1.18)$$

This is a common method of solving a lower triangular matrix, called forward substitution [51]. This is a purely monoenergetic problem in the sense that we can take:

$$S_g \equiv s_g - \sum_{g'=1}^{g-1} \hat{L}_{g'g} \psi_{g'} \quad (2.1.19)$$

which can be formed following solution of the group $g-1$. Then, the BTE we'd need to solve in any given iteration is just:

$$\hat{L}_{gg} \psi_g = S_g \quad (2.1.20)$$

where S_g is known. Note now that:

$$\hat{L}_{g'g} = -\hat{K}_{g'g}, \quad g' \neq g \quad (2.1.21)$$

$$\hat{L}_{gg} = \hat{\mathbf{k}} \cdot \nabla + \Sigma_{t,g}(\mathbf{r}) - \int d\Omega' \Sigma_{s,gg}(\hat{\mathbf{k}}' \rightarrow \hat{\mathbf{k}}) \quad (2.1.22)$$

So, our problem is the typical monoenergetic BTE if we take the symbolic substitutions $\psi_g \rightarrow \psi$, $S_g \rightarrow s$, $\Sigma_{s,gg} \rightarrow \Sigma_s(\hat{\mathbf{k}}' \rightarrow \hat{\mathbf{k}})$, and $\Sigma_{t,g} \rightarrow \Sigma_t$. From this point on, we will be discussing solely the monoenergetic problem, omitting group indices and reverting to s for the source rather than S .

Now, with respect to the first-collision scattering source, we would of course have:

$$\tilde{s}_g = \sum_{g'=1}^g \int d\Omega' \Sigma_{s,g'g} \tilde{\varphi}_{g'}^0 \delta^2[\hat{\mathbf{k}}' - \hat{\mathbf{k}}_0(\mathbf{r})] \quad (2.1.23)$$

But we must discuss how to get $\tilde{\varphi}_g^0$. Since we have formulated our problem as a series of monoenergetic problems, we can actually simply get $\tilde{\varphi}_g^0$ using the fact that $\Sigma_{t,g}$ is constant for a given group g , rather than forming $\tilde{\varphi}^0(E)$ and energy grouping that. That is, we just take:

$$\tilde{\varphi}_g^0 = f_g e^{-\int d\ell \Sigma_{t,g}} \quad (2.1.24)$$

where $\int d\ell \Sigma_{t,g}$ is the optical path length for particles in group g and $f_g = \int_g dE f(E)$. This is a quantity which, for a given beam origin \mathbf{r}_0 and a given point in the volume \mathbf{r} , can be obtained by ray-tracing through the various materials crossed between these points. Various fast algorithms exist for ray-tracing [37, 52, 53].

A note on the monoenergetic problem when using the FCS method, we take the prescription that $s_g \rightarrow \tilde{s}_g$ and $\psi_g \rightarrow \tilde{\psi}_g$ prior to forward substitution and formulation of the monoenergetic problem. Then, the $g' < g$ terms of the sum in \tilde{s}_g are separated out as terms which contribute to S_g during energy iteration, despite that all \tilde{s}_g are known prior to energy iteration. Thus, we write the energy-iterated source:

$$\tilde{S}_g \equiv \tilde{s}_g + \sum_{g'=1}^{g-1} \int d\Omega' \Sigma_{s,g'g} \tilde{\varphi}_{g'}^0 \delta^2[\hat{\mathbf{k}}' - \hat{\mathbf{k}}_0(\mathbf{r})] - \sum_{g'=1}^{g-1} \hat{L}_{g'g} \tilde{\psi}_{g'} \quad (2.1.25)$$

where we are re-defining \tilde{s}_g as:

$$\tilde{s}_g \leftarrow \int d\Omega' \Sigma_{s,gg} \tilde{\varphi}_g^0 \delta^2[\hat{\mathbf{k}}' - \hat{\mathbf{k}}_0(\mathbf{r})] \quad (2.1.26)$$

which will be the form of \tilde{s} in the monoenergetic problem with which we proceed.

2.1.2 Deposition cross sections

It is necessary to understand how a quantity such as dose is calculated in the multigroup approximation, but the discussion generalizes to so called ‘deposition’ calculations, where one can obtain, rather than energy deposition per unit mass (dose), deposition of ‘something’ per unit volume [30, 49]. Of course, dose is the special case of ‘energy’ deposition per unit volume, divided by mass density. One of the other interesting types of deposition is charge deposition, which describes the deposition or removal of charged particles, such as electrons or positrons, in a certain region. In general, however, the continuous expression of a deposition is:

$$D(\mathbf{r}) = \int dE d\Omega L(\mathbf{r}, E) \psi(\mathbf{r}, \hat{\mathbf{k}}, E) \quad (2.1.27)$$

where $L(\mathbf{r}, E)$ is the deposition of ‘something’ per unit path length of beam travel. The above is discretized in MGXS like:

$$D = \sum_{g'=1}^G L_g \varphi_g \quad (2.1.28)$$

where φ_g is the fluence in group g and L_g is the ‘deposition cross section’ for group g , and of course position dependence in L_g describes the material. Scattering interactions cause deposition, so L is generally related to the scattering cross sections and is usually constructed directly from the elements $\Sigma_{s,g'g}$, as well as those of $\Sigma_{t,g}$ and $\Sigma_{a,g}$ in certain instances. Precise expressions for deposition of energy and charge are beyond the scope of this document and are relegated to **wiscobolt physics**, however, a few notes are worthwhile here specifically for energy deposition.

First, due to the CSDA’s dependence on the energy group structure, energy deposition cross sections do not accurately describe the energy deposited by particles in group g [30]. That is to say, one can not suggest that the energy contributed by particles in group g is $L_g \varphi_g$. Rather, the entire sum in (2.1.28) is needed to accurately describe deposition. Additionally, particles which scatter from the lowest energy group $g = G$ to below the cutoff energy E_{G+1} are considered to depositing all of their energy locally, but this is done using an ‘absorption’ term that is particularly constructed, which accounts for numerical absorption of particles [30, 49]. That is, because the particles which scatter to below the cutoff energy disappear from the calculation, they are ‘numerically’ absorbed.

2.2 The spatial finite element method

In order to discretize the spatial part of the phase space, the finite element method (FEM) is used. The FEM is one of the most useful computational methods in recent history, and it is encountered in a number of engineering problems, and so one will have no trouble finding several resources which go into varying levels of depth on the topic. The reader is referred in particular to [17]. In regards to finite elements in the Boltzmann transport equation specifically, the reader is referred to [2] for a basic overview and [42, 54] for particular details and more rigorous work-throughs. The content in this section draws upon these sources, or is otherwise referenced directly.

First, we will introduce the FEM briefly. Then, we will switch gears and reformulate the BTE in a form to which the FEM can be applied, i.e., in terms of integral quantities over small volumes. Then, the FEM will be applied.

2.2.1 The finite element method

The rationale for the FEM is simple: one can convert a problem which takes place throughout a large, continuous volume V , to the composition of potentially co-dependent problems which take place in small pieces of the volume V^e , referred to as ‘elements’ e . To form elements, one first needs to construct a ‘mesh,’ which is a collection of points or nodes that are interconnected to form the aforementioned elements. The nodes are connected by lines, multiple lines enclose a face, and multiple faces enclose an element. If the elements are different shapes and/or sizes, then one must be using the so-called ‘discontinuous finite element method’ (DFEM) [17], whose distinction from a continuous FEM will be discussed briefly once our problem is formulated. If the elements are made up of straight edges, then the element is said to be ‘first-order,’ and one can only linearly interpolate within the element. If instead the elements have N nodes along the edges (distinct from vertices), then these elements are ‘ $(N + 1)$ th-order,’ and allow for $(N + 1)$ th-order polynomial interpolation. We will only discuss linear elements, but the use of higher-order elements makes some significant changes to the derivations soon to follow, the case of 2nd-order elements is well discussed in [42].

In general, the mesh should meet some criteria related to varying element size for the given problem, and there exist a number of programs which conveniently create meshes from user-defined geometry and ‘size fields,’ such as the Gmsh program [55]. An important note to be made for the BTE is how materials are defined. Material definition is a trait that is not general in the FEM, but, it is of great importance in the BTE. In the BTE, we need material identities to inform what cross sections Σ_s and Σ_t to use at some point in the volume. One can conveniently identify a set of finite elements with a particular material. Thus, the spatial dependence of these quantities is constant throughout a finite element. It is then noteworthy that one should use a mesh that is refined such that the size of a given element is not significantly greater than the ‘mean free path’ ($1/\Sigma_t$) of the particle in question travelling in the material of that element [18]. That is because the mean free path is a metric of the length over which our particle experiences scattering. If many scattering events are occurring over a certain distance, then one will need greater spatial resolution over that distance.

2.2.2 The weak form

The FEM is applied to formulate our problem as a matrix problem. However, before doing so, we should rephrase the BTE as an exact, albeit infinitely large, matrix problem. In principle, we can take the BTE $\hat{L}\psi = s$, and expand ψ and s in some basis $\{\phi_m(\mathbf{r})\}$. This basis needs to ‘span the entire space’ of possible angular fluences and sources, i.e., it needs

to satisfy:

$$\psi(\mathbf{r}, \hat{\mathbf{k}}) = \sum_{m=1}^{\infty} \psi_m(\hat{\mathbf{k}}) \phi_m(\mathbf{r}) \quad (2.2.1)$$

$$s(\mathbf{r}, \hat{\mathbf{k}}) = \sum_{m=1}^{\infty} s_m(\hat{\mathbf{k}}) \phi_m(\mathbf{r}) \quad (2.2.2)$$

where we'll suppress the angular variables from now on. Doing this expansion yields:

$$\sum_{m=1}^{\infty} \psi_m \hat{L} \phi_m(\mathbf{r}) = \sum_{m=1}^{\infty} s_m \phi_m(\mathbf{r}) \quad (2.2.3)$$

We can now find an equation for ϕ_m by projecting both sides of the equation onto an arbitrary basis vector ϕ_n , much like finding the components of a Euclidean vector in $\hat{\mathbf{x}}$, $\hat{\mathbf{y}}$, and $\hat{\mathbf{z}}$. That looks like:

$$\sum_{m=1}^{\infty} \psi_m \int_V d^3 \mathbf{r} \phi_n(\mathbf{r}) \hat{L} \phi_m(\mathbf{r}) = \sum_{m=1}^{\infty} s_m \int_V d^3 \mathbf{r} \phi_n(\mathbf{r}) \phi_m(\mathbf{r}) \quad (2.2.4)$$

If we take $L_{nm} \equiv \int_V d^3 \mathbf{r} \phi_n \hat{L} \phi_m$, and then suppose that our basis is orthonormal (in addition to being real), then:

$$\sum_{m=1}^{\infty} L_{nm} \psi_m = s_n \quad (2.2.5)$$

Of course, except for trivial cases, the problem above is not exactly soluble. In order to find a useful equation similar to (2.2.5), one may decide to be satisfied with a solution valid for a finite part of the basis, therefore yielding the solution in a correspondingly finite-dimensional subspace. The finite element method, however, is prior to this the division of the problem into different sub-volumes (elements), each of which will carry its own set of basis functions with which to prop up an approximate solution ψ , yielding the solution over the volume of the individual elements in the subspace spanned by the choice of basis functions. This makes a modular and more efficient problem.

So, we generalize the above so as not to commit to any basis such as ϕ_m , and that's what we'll work with until we can divide our problem into elements. This yields the 'weak form' of the BTE:

$$\int_V d^3 \mathbf{r} v(\mathbf{r}) \hat{L} \psi(\mathbf{r}) = \int_V d^3 \mathbf{r} v(\mathbf{r}) s(\mathbf{r}) \quad (2.2.6)$$

where, we recognize, the exact problem (2.2.5) is equivalent to demanding the above be satisfied for any (valid) function, equivalently all infinitely many bases $\phi_m(\mathbf{r})$ which span the space of (valid) functions. Now, the weak form of the BTE should be processed further before dividing the volume integrals into integrals over elements. In particular, this is so that we can remove direct differentiation of ψ itself, which takes place in the transport operator (specifically the streaming part). The whole weak form is:

$$\int_V d^3 \mathbf{r} (v \hat{\mathbf{k}} \cdot \nabla \psi + v \Sigma_t \psi) = \int_V d^3 \mathbf{r} v s + \int_V d^3 \mathbf{r} v \hat{K} \psi \quad (2.2.7)$$

We leave $\hat{K} \psi$ in this form because \hat{K} does not mix the spatial dependence of ψ (it is not an integral operator in \mathbf{r}), so we will find its treatment very simple. Frankly, the only nontrivial

term to consider is the streaming term $\hat{\mathbf{k}} \cdot \nabla \psi$. This integral is worked through as follows. Using chain rule then Gauss' theorem, we can take:

$$\int_V d^3\mathbf{r} v \hat{\mathbf{k}} \cdot \nabla \psi = \oint_{\Gamma} dA (\hat{\mathbf{k}} \cdot \hat{\mathbf{n}}) v \psi - \int_V d^3\mathbf{r} \psi \hat{\mathbf{k}} \cdot \nabla v \quad (2.2.8)$$

where $\Gamma = \partial V$. The surface integral may be split into two utilizing the boundary condition $\bar{\psi}$. If $\hat{\mathbf{k}}$ is pointing into the volume, we can use $\psi = \bar{\psi}$, which is known. Otherwise, we can not. Now, this means we are taking, within the integrand:

$$\psi = \begin{cases} \psi, & (\mathbf{r}, \hat{\mathbf{k}}) \in \Gamma_{\uparrow} \\ \bar{\psi}, & (\mathbf{r}, \hat{\mathbf{k}}) \in \Gamma_{\downarrow} \end{cases} \quad (2.2.9)$$

Given that Γ_{\uparrow} was defined as the composite space-angular domain when $\mathbf{r} \in V$ and $\hat{\mathbf{k}} \cdot \hat{\mathbf{n}} > 0$, and then Γ_{\downarrow} is when $\hat{\mathbf{k}} \cdot \hat{\mathbf{n}} < 0$, this can be written in one line:

$$(\hat{\mathbf{k}} \cdot \hat{\mathbf{n}})\psi = \frac{1}{2}(\hat{\mathbf{k}} \cdot \hat{\mathbf{n}} + |\hat{\mathbf{k}} \cdot \hat{\mathbf{n}}|)\psi + \frac{1}{2}(\hat{\mathbf{k}} \cdot \hat{\mathbf{n}} - |\hat{\mathbf{k}} \cdot \hat{\mathbf{n}}|)\bar{\psi} \quad (2.2.10)$$

For brevity, make the definitions:

$$\varsigma_{\uparrow}(\hat{\mathbf{n}}, \hat{\mathbf{k}}) \equiv \frac{1}{2}(\hat{\mathbf{k}} \cdot \hat{\mathbf{n}} + |\hat{\mathbf{k}} \cdot \hat{\mathbf{n}}|) \quad (2.2.11)$$

$$\varsigma_{\downarrow}(\hat{\mathbf{n}}, \hat{\mathbf{k}}) \equiv \frac{1}{2}(\hat{\mathbf{k}} \cdot \hat{\mathbf{n}} - |\hat{\mathbf{k}} \cdot \hat{\mathbf{n}}|) \quad (2.2.12)$$

Now, the surface integral of the streaming term is just:

$$\oint_{\Gamma} dA (\hat{\mathbf{k}} \cdot \hat{\mathbf{n}}) v \psi = \int_{\Gamma_{\uparrow}} dA \varsigma_{\uparrow} v \psi + \int_{\Gamma_{\downarrow}} dA \varsigma_{\downarrow} v \bar{\psi} \quad (2.2.13)$$

and this is as far as we will simplify the weak form of the BTE. The final weak form is, with no approximations:

$$\begin{aligned} \int_{\Gamma_{\uparrow}} dA \varsigma_{\uparrow} v \psi + \int_{\Gamma_{\downarrow}} dA \varsigma_{\downarrow} v \bar{\psi} - \int_V d^3\mathbf{r} \psi \hat{\mathbf{k}} \cdot \nabla v + \int_V d^3\mathbf{r} v \Sigma_t \psi \\ = \int_V d^3\mathbf{r} v s + \int_V d^3\mathbf{r} v \hat{K} \psi \end{aligned} \quad (2.2.14)$$

2.2.3 Applying the FEM

Now, our problem volume can be divided into many different sub-volumes, beginning formally the inexact, FEM treatment of the problem. We'll treat the volume integral terms fully first since they're more simple. The prescription for volume integrals is simple:

$$\int_V d^3\mathbf{r} \rightarrow \sum_{e=1}^{N_E} \int_{V^e} d^3\mathbf{r} \quad (2.2.15)$$

where N_E is the number of elements into which we've divided the volume (a domain, not a scalar) V , and V^e is the volume of the element e . Consequently, we can decide on a set of

basis functions within element e , over which to determine ψ . A typical choice in the FEM is to use interpolation. The order of interpolation (i.e., linear, quadratic, etc.) depends on the elements themselves. We will only discuss linear interpolation, in which the nodes in an element all define a corner. That said, quadratic interpolation with higher order elements can offer tremendous benefits, namely, the use of fewer elements, and competitive solve times for the same accuracy [42]. Nevertheless, we say:

$$\psi(\mathbf{r}) \approx \sum_{k=1}^{N_K^e} u_k^e(\mathbf{r}) \psi_k^e, \quad \mathbf{r} \in V^e \quad (2.2.16)$$

where:

$$\psi_k^e \equiv \psi(\mathbf{r}_k^e) \quad (2.2.17)$$

and \mathbf{r}_k^e is the position of the k th node in element e . For linear interpolation, the ‘shape function’ $u_k^e(\mathbf{r})$ is linear in \mathbf{r} . These shape functions take geometric information about the element’s nodes \mathbf{r}_k^e , and give us interpolation weights, which therefore sum to 1:

$$\sum_{k=1}^{N_K^e} u_k^e(\mathbf{r}) = 1, \quad \mathbf{r} \in V^e \quad (2.2.18)$$

This also follows from considering the above as ‘interpolation of $f(\mathbf{r}) = 1$.’ These functions also satisfy:

$$u_k^e(\mathbf{r}_{k'}^e) = \delta_{kk'} \quad (2.2.19)$$

which follows from evaluating some $f(\mathbf{r})$ at $\mathbf{r}_{k'}^e$. Both of these equations are useful to verify that one is able to accurately construct shape functions. For linear interpolation in 3D, shape functions most generally come in the form:

$$u_k^e(\mathbf{r}) = A_k^e + B_k^e x + C_k^e y + D_k^e z \quad (2.2.20)$$

where the coefficients depend on all \mathbf{r}_k^e for the element e in question. Now, with this being the chosen basis function, we’ll first expand ψ in our volume integrals as:

$$\int_V d^3\mathbf{r} v(\mathbf{r}) \hat{O} \psi(\mathbf{r}) = \sum_{e=1}^{N_E} \sum_{k'=1}^{N_K^e} \psi_{k'}^e \int_V d^3\mathbf{r} v(\mathbf{r}) \hat{O} u_{k'}^e(\mathbf{r}) \quad (2.2.21)$$

where \hat{O} is an arbitrary operator which only does as much as multiply in \mathbf{r} . This treats all but the surface integral terms in our weak form.

The surface integrals are a bit more complicated. Stokes’ theorem allows the surface integral over Γ to be broken into a series of surface integrals over every internal element face. Now, however, we must decide how to speak about element faces. We will later want to index element faces on a local basis (i.e., each element has its own face indexing system, $f = 1, 2, \dots, N_F^e$). Right now we will just define any face within the mesh by stating the two elements which share the face, as in (e, e') . In that case, we take:

$$\oint_{\Gamma} dA \rightarrow \sum_{e=1}^{N_E} \sum_{e'} \int_{\Gamma^{ee'}} dA \quad (2.2.22)$$

where $\Gamma^{ee'}$ is the face shared by elements e and e' . The sum over e' is not stated as running from 1 to N_E , because the element e has only N_F^e faces, and no more than that many pairs (e, e') exist. However, Stokes' theorem would necessitate that one considers (e, e') and (e', e) as distinct faces in this sum, and indeed the two faces are distinct insofar as they have different normal vectors (up to a sign).

Now that these surface integrals run over the elements themselves, the ‘boundary condition’ $\bar{\psi}$ for a given element is the value of ψ in the neighboring element, which will only ever be referenced on the shared face of course. Thus, we’d expand ψ in the $\Gamma_{\downarrow}^{ee'}$ term not as $\psi_{k'}^e$ but as $\psi_{k'}^{e'}$. But, you may suggest that ψ_k^e should have the same value as $\psi_{k'}^{e'}$ if $\mathbf{r}_k^e = \mathbf{r}_{k'}^{e'}$. This is simply not the case in the DFEM [17], because we are using a different subspace to expand ψ in each element. The problem being formulated is not a problem that describes transfer between nodes of a mesh, but rather, one that describes transfer between two elements, and then between the nodes in these two elements. Typically, only at the end of a solution would one assign to ‘global’ mesh nodes a single value of ψ , for instance by taking the average across all elemental nodes that coincide at that global mesh node. Conversely, volume integrated-quantities may be the primary goal of the solution, for which the elemental solutions ψ_k^e are indeed more appropriate. Nevertheless, the Γ_{\downarrow} integrand is only nonzero when $\hat{\mathbf{k}}$ is incident upon the volume, thus, a $\Gamma_{\downarrow}^{ee'}$ integrand is similarly only nonzero when $\hat{\mathbf{k}}$ is incident on the face (e, e') from the perspective of e . This is also enforced by the presence of $\varsigma_{\downarrow}^{ee'}$, so there is no need to reiterate that integration occurs only over $\Gamma_{\uparrow}^{ee'}$ or $\Gamma_{\downarrow}^{ee'}$. Physically, this means we are allowing fluence from e' to propagate into e when e' is ‘upstream’ of e for the given $\hat{\mathbf{k}}$, and we are allowed fluence from e to propagate into e' when e' is ‘downstream’ of e . The whole area integral is thus:

$$\oint_{\Gamma} dA (\hat{\mathbf{k}} \cdot \hat{\mathbf{n}}) v \psi = \sum_{e=1}^{N_E} \sum_{e'=1}^{N_F^e} \sum_{k'=1}^{N_K} \left(\begin{array}{l} \psi_{k'}^e \int_{\Gamma^{ee'}} dA \varsigma_{\uparrow}^{ee'} u_{k'}^e v \\ + \psi_{k'}^{e'} \int_{\Gamma^{ee'}} dA \varsigma_{\downarrow}^{ee'} u_{k'}^{e'} v \end{array} \right) \quad (2.2.23)$$

If e lies on the boundary of V , then although there is no meaning to e' , the faces must still be accounted for. In this case, we do just use the boundary condition, $\psi_{k'}^{e'} = \bar{\psi}(\mathbf{r}_{k'}^e)$. That is, use the boundary condition evaluated at the physical point $\mathbf{r}_{k'}^e$. We will make more precise the e' sum used here shortly, for now it just says to sum over all faces (including boundary faces).

Now, we have expanded ψ and transformed our integrals to the mesh. If we write out our discretized weak form, we find a persistent sum over e on both sides of the equation. This sum can be thrown off while maintaining equality, meaning that we have a system of N_E equations to this point. We find:

$$\begin{aligned} & \sum_{k'=1}^{N_K} \left(\sum_{e'} \varsigma_{\uparrow}^{ee'} \int_{\Gamma^{ee'}} dA u_{k'}^e v - \int_{V^e} d^3 \mathbf{r} u_{k'}^e \hat{\mathbf{k}} \cdot \nabla v + \sum_t^e \int_{V^e} d^3 \mathbf{r} u_{k'}^e v \right) \psi_{k'}^e \\ &= \sum_{k'=1}^{N_K} \left(\int_{V^e} d^3 \mathbf{r} u_{k'}^e v \right) \int d\Omega' \sum_s^e \psi_{k'}^e - \sum_{k'=1}^{N_K} \sum_{e'} \left(\varsigma_{\downarrow}^{ee'} \int_{\Gamma^{ee'}} dA u_{k'}^{e'} v \right) \psi_{k'}^{e'} \\ & \quad + \int_{V^e} d^3 \mathbf{r} v s \end{aligned} \quad (2.2.24)$$

Importantly, note again that we are using first-order elements, so normal vectors $\hat{\mathbf{n}}$ are constant over the faces of an element, and the $\varsigma^{ee'}$ factors are constant and were removed from spatial integration.

The last step is to limit the space of test functions v in a given element. Rather than search for a solution to the equation above over every possible function v , for a given element one searches for a solution which satisfies the discretized weak form in a subspace that is relevant to that element, namely, the subspace formed by shape functions. This means we take $v = u_k^e$, and impose that the weak form is satisfied for every k in an element e , finally forming a matrix problem. Thus, the use of a mesh not only discretizes the problem, but also allows one to avoid the use of a global test function subspace. To write the full result of this section, let's define the various shape function integrals that we appear to need:

$$I_{1,kk'}^e \equiv \int_{V^e} d^3\mathbf{r} u_{k'}^e u_k^e \quad (2.2.25)$$

$$I_{2\uparrow,kk'}^{ee'} \equiv \int_{\Gamma^{ee'}} dA u_{k'}^e u_k^e \quad (2.2.26)$$

$$I_{2\downarrow,kk'}^{ee'} \equiv \int_{\Gamma^{ee'}} dA u_{k'}^e u_k^e \quad (2.2.27)$$

$$\mathbf{I}_{3,kk'}^e \equiv \int_{V^e} d^3\mathbf{r} u_{k'}^e \nabla u_k^e \quad (2.2.28)$$

With these definitions, the problem can be written a lot more succinctly:

$$\sum_{k'=1}^{N_K^e} \left(-\hat{\mathbf{k}} \cdot \mathbf{I}_{3,kk'}^e + \sum_{e'} \varsigma_{\uparrow}^{ee'} I_{2\uparrow,kk'}^{ee'} + \Sigma_t^e I_{1,kk'}^e \right) \psi_{k'}^e = \int_{V^e} d^3\mathbf{r} u_{k'}^e s + \sum_{k'=1}^{N_K^e} I_{1,kk'}^e \int d\Omega' \Sigma_s^e \psi_{k'}^e - \sum_{k'=1}^{N_K^e} \sum_{e'} \varsigma_{\downarrow}^{ee'} I_{2\downarrow,kk'}^{ee'} \psi_{k'}^{e'} \quad (2.2.29)$$

Now, the integral $I_{1,kk'}^e$ is rather persistent, and it our preference to explicitly invert it on both sides before proceeding. Noting that the units of $I_{1,kk'}^e$ are volume, a factor introduced during creation of the weak form, with this inversion, the matrices multiplying ψ_k^e once again have units of inverse length, and more importantly, the matrix responsible for scattering will not have any dependence on the node, only the element. The integral operators, with $(I_1^e)^{-1}$ applied, will be designated by the same symbols, except with a prime next to their numbering. Now, borrowing notation from [42], we will define:

$$G_{kk'}^e \equiv -\hat{\mathbf{k}} \cdot \mathbf{I}_{3',kk'}^e \quad (2.2.30)$$

$$F_{\uparrow,kk'}^e \equiv \sum_{e'} \varsigma_{\uparrow}^{ee'} I_{2'\uparrow,kk'}^{ee'} \quad (2.2.31)$$

$$F_{\downarrow,kk'}^{ee'} \equiv \varsigma_{\downarrow}^{ee'} I_{2'\downarrow,kk'}^{ee'} \quad (2.2.32)$$

$$M_{kk'}^e \equiv \Sigma_t^e \delta_{kk'} \quad (2.2.33)$$

It is also worth noting that all but the last of these matrix elements are continuous functions of $\hat{\mathbf{k}}$ at this stage.

Now, we should briefly discuss in more depth the sources, boundary conditions, and the integrals of $u_k^e s$. We discussed earlier the form of s for external beam sources. One may rightfully wonder whether $\int_{V^e} d^3\mathbf{r} u_k^e s = 0$ since s is in the form of a delta function localized outside of V . Indeed, this is the case, however, that is because our problem uses as its ‘source’ the terms in the sum of $F_{\downarrow, kk'}^{ee'} \psi_{k'}^{e'}$ over boundary faces, which we noted use the boundary condition $\psi_{k'}^{e'} = \bar{\psi}_{k'}^{e'}$. That is, we can separate from the F_{\downarrow} term all terms of the sum which go over boundary faces. Note that, as we mentioned earlier, these terms have no corresponding e' , and in this sense, the sum $\sum_{e'}$ is more of an abbreviated notation. A local face indexing system will soon be introduced, but in the meantime, we can write the source term that is left out of $\sum_{e'}$ as:

$$s_k^{\Gamma, e} \equiv - \sum_{k'=1}^{N_K^e} \sum_{f \in \Gamma} F_{\downarrow, kk'}^{ef} \bar{\psi}_{k'}^e \quad (2.2.34)$$

where $\sum_{f \in \Gamma}$ means that we sum over the faces that have no neighbor, i.e., there is no valid (e, e') pair. We will see shortly how $F_{\downarrow, kk'}^{ef}$ is formed for the above to hold. Now, $s_k^{\Gamma, e} \neq 0$ only for elements (and we will see soon, nodes) that are on the very boundary of the problem.

That said, we also discussed the FCS method, for which s is replaced symbolically by \tilde{s} that is a continuous function over the entire volume V . In this case of course, $\bar{\psi} = 0$, but the integrals $\int_{V^e} d^3\mathbf{r} u_k^e \tilde{s}$ can now be formed and are generally nonzero, because FCS converts an external beam problem to an internal source problem. So, can we now expand \tilde{s} in terms of u_k^e and form a matrix multiplication with I_1^e (which is subsequently inverted)? The expansion of \tilde{s} in terms of u_k^e is only acceptable if \tilde{s} varies linearly in the element in question. We saw that the spatial dependence of \tilde{s} is essentially that of $\tilde{\varphi}^0$. We know that $\tilde{\varphi}^0$ is related to the exponential of the optical path length from an external beam source to the point \mathbf{r} . So given that the mean free path of electrons in typical materials [29] is typically on the order of microns to nanometers, much smaller than the scale typical radiotherapy problems, the elements used do not generally satisfy linear expansion of \tilde{s} , and significant errors will be introduced. For electrons, to approximate $\tilde{\varphi}^0$ as being linear with depth, we would need to have an extremely refined mesh towards the surface of our volume that is facing the beam. Importantly, that is not to say that linearity is not a good approximation for $\tilde{\psi}$ in macroscopic elements, because $\tilde{\psi}$ corresponds to electrons which have scattered arbitrarily many times, generally smoothing out the population of electrons over a somewhat larger scale. So, the solution is to perform the integrals we reference in a more sophisticated manner, rather than using an expansion of $\tilde{\varphi}^0$. That is to say, we will take the most un-simplified expression of \tilde{s}_k^e :

$$\tilde{s}_k^e \equiv \sum_{k'=1}^{N_K^e} (I_1^{-1})_{kk'}^e \int_{V^e} d^3\mathbf{r} u_{k'}^e(\mathbf{r}) \tilde{s}(\mathbf{r}) \quad (2.2.35)$$

In principle, $\tilde{s}(\mathbf{r})$ is indeed able to be determined at any point in the volume, because we need only to determine $\tilde{\varphi}^0$ at some given point in the volume. The form of $\tilde{\varphi}^0(\mathbf{r})$ is, as we discussed in Section 1.4, able to be determined for any choice of \mathbf{r} . So, rather than expand \tilde{s} , we will want to discuss the case and methodology wherein one must evaluate this integral

numerically. This will be discussed in Section 3.2.2. Additionally, this is only a relevant note for massive charged particles, such as electrons, rather than photons. In the case of photons, one can generally safely take $\tilde{s}_k^e = \tilde{s}(\mathbf{r}_k^e)$, provided that the elements in question are on the order of 1 cm in size, a typical mean free path [56], and not dramatically larger.

Now, the final form of the spatially discretized monoenergetic BTE is:

$$\sum_{k'=1}^{N_K^e} \left(G_{kk'}^e + M_{kk'}^e + F_{\uparrow, kk'}^e \right) \psi_{k'}^e + \sum_{k'=1}^{N_K^e} \sum_{e'} F_{\downarrow, kk'}^{ee'} \psi_{k'}^{e'} = s_k^e + \int d\Omega' \Sigma_s^e \psi_k^e \quad (2.2.36)$$

where s_k^e is either \tilde{s}_k^e (for a continuous source such as \tilde{s}) or $s_k^{\Gamma, e}$ (for an external beam source), and the sum over e' on the LHS does not (as it can not) run over faces on the boundary of the volume. Importantly, this equation describes a matrix problem not just in (k, k') (i.e., two nodes of the same element), but also in (e, e') . Thus, it can be considered a block-matrix problem, where (e, e') indexes blocks and (k, k') indexes elements within a block. Since all interior elements only share N_F^e faces with their neighbors, the row e (if it describes an interior element) will only have at most $N_F^e + 1$ nonzero blocks, where N_F^e are due to off-diagonal blocks (only $F_{\downarrow, kk'}^{ee'}$ has these) and 1 is due to diagonal terms. In Figure 1, we show a real 16 element mesh that was created by hand, then in Figure 2, we show the structure of the resulting finite element method matrix problem. Note that, without angular discretization, this ‘matrix problem’ still involves functions and operators of $\hat{\mathbf{k}}$. These are to be resolved shortly, and in the case of S_N [42] (but actually not P_N [34], to be discussed in this document on a later update), this will eliminate many of the off-diagonal (e, e') elements in $L_{kk'}^{ee'}$. It is worth noting that this system matrix will generally be very large, since the number of its entries (including zeros) scales as $N_E \times N_E$.

One may suspect, or suggest, that because so many elemental nodes \mathbf{r}_k^e correspond to the same physical point, the problem’s size can somehow be truncated to only as many nodes as are in the mesh, say N_K , but this is not meaningful in the DFEM [17]. The problem formulated thus far is indeed of shape $(N_E N_K^e) \times (N_E N_K^e)$, not $N_K \times N_K$.

2.2.4 Evaluation of spatial integrals for tetrahedra

We can now discuss solutions of the integrals $I_{1, kk'}^e$, $I_{2\uparrow, kk'}^e$, $I_{2\downarrow, kk'}^{ee'}$, and $\mathbf{I}_{3, kk'}^e$ put explicitly in terms of \mathbf{r}_k^e . Part of this discussion closely follows [2]. We restate each integral here:

$$I_{1, kk'}^e = \int_{V^e} d^3 \mathbf{r} u_{k'}^e u_k^e \quad (2.2.37)$$

$$I_{2\uparrow, kk'}^{ee'} = \int_{\Gamma^{ee'}} dA u_{k'}^e u_k^e \quad (2.2.38)$$

$$I_{2\downarrow, kk'}^{ee'} = \int_{\Gamma^{ee'}} dA u_{k'}^{e'} u_k^e \quad (2.2.39)$$

$$\mathbf{I}_{3, kk'}^e = \int_{V^e} d^3 \mathbf{r} u_{k'}^e \nabla u_k^e \quad (2.2.40)$$

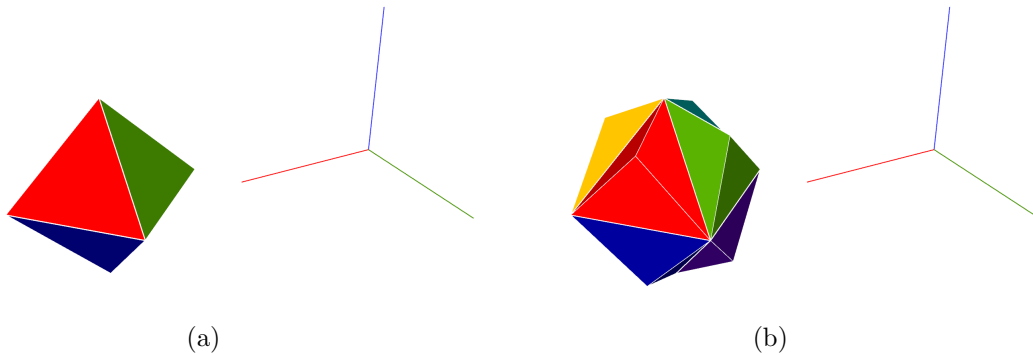


Figure 1: Axis shown in RGB. (a) The inner shell of the mesh, which is eight tetrahedra color-coded for distinction. (b) The outer shell of the mesh, which is eight tetrahedra and color-coded.

Figure 2: A hypothetical problem structure for the mesh in Figure 1. Each (block) matrix entry corresponds to a $N_K^e \times N_K^e$ matrix, potentially with operators such as $\int dE d\Omega$, while each vector entry corresponds to a column vector of length 4. This is a highly nontrivial problem due to its size. A discussion on how it is approached is relegated to Section 2.4.2 once angular discretization is complete.

Rather than work out expressions which are valid for arbitrary linear elements, which are generally difficult because of the expression of arbitrary 3D integrals, we will take tetrahedra as a simple example case that demonstrates how these integrals can be approached. The number of nodes in a tetrahedron are $N_K^e = 4$, and the number of faces are $N_F^e = 4$. The shape functions for tetrahedral elements are given as [2]:

$$u_k^e(\mathbf{r}) = \frac{1}{6\tau^e}(a_k^e + b_k^e x + c_k^e y + d_k^e z) \quad (2.2.41)$$

where:

$$\tau^e = \frac{1}{6} \det S^e \quad (2.2.42)$$

is simply the volume of the element, and:

$$a_k^e = \text{cofactor}(S^e)_{k1} \quad (2.2.43)$$

$$b_k^e = \text{cofactor}(S^e)_{k2} \quad (2.2.44)$$

$$c_k^e = \text{cofactor}(S^e)_{k3} \quad (2.2.45)$$

$$d_k^e = \text{cofactor}(S^e)_{k4} \quad (2.2.46)$$

while the matrix S^e is:

$$S^e \equiv \begin{pmatrix} 1 & x_1^e & y_1^e & z_1^e \\ 1 & x_2^e & y_2^e & z_2^e \\ 1 & x_3^e & y_3^e & z_3^e \\ 1 & x_4^e & y_4^e & z_4^e \end{pmatrix} \quad (2.2.47)$$

We will conventionally define a vector containing the last three coefficients in the shape function, as:

$$\mathbf{b}_k^e \equiv (b_k^e, c_k^e, d_k^e) \quad (2.2.48)$$

and so it could be said:

$$u_k^e(\mathbf{r}) = \frac{1}{6\tau^e}(a_k^e + \mathbf{b}_k^e \cdot \mathbf{r}) \quad (2.2.49)$$

One way to work with these integrals is, for a given element, to transform the coordinate system to one in which the integral becomes easier to solve [2, 42]. This method is used for various types of elements, regardless of order [42]. With a first-order tetrahedron, we transform an element to a ‘linear tetrahedron.’ This is depicted in Figure 3. A linear tetrahedron always has the structure in Table 3, while its shape functions are consequently:

$$u_1(\mathbf{r}') = 1 - x' - y' - z' \quad (2.2.50)$$

$$u_2(\mathbf{r}') = x' \quad (2.2.51)$$

$$u_3(\mathbf{r}') = y' \quad (2.2.52)$$

$$u_4(\mathbf{r}') = z' \quad (2.2.53)$$

These are used to write the coordinate transformations. We can exactly expand, say, $x(\mathbf{r}')$ in terms of these shape functions, giving:

$$x(\mathbf{r}') = \sum_{k=1}^{N_K^e} x_k^e u_k(\mathbf{r}') \quad (2.2.54)$$

Table 3: The coordinates for the k th node of a linear tetrahedron.

k	x'_k	y'_k	z'_k
1	0	0	0
2	1	0	0
3	0	1	0
4	0	0	1

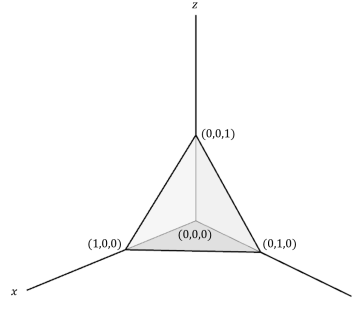


Figure 3: Linear tetrahedron.

and likewise for y and z . This expansion is valid within the element e only. One then converts an integral in \mathbf{r} to one in \mathbf{r}' using the Jacobian:

$$J^e(\mathbf{r}') = \begin{pmatrix} \partial x / \partial x' & \partial y / \partial x' & \partial z / \partial x' \\ \partial x / \partial y' & \partial y / \partial y' & \partial z / \partial y' \\ \partial x / \partial z' & \partial y / \partial z' & \partial z / \partial z' \end{pmatrix} \quad (2.2.55)$$

with x , y , and z expressed in e . Generally, one major utility of the Jacobian is that:

$$\int_{V^e} d^3\mathbf{r} f(\mathbf{r}) = \int_{V^e} d^3\mathbf{r}' \det [J^e(\mathbf{r}')] f[\mathbf{r}(\mathbf{r}')] \quad (2.2.56)$$

Of course, this holds for a general coordinate transformation, but ours is affine (all derivatives are constant), so we know $\det J^e$ is constant and can be removed from integration. As a matter of fact, one can quite easily derive the precise value $\det J^e$ should take. Suppose we examined $f(\mathbf{r}) = 1$:

$$\int_{V^e} d^3\mathbf{r} = \det J^e \int_{V^e} d^3\mathbf{r}' \quad (2.2.57)$$

Since the volume of a linear tetrahedron is $1/6$:

$$\det J^e = 6\tau^e \quad (2.2.58)$$

which is fundamentally a statement of what J^e geometrically means. Thus, we will eliminate all use of $\det J^e$, preferring to use $6\tau^e$. Finally note that, for a linear tetrahedron:

$$\int_{V^e} d^3\mathbf{r}' f(\mathbf{r}') = \int_0^1 dx' \int_0^{1-x'} dy \int_0^{1-x'-y'} dz' f(\mathbf{r}') \quad (2.2.59)$$

Now, the first integral, which is just an overlap integral for the basis of the element e , is:

$$I_{1,kk'}^e = 6\tau^e \int_{V^e} d^3\mathbf{r}' u_k(\mathbf{r}') u_{k'}(\mathbf{r}') \quad (2.2.60)$$

and then:

$$\int_{V^e} d^3\mathbf{r}' u_k(\mathbf{r}') u_{k'}(\mathbf{r}') = \int_0^1 dx' \int_0^{1-x'} dy' \int_0^{1-x'-y'} dz' u_k(\mathbf{r}') u_{k'}(\mathbf{r}') \quad (2.2.61)$$

This integration is easily carried out for any combination of (k, k') . The final result is:

$$I_{1,kk'}^e = \frac{1}{20} \tau^e (1 + \delta_{kk'}) \quad (2.2.62)$$

From here we can show:

$$(I_1^{-1})_{kk'}^e = \frac{4}{\tau^e} (-1 + 5\delta_{kk'}) \quad (2.2.63)$$

Next, we'll deal with $I_{2\uparrow,kk'}^{ee'}$. This is an overlap integral exclusively over a single face. Here, we will begin to adopt the convention that faces are labelled by (e, f) , where f is an index of the faces belonging to e , instead of describing a face by the two elements which share it, (e, e') . We could then say that we can determine e' by specifying e and f , i.e., $e' = e'(e, f)$. We could also determine the face's index in e' , i.e., $f' = f'(e, f)$. The meaning of these maps is simple: $e'(e, f)$ says that if you pick an element e , and a face within that element f , then $e'(e, f)$ is the element sharing that face. Then, $f'(e, f)$ is the index of this face within e' . This leads to a useful identity:

$$e'[e'(e, f), f'(e, f)] = e \quad (2.2.64)$$

$$f'[e'(e, f), f'(e, f)] = f \quad (2.2.65)$$

For a surface integral, our coordinate transformation takes a slightly different form. Namely, rather than transform to a linear tetrahedron, we will consider transformations to map a given face to a simple unit right triangle. Our coordinates will be x' and y' . Now, we can do this because, if shape functions are evaluated on $\mathbf{r} \in \Gamma^{ef}$, then the shape function for the node which is not on the face will be zero entirely (in a tetrahedron, only one node lies outside of a given face). Before proceeding, let's define face indices with respect to node indices. Let the face f be the one which contains all nodes except node f , i.e., the face opposite to node f . Our integrals will obey the transformation relationship:

$$\int_{\Gamma^{ef}} dA = \int_{\Gamma^{ef}} dx' dy' |\mathbf{J}_{s,f}^e(\mathbf{r}')| \quad (2.2.66)$$

where $\mathbf{J}_{s,f}^e(\mathbf{r}')$ is the surface Jacobian, a vector given by:

$$\mathbf{J}_{s,f}^e = \left(\frac{\partial x}{\partial x'}, \frac{\partial y}{\partial x'}, \frac{\partial z}{\partial x'} \right) \times \left(\frac{\partial x}{\partial y'}, \frac{\partial y}{\partial y'}, \frac{\partial z}{\partial y'} \right) \quad (2.2.67)$$

which is useful when working with nonlinear shape functions. However, we can forego this technical description. With linear shape functions, the derivatives featured in (2.2.67) come out to be constant again. Then:

$$\int_{\Gamma^{ef}} dA = |\mathbf{J}_{s,f}^e| \int_{\Gamma'^{ef}} dx' dy' \quad (2.2.68)$$

On the LHS, we have the area of a face f in element e . On the RHS, we have the magnitude of the surface Jacobian multiplied by the area of our unit right triangle, which is just $1/2$. Therefore:

$$|\mathbf{J}_{s,f}^e| = 2A_f^e \quad (2.2.69)$$

A simple formula for the areas, which can be supplied by knowledge of the mesh, is Heron's formula, which gives the area of a tetrahedral face based solely on its side lengths:

$$A = \sqrt{s(s - \alpha)(s - \beta)(s - \gamma)} \quad (2.2.70)$$

where α , β , and γ describe the side lengths of the tetrahedral face, and:

$$s = \frac{1}{2}(\alpha + \beta + \gamma) \quad (2.2.71)$$

Using our convention for naming faces, we would have:

$$\alpha_f^e = |\mathbf{r}_{k'}^e - \mathbf{r}_{k''}^e| \quad (2.2.72)$$

$$\beta_f^e = |\mathbf{r}_{k'}^e - \mathbf{r}_{k'''}^e| \quad (2.2.73)$$

$$\gamma_f^e = |\mathbf{r}_{k''}^e - \mathbf{r}_{k'''}^e| \quad (2.2.74)$$

Where $k', k'', k''' \neq f$. We can then proceed to perform integration. The shape functions are the same as for the linear tetrahedron, but $z' = 0$, and we eliminate $u_4(\mathbf{r}')$ entirely. Working it through yields an answer that is intuitive in form:

$$I_{2\uparrow, kk'}^{ef} = \frac{1}{12} A_f^e (1 - \delta_{kf})(1 - \delta_{k'f})(1 + \delta_{kk'}) \quad (2.2.75)$$

Specifically, we see that if the face f does not contain either the node k or k' (i.e., if $f = k$ or if $f = k'$), then the entire integral is zero. If $k = k'$, the integral is doubled.

We use this form to write the next integral, $I_{2\downarrow, kk'}^{ef}$. If the node k , which is in element e , refers to a node not on the face f (i.e., $k = f$), then the integral should be zero. Similarly, if the node k' , which is in element $e'(e, f)$, refers to a node not on the face $f'(e, f)$ (i.e., $k' = f'(e, f)$), then again the integral should be zero. Lastly, if the nodes k and k' refer to the same physical node, then the integral should double, as it does above. Let's say we have some node, \mathbf{r}_k^e . The element neighboring e on f is $e'(e, f)$. We define $k'(e, f, k)$ as the address of node $\mathbf{r}_{k'}^{e'(e,f)} = \mathbf{r}_k^e$, i.e., k' in the neighboring element e' (which shares face f with e) refers to the same physical node as k in the original element e . Now, if $k' = k'(e, f, k)$, then in fact we are referring to transport between the same physical node across two elements, and the integral above doubles. We finally have:

$$I_{2\downarrow, kk'}^{ef} = \begin{cases} I_{2\uparrow, kk'}^{ef}, & (e, f) \text{ on bdy} \\ \frac{1}{12} A_f^e (1 - \delta_{kf})(1 - \delta_{k'f})(1 + \delta_{kk'})[1 + \delta_{k'k'(e,f,k)}], & \text{else} \end{cases} \quad (2.2.76)$$

where we use $I_{2\downarrow, kk'}^{ef} = I_{2\uparrow, kk'}^{ef}$ on boundary faces because these faces will be supplied by the boundary condition $\bar{\psi}(\mathbf{r}_k^e)$, essentially taking a virtual element to be the neighbor that has the same node indexing on the face (e, f) . This way, the construction of a term like $s_k^{\Gamma, e}$ from $F_{\downarrow, kk'}^{ef}$ is fully defined and rigorous.

We lastly treat $\mathbf{I}_{3, kk'}^e$. We need not perform a coordinate transformation here. That is because, if $u_k^e = (1/6\tau^e)(a_k^e + \mathbf{b}_k^e \cdot \mathbf{r})$, then $\nabla u_k^e = (1/6\tau^e)\mathbf{b}_k^e$, which can be removed from integration as it does not involve \mathbf{r} . Now we are treating:

$$\mathbf{I}_{3, kk'}^e = \frac{1}{6\tau^e} \mathbf{b}_k^e \int_{V^e} d^3 \mathbf{r} u_{k'}^e(\mathbf{r}) \quad (2.2.77)$$

The above integral can be performed without a transformation. The a_k^e term is simple, then:

$$\frac{1}{6\tau^e} \mathbf{b}_k^e \cdot \int_{V^e} d^3 \mathbf{r} \mathbf{r} = \frac{1}{6} \mathbf{b}_k^e \cdot \left(\frac{1}{\tau^e} \int_{V^e} d^3 \mathbf{r} \mathbf{r} \right) \quad (2.2.78)$$

The quantity in parenthesis on the RHS is the center of gravity of the given element, which for linear elements is just the sum of nodes normalized by the number of nodes. Thus:

$$\frac{1}{6\tau^e} \mathbf{b}_k^e \cdot \int_{V^e} d^3 \mathbf{r} \mathbf{r} = \frac{1}{6N_K^e} \mathbf{b}_k^e \cdot \sum_{k''=1}^{N_K^e} \mathbf{r}_{k''}^e \quad (2.2.79)$$

When we combine this with the a_k^e term:

$$\int_{V^e} d^3 \mathbf{r} u_{k''}^e(\mathbf{r}) = \frac{1}{6N_K^e} \left(N_K^e a_k^e + \mathbf{b}_k^e \cdot \sum_{k''=1}^{N_K^e} \mathbf{r}_{k''}^e \right) = \frac{1}{6N_K^e} \sum_{k''=1}^{N_K^e} \left(a_k^e + \mathbf{b}_k^e \cdot \mathbf{r}_{k''}^e \right) \quad (2.2.80)$$

The quantity in parenthesis on the RHS is just $6\tau^e u_k^e(\mathbf{r}_{k''}^e)$, and we know is $u_k^e(\mathbf{r}_{k''}^e) = \delta_{kk''}$. Thus:

$$\int_{V^e} d^3 \mathbf{r} u_{k'}^e(\mathbf{r}) = \frac{\tau^e}{N_K^e} \quad (2.2.81)$$

and finally, for tetrahedra:

$$\mathbf{I}_{3, kk'}^e = \frac{1}{24} \mathbf{b}_k^e \quad (2.2.82)$$

which generalizes to an arbitrary linear finite element with multiplication by $4/N_K^e$ an expression of u_k^e as per $(1/6\tau^e)(a_k^e + \mathbf{b}_k^e \cdot \mathbf{r})$, which can always be done.

2.3 PN scattering

A major difficulty in solving the Boltzmann transport equation is the presence of angular integral operators, particularly the scattering operators. This is typically simplified by expanding the quantities in the integrand, namely ψ and Σ_s , in moments of (real or complex) spherical harmonics and Legendre polynomials, respectively. These expansions will constitute the ‘ P_N scattering’ treatment, which is frequently taken regardless of the angular

discretization of the rest of the BTE [2, 19, 30, 34]. Taken alone, these moments re-cast the BTE scattering operator in a useful form which is exact until truncation of infinite sums.

To begin, it is necessary we outline the conventions we will be using, which are not always consistent among the literature. First, our unit vectors $\hat{\mathbf{k}}$ are given in spherical coordinates as:

$$\hat{\mathbf{k}}(\mu, \phi) = \sqrt{1 - \mu^2} \cos \phi \hat{\mathbf{x}} + \sqrt{1 - \mu^2} \sin \phi \hat{\mathbf{y}} + \mu \hat{\mathbf{z}} \quad (2.3.1)$$

where $\mu \equiv \cos \theta = k_z$ is the ‘polar angle cosine,’ and ϕ is the azimuth of $\hat{\mathbf{k}}$. The spherical harmonic of degree ℓ and order m , Y_ℓ^m , will be given as [57]:

$$Y_\ell^m(\hat{\mathbf{k}}) = \sqrt{\frac{(2\ell + 1)}{4\pi} \frac{(\ell - m)!}{(\ell + m)!}} P_\ell^m(\mu) e^{im\phi} \quad (2.3.2)$$

where the Condon-Shortley phase is included in the associated Legendre polynomial $P_\ell^m(\mu)$, which is given by:

$$P_\ell^m(\mu) = (-1)^m (1 - \mu^2)^{m/2} \frac{d^m}{d\mu^m} P_\ell(\mu) \quad (2.3.3)$$

and finally $P_\ell(\mu)$ is a Legendre polynomial, given by:

$$P_\ell(\mu) = \frac{1}{2^\ell \ell!} \frac{d^\ell}{d\mu^\ell} [(\mu^2 - 1)^\ell] = P_\ell^0(\mu) \quad (2.3.4)$$

Now, we are using complex spherical harmonics, but it is worth noting that the utility of the real spherical harmonics in the context of the BTE is evident primarily in the P_N discretization method [19, 34]. In the S_N discretization method, the expansions we make with complex spherical harmonics will conveniently collapse, foregoing the use of any complex numbers and becoming identical whether they were made with real or complex spherical harmonics. Specifically, both the real and complex forms of the spherical harmonics obey the following important identities [57]:

$$\int_{4\pi} d\Omega Y_\ell^{m*}(\theta, \phi) Y_{\ell'}^{m'}(\theta, \phi) = \delta_{\ell\ell'} \delta_{mm'} \quad (2.3.5)$$

$$P_\ell(\hat{\mathbf{k}} \cdot \hat{\mathbf{k}}') = \frac{4\pi}{2\ell + 1} \sum_{m=-\ell}^{\ell} Y_\ell^m(\hat{\mathbf{k}}) Y_\ell^{m*}(\hat{\mathbf{k}}') \quad (2.3.6)$$

$$\int d\Omega' Y_\ell^m(\hat{\mathbf{k}}') P_{\ell'}(\hat{\mathbf{k}} \cdot \hat{\mathbf{k}}') = \frac{4\pi}{2\ell + 1} Y_\ell^m(\theta, \phi) \delta_{\ell\ell'} \quad (2.3.7)$$

$$\sum_{\ell=0}^{\infty} \frac{2\ell + 1}{2} P_\ell(\mu) P_\ell(\mu') = \delta(\mu - \mu') \quad (2.3.8)$$

$$\delta^2(\hat{\mathbf{k}} - \hat{\mathbf{k}}') = \sum_{\ell=0}^{\infty} \sum_{m=-\ell}^{\ell} Y_\ell^m(\hat{\mathbf{k}}) Y_\ell^{m*}(\hat{\mathbf{k}}') = \frac{1}{2\pi} \delta(\hat{\mathbf{k}} \cdot \hat{\mathbf{k}}' - 1) \quad (2.3.9)$$

$$\sum_{m=-\ell}^{\ell} Y_{\ell}^m(\hat{\mathbf{k}}) Y_{\ell}^{m*}(\hat{\mathbf{k}}') = \frac{2\ell+1}{4\pi} \times \\ \left[2 \sum_{m=0}^{\ell} \frac{(\ell-m)!}{(\ell+m)!} P_{\ell}^m(\mu) P_{\ell}^m(\mu') \cos(m(\phi - \phi')) - P_{\ell}(\mu) P_{\ell}(\mu') \right] \quad (2.3.10)$$

Now, the first of these identities allows us to expand a function on the unit sphere $f(\hat{\mathbf{k}})$ like:

$$f(\hat{\mathbf{k}}) = \sum_{\ell=0}^{\infty} \sum_{m=-\ell}^{\ell} f_{\ell}^m Y_{\ell}^m(\hat{\mathbf{k}}) \quad (2.3.11)$$

which is synonymous with:

$$f_{\ell}^m = \int d\Omega' f(\hat{\mathbf{k}}') Y_{\ell}^{m*}(\hat{\mathbf{k}}) \quad (2.3.12)$$

The Legendre polynomials themselves will be interesting as well. They happen to obey [58]:

$$\int_{-1}^1 d\mu P_{\ell}(\mu) P_{\ell'}(\mu) = \frac{2}{2\ell+1} \delta_{\ell\ell'} \quad (2.3.13)$$

Since Legendre polynomials are, by definition, not normalized (rather, they are defined to obey $P_{\ell}(1) = 1$), there is more than one convention for expansion of a function $g(\mu)$. We use the following convention:

$$g(\mu) = \sum_{\ell=0}^{\infty} \frac{2\ell+1}{4\pi} g_{\ell} P_{\ell}(\mu) \quad (2.3.14)$$

which then implies:

$$g_{\ell} = 2\pi \int_{-1}^1 d\mu g(\mu) P_{\ell}(\mu) \quad (2.3.15)$$

Other conventions move around factors of 2π as well as $(2\ell+1)/2$, but these of course only affect the ℓ -by- ℓ expression of the moments g_{ℓ} .

With these expansions, as well as identity (2.3.7), it can be shown that:

$$\hat{K}\psi = \sum_{\ell=0}^{\infty} \sum_{m=-\ell}^{\ell} Y_{\ell}^m(\theta, \phi) \Sigma_{s,\ell}(\mathbf{r}) \psi_{\ell}^m(\mathbf{r}) \quad (2.3.16)$$

Thus far, there is no approximation. However, to make this computationally useful, one must truncate the ℓ sum to a finite degree, which we will write as L . That is:

$$\hat{K}\psi \approx \sum_{\ell=0}^L \sum_{m=-\ell}^{\ell} Y_{\ell}^m(\theta, \phi) \Sigma_{s,\ell}(\mathbf{r}) \psi_{\ell}^m(\mathbf{r}) \quad (2.3.17)$$

which we take as an equality moving forward. There is a good rationale for choosing L : It can be reasoned that a highly anisotropic $g(\mu)$ leads to larger magnitudes of g_{ℓ} for higher degrees ℓ . Thus, one chooses L such that $\Sigma_{s,(\ell>L)} \approx 0$, which we know is to say that scattering is not significantly anisotropic beyond degree L . This discussion is much more important when constructing discretized cross sections [30], especially in the context of electron elastic

scattering, wherein an approximation referred to as the ‘extended transport correction’ or ‘delta-down scattering’ must be made to the Legendre-moments of the cross section since they are extremely anisotropic, favoring forward scattering. This creates unrealistically slowly converging solutions, rather than the need to use larger L . We will describe this approximation later in this document. Nevertheless, returning ψ to the quantity of interest in $\hat{K}\psi$, the primary result of this subsection is:

$$\hat{K}\psi = \sum_{\ell=0}^L \sum_{m=-\ell}^{\ell} Y_{\ell}^m(\theta, \phi) \Sigma_{s,\ell}(\mathbf{r}) \int d\Omega' Y_{\ell}^{m*}(\hat{\mathbf{k}}') \psi(\mathbf{r}, \hat{\mathbf{k}}') \quad (2.3.18)$$

Now one must treat sources of the form found in \tilde{s} , i.e., sources constructed by applying a scattering operator to some uncollided fluence. Recall that we wrote:

$$\tilde{s} = \int d\Omega' \Sigma_s \tilde{\varphi}^0 \delta^2[\hat{\mathbf{k}}_0(\mathbf{r}) - \hat{\mathbf{k}}'] \quad (2.3.19)$$

When this is discretized, and the identity (2.3.6) is applied, the result is:

$$\tilde{s} = \sum_{\ell=0}^L \sum_{m=-\ell}^{\ell} Y_{\ell}^m(\hat{\mathbf{k}}) Y_{\ell}^{m*}[\hat{\mathbf{k}}_0(\mathbf{r})] \Sigma_{s,\ell}(\mathbf{r}) \tilde{\varphi}^0(\mathbf{r}) \quad (2.3.20)$$

Note that this is essentially the expansion of $\Sigma_s(\hat{\mathbf{k}}_0 \cdot \hat{\mathbf{k}})$ in spherical harmonics. Generally speaking however, this may still be singular, if Σ_s is singular in scattering angle. It so happens, this is the case for an inelastic cross section which is kinematically restrained. That is, one for which scattering from $E' \rightarrow E$ necessarily requires some scattering angle cosine $\bar{\mu}(E' \rightarrow E)$. Examples are electron inelastic scattering and Compton scattering. However, when energy grouped, these cross sections represent aggregate ‘transfer’ from some group g' to g , so the singularity is in principle removed. Were this not the case, \tilde{s} would also be singular, and any choice of L would lead to a rather poor expansion in \tilde{s} .

The final note concerns $\hat{R}\psi$, which, as stated in Section 2.1, is treated as a source term which populates a group g from groups $g' > g$. The angular moments of this cross section are straightforward; literally, the angular distribution of \hat{R} when treated (as in this case) as an integral operator is just $\delta(\mu - 1)/2\pi$, corresponding to no angular deflection, since \hat{R} acts only upon the energy coordinate of ψ . Thus, we could simply say:

$$R_{\ell,g'g} = R_{0,g'g} \quad (2.3.21)$$

for all ℓ . This indeed yields the angular distribution $\delta(\mu - 1)/2\pi$. This is useful if we are lumping $R_{g'g}$ into our other multigroup cross sections $\Sigma_{s,\ell g'g}$. However, it is also possible to consider $R_{g'g}$ a distinct term which simply has no mapping in angle, essentially being a special source term constructed as $R_{g'g}\psi_{g'i}$.

2.4 SN angular discretization

A common method of discretizing the angular space in Boltzmann transport is discrete ordinates, or S_N [2, 42, 54, 59]. In discrete ordinates, we discretize $\hat{\mathbf{k}}$ simply by considering our

functions evaluated at discrete values of $\hat{\mathbf{k}}$. The treatment of operators which don't mix angular coordinates (i.e., those not involving angular derivatives/integrals) is straightforward. One such example is the transport operator. On the other hand, the scattering operator does mix angular coordinates via angular integration of ψ with a spherical harmonic Y_ℓ^{m*} . Thus, one must write an expression for this angular integral in terms of ψ and Y_ℓ^{m*} evaluated at various points in the angular domain. Such a problem is referred to as quadrature, and it motivates the choice of a discrete ordinates set [2, 60, 61].

2.4.1 Angular quadrature

For Gauss-Legendre quadrature, we follow closely a basic treatment described in [2] with one minor deviation in treatment of the ϕ coordinate. In any case, quadrature is the use of knowledge of a function only at certain points in order to evaluate an integral. Generally, quadrature goes as [2]:

$$\int_{-1}^1 dx f(x) = \int_{-1}^1 dx w(x)g(x) \approx \sum_{i=1}^n w_{ni}g(x_{ni}) \quad (2.4.1)$$

where we recognize that a coordinate transformation can phrase any definite integral with finite bounds as one over $x \in [-1, 1]$. The function $w(x)$ is a ‘weight function,’ n is the quadrature order, w_{ni} is the i th quadrature weight of the given form of quadrature of the n th order, and finally x_{ni} is the i th ‘abscissa’ of n th order quadrature. The use of a weight function $w(x)$ is because the various quadrature schemes rely on the exact integration of some set of basis polynomials up to some order depending on n . That is, the integrand $f(x)$ may not be easily represented by a polynomial in x , but in some cases can be factored into an arbitrary polynomial $g(x)$ and a weight function $w(x)$ that corresponds to the orthogonalization procedure of some polynomial set [62]. After choosing the weight function such that $g(x)$ is well-represented by a polynomial, one can determine the weights w_{ni} and abscissae x_{ni} by enforcing exact integration of the basis polynomials up to order n .

In Boltzmann transport, the integrals are typical unit sphere integrals:

$$I = \int_{-1}^1 d\mu \int_0^{2\pi} d\phi f(\mu, \phi) \quad (2.4.2)$$

We will introduce two schemes of performing quadrature: the first is to separately treat μ and ϕ [2], the second is to treat them both simultaneously [60].

To do μ quadrature in Boltzmann transport, it is adequate to treat the integrand as a polynomial in μ . Thus, we take $w(\mu) = 1$, at which point we should have the quadrature scheme which exactly integrates Legendre polynomials, referred to as Gauss-Legendre quadrature. The weights for this quadrature scheme are known:

$$w_i = \frac{2}{(1 - \mu_i^2) [P'_n(\mu_i)]^2} \quad (2.4.3)$$

where, omitting the n index, μ_i is the i th root of the Legendre polynomial $P_n(\mu)$, given by:

$$P_n(\mu_i) = 0 \quad (2.4.4)$$

which is typically solved numerically and tabulated. The functions which can be well treated by Gauss-Legendre quadrature of order n are specifically those which can be approximated by any polynomial of order $2n - 1$. As for ϕ , our integrands are not generally polynomials of ϕ , but we can attempt to represent them as polynomials of $\cos \phi$ [2]. So, we must transform our integral. Let:

$$\nu \equiv \cos \phi \quad (2.4.5)$$

then we can say:

$$\begin{aligned} \int_0^{2\pi} d\phi f(\phi) &= \int_{-1}^1 d\nu \frac{1}{\sqrt{1-\nu^2}} f(\arccos \nu) \\ &+ \int_{-1}^1 d\nu \frac{1}{\sqrt{1-\nu^2}} f(2\pi - \arccos \nu) \end{aligned} \quad (2.4.6)$$

for any $f(\phi)$. Unlike in θ integration, for ϕ we have to run over 2π , which necessitates the second term that has $\phi = 2\pi - \arccos \nu$. Our problem does not necessarily permit such symmetry as to take $f(\arccos \nu) = f(2\pi - \arccos \nu)$. Quadrature may then follow from the weight function $w(\nu) = 1/\sqrt{1-\nu^2}$. The corresponding polynomials are the Chebyshev polynomials of the first kind, which are polynomials in $\cos x$, $T_n(\cos x) = \cos(nx)$. Subsequently, abscissae and weights are:

$$w_i = \frac{\pi}{n} \quad (2.4.7)$$

$$\nu_i = \cos \left(\frac{2i-1}{2n}\pi \right) \quad (2.4.8)$$

starting from $i = 1$. This is a scheme which exactly integrates functions which involve Chebyshev polynomials up to order $n - 1$. We'll write this one out because there's an important note to make:

$$\int_0^{2\pi} d\phi f(\phi) = \frac{\pi}{n} \sum_{i=1}^n f(\arccos \nu_i) + \frac{\pi}{n} \sum_{i=1}^n f(2\pi - \arccos \nu_i) \quad (2.4.9)$$

Here, let's define:

$$f_i = \begin{cases} f(\arccos \nu_i), & i = 1, \dots, n \\ f(2\pi - \arccos \nu_{2n+1-i}), & i = n+1, \dots, 2n \end{cases} \quad (2.4.10)$$

Then, we can say:

$$\int_0^{2\pi} d\phi f(\phi) = \frac{\pi}{n} \sum_{i=1}^{2n} f_i \quad (2.4.11)$$

This way, we have essentially defined ϕ ordinates such that they wrap from 0 to 2π , and there are $2n$ such ordinates:

$$\phi_i = \begin{cases} \arccos \nu_i, & i = 1, \dots, n \\ 2\pi - \arccos \nu_{2n+1-i}, & i = n+1, \dots, 2n \end{cases} = \frac{2j-1}{2N_\phi}\pi \quad (2.4.12)$$

noting $f_i = f(\phi_i)$.

Finally, the whole ‘Legendre-Chebyshev’ integration scheme is:

$$\int_{4\pi} d\Omega f(\hat{\mathbf{k}}) \approx \frac{2\pi}{N_\phi} \sum_{i=1}^{N_\mu} \sum_{j=1}^{N_\phi} w_i f(\mu_i, \phi_j) \quad (2.4.13)$$

where w_i is a Gauss-Legendre weight, N_μ is the order of μ quadrature (and hence the number of θ or μ discrete ordinates), but N_ϕ is twice the order of ν quadrature (and so the total number of unique ϕ values).

The second scheme is one which prefers to treat integration over Ω as a single quadrature problem. It is an inherently 2D quadrature specified to spherical harmonics [60]. Conventionally:

$$\int_{4\pi} d\Omega f(\hat{\mathbf{k}}) \approx 4\pi \sum_{i=1} w_i f(\hat{\mathbf{k}}_i) \quad (2.4.14)$$

Determination of the weights w_i and ‘grid points’ $\hat{\mathbf{k}}_i$ is rather involved and won’t be discussed here. We note, however, that an n -point Lebedev quadrature scheme exactly integrates spherical harmonics up to a certain order N , but the relationship of N to n is not straightforward. Generally, tables are used with weights and points, such as [61, 63], and in some cases these tables include the order of spherical harmonics that is exactly integrated by the n -point set.

Moving forward, we will carry only one angular index, i . Applying discrete ordinates to the scattering operator, one finds the matrix multiplication problem:

$$(\hat{K}\psi)_i = \sum_{i'=1}^{N_\Omega} \sum_{\ell=0}^L \sum_{m=-\ell}^{\ell} w_{i'} Y_{\ell i}^m Y_{\ell i'}^{m*} \Sigma_{s, \ell}(\mathbf{r}) \psi_{i'}(\mathbf{r}) \quad (2.4.15)$$

where N_Ω may represent both N_μ and N_ϕ , or just stand for the number of points used in Lebedev quadrature. If one is using the first-collision scattering source, there is no quadrature anyway:

$$\tilde{s}_i = \sum_{\ell=0}^L \sum_{m=-\ell}^{\ell} Y_{\ell i}^m Y_{\ell}^{m*} [\hat{\mathbf{k}}_0(\mathbf{r})] \Sigma_{s, \ell}(\mathbf{r}) \tilde{\varphi}^0(\mathbf{r}) \quad (2.4.16)$$

The terms above are straightforwardly coupled with the spatial FEM. In $(\hat{K}\psi)_i$, no matrix multiplication occurs in e nor k . Instead, Σ_s is given a superscript e , which just says that a given element has its own cross sections corresponding to the material in that element. As for \tilde{s}_i , one again gives Σ_s the index e , then integrates over element volume with a shape function, only after which is $(I_1^{-1})^e$ applied. See the notes surrounding (2.2.35).

It is to be noted that the separation of a μ index and a ϕ index as per Legendre and Chebyshev quadrature may lead to computationally more convenient evaluations of $(\hat{K}\psi)_i$ via the use of purely real numbers and matrix-less multiplication, particularly if the spherical harmonics sum product $\sum_{m=-\ell}^{\ell} Y_{\ell}^m(\mu_i, \phi_j) Y_{\ell}^{m*}(\mu_{i'}, \phi_{j'})$ is separated as per (2.3.10). Otherwise, one can still forego imaginary numbers by simply swapping the spherical harmonics with real spherical harmonics.

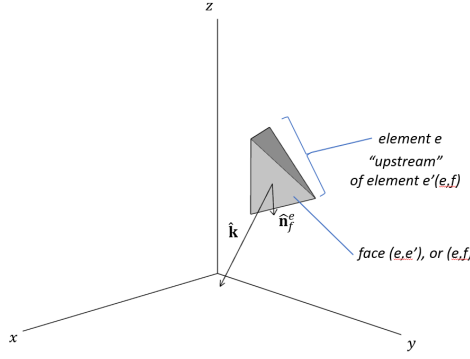


Figure 4: Depiction of the definition of an ‘upstream’ element, whose neighbor on the given face is then the ‘downstream’ element, for a chosen angle $\hat{\mathbf{k}}$.

2.4.2 Sweep

Regarding the transport matrix, coupling with the FEM deserves quite a bit of attention, as it introduces a peculiar structure to our spatial block matrices, which is to be taken into account if one wishes to feasibly invert anything involving T . As we will discuss, in the process of solving the BTE numerically, it is generally advantageous, or entirely sufficient, to invert T alone. Now, returning to (2.2.37), the terms G , F_\uparrow , and F_\downarrow remain to be treated in the context of discrete ordinates. These are treated by evaluating them at $\hat{\mathbf{k}}_i$:

$$G_{ikk'}^e = -\hat{\mathbf{k}}_i \cdot \mathbf{I}_{3',kk'}^e \quad (2.4.17)$$

But the F terms involve the quantities ς_\uparrow and ς_\downarrow . Plugging in $\hat{\mathbf{k}}_i$, one will find the terms:

$$\varsigma_{\uparrow,i}^{ee'} = \frac{1}{2}(\hat{\mathbf{k}}_i \cdot \hat{\mathbf{n}}^{ee'} + |\hat{\mathbf{k}}_i \cdot \hat{\mathbf{n}}^{ee'}|) \quad (2.4.18)$$

$$\varsigma_{\downarrow,i}^{ee'} = \frac{1}{2}(\hat{\mathbf{k}}_i \cdot \hat{\mathbf{n}}^{ee'} - |\hat{\mathbf{k}}_i \cdot \hat{\mathbf{n}}^{ee'}|) \quad (2.4.19)$$

Importantly, $\varsigma_{\downarrow,i}^{ee'}$ is zero for particular combinations of (e, e', i) . Specifically, for those that describe a face whose normal vector is pointing along the chosen direction $\hat{\mathbf{k}}_i$, i.e., one that points to the ‘downstream,’ making e the ‘upstream’ element, as depicted in Figure 4. Since element e is upstream of element $e'(e, f)$, it should not receive any fluence from $e'(e, f)$. This relationship dictates the connectivity of our problem, and therefore the sparsity pattern of the full (e, e') system matrix that we wish to invert. Let’s describe this fully. First, consider a modified form of the block-structure conceptualization of our spatial matrix problem that we introduced in Figure 2. We consider only the problem of $T\psi = s$, which is depicted in Figure 5.

If we discretize this problem simply by specifying $\hat{\mathbf{k}} = \hat{\mathbf{k}}_i$, the problem is formally:

$$\sum_{k'=1}^{N_K^e} (G_{ikk'}^e + M_{kk'}^e + F_{\uparrow,ikk'}^e) \psi_{ik'}^e + \sum_{e'} \sum_{k'=1}^{N_K^e} F_{\downarrow,ikk'}^{ee'} \psi_{ik'}^{e'} = s_{ik}^e \quad (2.4.20)$$

or, more succinctly, as a block matrix problem with i suppressed:

$$(G + M + F_\uparrow)\psi + F_\downarrow\psi = s \quad (2.4.21)$$

$$(G + M + F_\uparrow)\psi + F_\downarrow\psi + F_\downarrow\bar{\psi} = s$$

Figure 5: The problem of $T\psi = s$ over all angles simultaneously, with no angular discretization. Each matrix element is actually a $N_K^e \times N_K^e$ matrix that is continuously parametrized by $\hat{\mathbf{k}}$. Notably, the two known constants are s and $F_\downarrow\bar{\psi}$.

Now, a given row in the overall system matrix T refers to a given element, say e . In general, due to off-diagonal elements in the system matrix, the solution ψ^e to the row e requires the solution $\psi^{e'}$ to all rows e' such that the block matrix at (e, e') , i.e., $T^{ee'}$, is nonzero. Now, T has a diagonal part, $G + M + F_\uparrow$, and an off-diagonal part F_\downarrow . However, for a chosen discrete ordinate $\hat{\mathbf{k}}_i$, the matrix element $F_\downarrow^{ee'}$ will be entirely zero if $\zeta_{\downarrow, i}^{ee'} = 0$, i.e., if the normal vector on e that points to e' is pointing downstream. We should expect that there are some boundary elements which are ‘all the way upstream,’ i.e., their neighbors are all either downstream, or boundary faces. For such elements, $F_\downarrow^{ee'} = 0$ for all e' , and so row e would be soluble. This solution then satisfies one required solution for its immediately downstream neighbors. Then, one can identify the set of elements for which all upstream faces are either on the boundary, or already solved, and these elements can be solved. This procedure is then repeated until every element is solved. This is technically a form of forward substitution following a reorganization of the elements to form a lower triangular matrix.

For example, in the hypothetical problem structure created in Figure 2, if we eliminate those entries (e, e') where e' is downstream of e , then we get Figure 6. Indeed, Figure 6 represents a problem which is soluble (provided that one can invert a matrix of shape $N_K^e \times N_K^e$) via a simple iterative scheme like forward substitution. We will demonstrate this by working through two iterates by hand.

The elements on the boundary are the last 8 elements. In the last 8 rows of F_\downarrow , we see that rows 11, 14, 15, and 16 are fully zero. This means that the neighbors of these elements are all downstream, so these elements can not possibly receive fluence from any elements. Meanwhile, rows 9, 10, 12, and 13 have some nonzero blocks, meaning that while they are on the boundary, they are still downstream of at least one neighbor (respectively, elements 1, 2, 4, and 5). Now, the equation for rows 11, 14, 15, and 16 can be written. For instance, row 11:

$$\sum_{k'=1}^{N_K^e} (G + M + F_\uparrow)_{kk'}^{11} \psi_{k'}^{11} = s_k^{11} - \sum_{k'=1}^{N_K^e} F_{\downarrow, kk'}^{11} \bar{\psi}_{k'}^{11} \quad (2.4.22)$$

where the last term represents the (known) source due to any possible boundary condition (which may be the sole source in a fully external beam problem). This problem can be solved

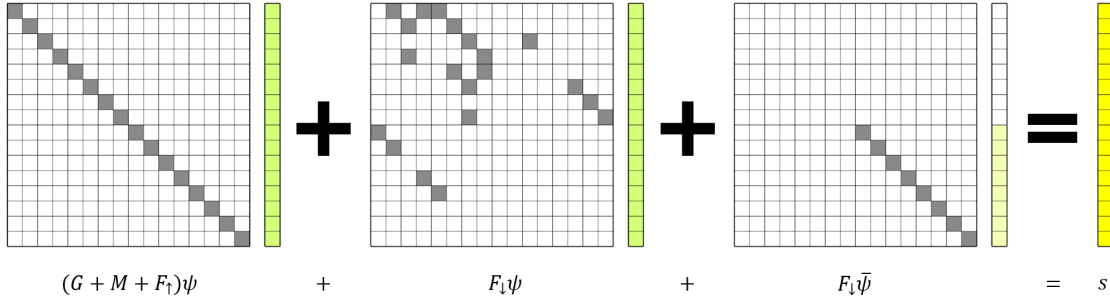


Figure 6: The problem of $T\psi = s$ for the particular direction $\hat{\mathbf{k}} = (1, 1, 1)/\sqrt{3}$. The choice of angle kills several elements of F_\downarrow and makes the problem soluble with forward substitution based on a particular order of elements.

if the $N_K^e \times N_K^e$ matrix $(G + M + F_\uparrow)^{11}$ is inverted (which is feasible to do manually in the case of $N_K^e = 4$). With the incident boundary elements $\psi^{11}, \psi^{14}, \psi^{15}$, and ψ^{16} being solved, we can scan the matrix F_\downarrow for rows which depend only on these elements. Indeed, we find that row 7, although an element on the interior, has only one upstream neighbor, which is 15. The equation for ψ^7 is then:

$$\sum_{k'=1}^{N_K^e} (G + M + F_\uparrow)_{kk'}^7 \psi_{k'}^7 + \sum_{k'=1}^{N_K^e} F_{\downarrow, kk'}^{7, 15} \psi_{k'}^{15} = s_k^7 - \sum_{k'=1}^{N_K^e} F_{\downarrow, kk'}^7 \bar{\psi}_{k'}^7 \quad (2.4.23)$$

Since ψ^{15} is known at this point, this is soluble with inversion of the matrix $(G + M + F_\uparrow)^7$. Now, element 7 can be added to the pool of solved fluences. We repeat this procedure until we have solved for all ψ^e . This procedure is referred to as the ‘sweep.’ Determination of a sweep order for any given mesh and $\hat{\mathbf{k}}$ becomes a task which could be performed as a pre-processing step to solving the Boltzmann transport equation. Generally speaking, the sweep order is determined by rearranging the system matrix in Figure 6 to fit the form of a lower-triangular matrix, however, each discrete ordinate generally requires a distinct sweep order, so this isn’t just a rearrangement of element indices globally. Consider the following, very basic algorithm, whose goal is to determine an array `sweeplist(k, i)`, which provides the k th soluble element for the i th discrete ordinate.

1. Choose a discrete ordinate $\hat{\mathbf{k}}_i$.
2. Initialize an array `parents(e, f) = 0`, where e is an element and f is a face in the element’s indexing system.
3. Visit each e and f . If $\hat{\mathbf{k}}_i \cdot \hat{\mathbf{n}}_f^e \leq 0$, then record $e'(e, f)$ as an upstream element of e . Note that we take $e'(e, f) = 0$ if the face is on the boundary. Note that zeros in `parents(e, f)` represent a neighbor which does not need to be solved prior to solving e .
4. Create an array which contains all element indices e such that $\sum_f \text{parents}(e, f) = 0$. We’ll call this array `zerorows(k)`, with the k th entry thus being the k th smallest element e satisfying the aforementioned rule.

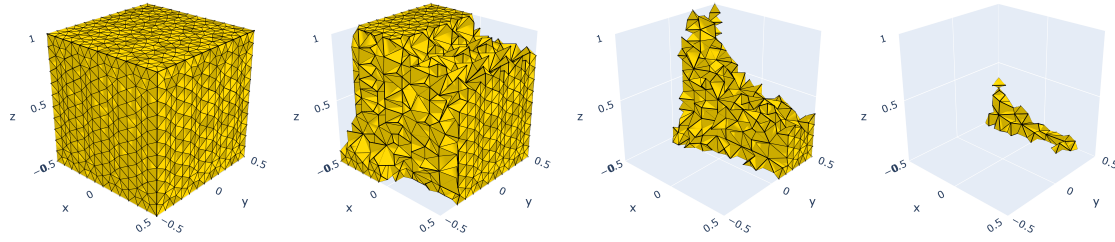


Figure 7: 3D tetrahedral mesh of a cube being swept by wiscobolt for a given discrete ordinate roughly corresponding to the camera angle. From left to right, elements are being removed as they become soluble, with of course many stills removed for brevity. The mesh has $N_E = 9,312$ elements and the sweep is 105 distinct iterates, each iterate containing multiple elements that don't interact and are thus soluble in parallel. Mesh was created with the Gmsh program [55].

5. Append `zerorows` to an array `sweeplist`.
6. For every k , take `parents(zerorows(k), :) = -1`, indicating that the element `zerorows(k)` is solved, so it will not be inserted back into `zerorows` on the next iteration.
7. For every k , find the (e, f) addresses such that `parents(e, f) = \zerorows(k)`, and set `parents(e, f) = 0`, so that the element e is informed that it shares face f with a solved element.
8. Return to Step (iv) and repeat until the size of `sweeplist` in the k index position is the same as the number of elements in the mesh.
9. Return to Step (i) and repeat until all discrete ordinates have been treated.

As is needed in wiscobolt's implementation of this algorithm, it is also useful to determine how many elements can be solved simultaneously, as the sweep by no means imposes that only one element is soluble at a time (as we saw with the four incident boundary elements in our exemplary problem), thus there is a major opportunity for parallelization [64]. Nevertheless, with the sweep order determined, one could proceed element-by-element and solve the problem (2.4.20) as an indirectly-addressed-but-otherwise-typical forward substitution problem using the face indexing system (e, f) .

A brief depiction of how the sweep may act on a three dimensional mesh, in a sweep order determined by wiscobolt, is shown in Figure 7.

2.4.3 Summary

Now absorbing the boundary term into the source, the simultaneous space-angle monoenergetic BTE has been formulated as:

$$\sum_{k'=1}^{N_K^e} \left(G_{ikk'}^e + M_{kk'}^e + F_{\uparrow,ikk'}^e \right) \psi_{ik'}^e = s_{ik}^e - \sum_{k'=1}^{N_K^e} \sum_{f \notin \Gamma} F_{\downarrow,ikk'}^{ef} \psi_{ik'}^{e'(e,f)} + \sum_{i'=1}^{N_\Omega} K_{ii'}^e \psi_{i'k}^e \quad (2.4.24)$$

where:

$$G_{ikk'}^e = -\hat{\mathbf{k}}_i \cdot \mathbf{I}_{3',kk'}^e \quad (2.4.25)$$

$$M_{kk'}^e = \Sigma_t^e \delta_{kk'} \quad (2.4.26)$$

$$F_{\uparrow,ikk'}^e = \sum_{f=1}^{N_F^e} \zeta_{\uparrow,i}^{ef} I_{2'\uparrow,kk'}^{ef} \quad (2.4.27)$$

$$F_{\downarrow,ikk'}^{ef} = \zeta_{\downarrow,i}^{ef} I_{2'\downarrow,kk'}^{ef} \quad (2.4.28)$$

$$K_{ii'}^e = \sum_{\ell=0}^L \sum_{m=-\ell}^{\ell} Y_{\ell i}^m Y_{\ell i'}^{m*} w_{i'} \Sigma_{s,\ell}^e \quad (2.4.29)$$

$$s_{ik}^e = \begin{cases} -\sum_{k'=1}^{N_K^e} \sum_{f \in \Gamma} F_{\downarrow,ikk'}^{ef} \tilde{\psi}_{ik'}^{0,e}, & \text{no FCS} \\ \tilde{s}_{ik}^e, & \text{FCS} \end{cases} \quad (2.4.30)$$

$$\tilde{s}_{ik}^e = \sum_{\ell=0}^L \sum_{m=-\ell}^{\ell} Y_{\ell i}^m \Sigma_{s,\ell}^e \sum_{k'=1}^{N_K^e} (I_1^{-1})_{kk'}^e \int_{V_e} d^3 \mathbf{r} u_{k'}^e(\mathbf{r}) Y_{\ell}^{m*} [\hat{\mathbf{k}}_0(\mathbf{r})] \tilde{\varphi}^0(\mathbf{r})$$

To turn this into a polyenergetic problem is as simple as applying energy iteration, taking care to update the source term appropriately with the expression corresponding to whether one is using the FCS. Note that because the scattering operator mixes angular indices, thereby mixing sweep orders, $(T - K)$ is not able to be directly inverted using any sort sweep/forward substitution. Only inversion of T is possible via a sweep. Nevertheless, our solution methods to be discussed shortly will invoke not more than the sweep and direct multiplication by T and K .

3 Solution

What has been formulated for a single particle (and single energy group) is, most naively, a numerical system of shape $(N_E N_K^e N_\Omega) \times (N_E N_K^e N_\Omega)$. Let's take a rather coarse spatial discretization with reasonable angular discretization. Say we have $N_E = 10,000$, $N_K^e = 4$, $N_\Omega = 512$. Then, we'd have a matrix problem with $>4.194 \cdot 10^{14}$ entries. This estimate, obviously, is prohibitively large. However, in reality this system is extremely sparse in the indices for finite element at least. So this problem, though discretized, needs solution methods that take advantage of the structure of the system. In this section of the document, we will outline what an interested reader should know that goes beyond simply discretizing the problem.

3.1 Iterative methods

3.1.1 Source iteration

The first iterative method we discuss is source iteration (SI) [2, 16, 42]. Simultaneous inversion of the matrix $L = T - K$ requires simultaneous inversion of the spatial and angular indices. However, T mixes spatial indices but not angular indices, and K mixes angular indices but not spatial indices. Also, K^{-1} is undefined (being the discrete form of a definite integral), but T^{-1} is (and it is the sweep described earlier). Thus, in this method, one lags the K operator. That leads to the easily soluble iterative scheme:

$$T\psi^0 = s \quad (3.1.1)$$

$$T\psi^{p+1} = K\psi^p + s, \quad p = 0, 1, \dots \quad (3.1.2)$$

where $\psi^0 = \tilde{\psi}^0$ could or could not be immediately supplied by the FCS method, depending on whether or not the method is being used. The use of FCS only shifts the iteration index. The iterates ψ^{p+1} , or rather their difference, have an interpretation related to the FCS. That is, expand ψ as:

$$\psi = \sum_{p=0}^{\infty} \tilde{\psi}^p \quad (3.1.3)$$

where $\tilde{\psi}^p$ is the fluence of particles that have scattered exactly p times. Now, suppose we truncate the expansion of ψ to some M such that not a negligible fraction particles have scattered more than M times. That is, we'd say:

$$\psi = \sum_{p=0}^M \tilde{\psi}^p \quad (3.1.4)$$

If we are assuming that no particles scatter more than M times, then we are really saying:

$$K\tilde{\psi}^M = 0 \quad (3.1.5)$$

Thus:

$$T\psi - K\psi = \sum_{p=0}^M T\tilde{\psi}^p - \sum_{p=0}^{M-1} K\tilde{\psi}^M = s \quad (3.1.6)$$

Now, $T\tilde{\psi}^0 = s$, so we can say:

$$\sum_{p=1}^M T\tilde{\psi}^p - \sum_{p=0}^{M-1} K\tilde{\psi}^M = 0 \quad (3.1.7)$$

After shifting indices in the sums we have:

$$T\tilde{\psi}^{p+1} = K\tilde{\psi}^p, \quad p = 0, 1, \dots \quad (3.1.8)$$

which is identical to the original SI scheme. This therefore demands a convergence metric which can be used to determine a suitable stopping point M for iteration. One option is the residual of the problem at the M th iteration:

$$r^M = |s - L\psi^M|_2 \quad (3.1.9)$$

where $|x|_2$ is the L2-norm of the vector x . Or, one can look at the ratio of the L2-norm of the fluence at M to the fluence up to the previous iterate:

$$\epsilon^M = \frac{|\tilde{\varphi}^M|_2}{|\varphi^{M-1}|_2} = \frac{|\varphi^M - \varphi^{M-1}|_2}{|\varphi^{M-1}|_2} \quad (3.1.10)$$

and so on.

Note that one can get an idea of how many times a particle scatters until leaving the volume being irradiated by comparing the longest dimension of the volume and the mean free path of the particle, the mean free path being the average distance a particle travels between scattering events. Thus, if the mean free path is much smaller than the volume, a particle will scatter often and consequently SI will generally be very slow. More rigorously, this is because the elements of K will be large compared to T , so lagging K will result in a poor iterative procedure [65]. If, however, the mean free path is only a handful of times smaller than the dimension of the volume, then SI will be faster. For $\sim 10^{-1} - 10^1$ MeV photons in water, mean free paths are on the scale of centimeters to tens of centimeters [29, 56], and in volumes of size tens to hundreds of centimeters, SI will be very efficient. For electrons however, SI is generally extremely slow, because mean free paths can be as little as microns or nanometers [29]. One can remedy this by: using a different solution method, accelerating SI, or lag an operator which is not just K , in other words giving T some terms from K (provided that the newly defined T still won't mix angular indices). All of these approaches are to be discussed, though the last won't be discussed until Section 3.2.1.

3.1.2 Acceleration of SI

Acceleration of SI involves applying a correction to ψ^M following every iterate which is an estimate of the true error at this iterate [66]. That is, the residual function at iterate p is:

$$r = s - (T - K)\psi^p = K(\psi^p - \psi^{p-1}) \quad (3.1.11)$$

while the error is:

$$\varepsilon = \psi - \psi^p \quad (3.1.12)$$

We can show that:

$$(T - K)\varepsilon = r \quad (3.1.13)$$

Therefore:

$$\psi = \psi^p + L^{-1}r \quad (3.1.14)$$

One then can approximate $L^{-1}r = \varepsilon$, for instance, with some $\mathcal{L} \approx L$:

$$\varepsilon \approx \mathcal{L}^{-1}r \quad (3.1.15)$$

Then, this can be added to ψ^p , before continuing to iterate. That said, one would no longer maintain the interpretation that ψ^p represents particles which have scattered up to p times, but despite this further iterates on ψ^p added to ε do converge to ψ . One can then take the following iteration scheme:

$$\psi^0 = T^{-1}s \quad (3.1.16)$$

$$\psi^{p+1/2} = T^{-1}(K\psi^p + s) \quad (3.1.17)$$

$$r^p = K(\psi^{p+1/2} - \psi^p) \quad (3.1.18)$$

$$\varepsilon^p = \mathcal{L}^{-1}r^p \quad (3.1.19)$$

$$\psi^{p+1} = \psi^{p+1/2} + \varepsilon^p \quad (3.1.20)$$

where ‘half-iterates’ $p + 1/2$ are conventionally used to distinguish the corrected ($p + 1$) and uncorrected ($p + 1/2$) iterates. We will discuss methods of expressing and applying an approximate system \mathcal{L} at the end of this subsection.

3.1.3 Generalized minimal residual method

The linear system $L\psi = s$, most notably, is extremely large when discretized, but also extremely sparse, because first-order elements only have diagonal elements with their neighbors, and even then, no more than 3 of them when using discrete ordinates. Additionally, it is not symmetric nor necessarily positive-definite. For problems of this nature, an incredibly practical and successful algorithm was developed by Saad and Schultz [67], known as the generalized minimum residual method (GMRES). We will not describe the algorithm as it is rather long, but it is quite simple and well described by its authors in the original text. We will instead give a high-level overview of GMRES and the implications it has for solution of the Boltzmann transport equation.

With the GMRES algorithm, one can form an approximate solution to the linear system $Ax = b$ using only multiplication with A , as well as some generic, much smaller-sized matrix multiplications, and a backwards substitution. The solution that GMRES gives us is exactly the one which minimizes the residual $b - Ax$ in a t -dimensional ‘Krylov subspace,’ using only t multiplications with A . The Krylov subspace, for what its worth, can be defined by what vectors span it:

$$K_t(A, x_0) = \text{span} \left\{ v_0, Av_0, A^2v_0, \dots, A^{t-1}v_0 \right\} \quad (3.1.21)$$

where x_0 is an initial guess solution, and $v_0 = (b - Ax_0)/|b - Ax_0|$, i.e., the normalized residual of the initial guess. Note that the Krylov subspace does not specify anything about the structure of the multiplication Av_0 , although for our purposes, it will be matrix multiplication. Now, GMRES iteratively and efficiently appends vectors and orthogonalizes them to the Krylov subspace until such a t is reached that a residual below some given convergence criterion is guaranteed. That said, the choice of x_0 typically has a significant impact on the convergence of the problem.

Thus, GMRES in Boltzmann transport allows for a solution to be obtained if only one can apply the operator L to an arbitrary vector. To turn a given GMRES implementation

into one that applies to Boltzmann transport, one must only replace multiplication by the system matrix A with multiplication by L , how ever the latter is implemented in a given solver. Every other step of GMRES will be the same regardless of the problem at hand. Since most terms in L are diagonal in (e, e') (only F_\downarrow is not), multiplication by L is of course not exceedingly difficult.

Note that GMRES can be exceedingly storage-costly if t grows large. To solve this issue, the creators of GMRES have also presented GMRES ‘with restart,’ or, GMRES(m), in the same paper [67]. The idea is that a user can specify a maximum iterate m , for which pre-allocated arrays of known size can be generated. Once this iterate is reached, the original GMRES procedure will restart with the latest iterate as the initial guess. However, it is not guaranteed to converge at all [67], unlike GMRES. In the context of Boltzmann transport, it is generally necessary to use GMRES(m) despite the possible degradation of convergence [66].

3.1.4 Acceleration of GMRES

GMRES can be accelerated by considering the system matrix to be not L , but rather $\mathcal{L}^{-1}L$, where again $\mathcal{L} \approx L$. Most generally, this is referred to as ‘preconditioning’ [51, 66]. We will shortly discuss useful expressions for \mathcal{L} , notably, that also work for estimation of error in SI. However, peculiar to GMRES is the ability to use $\mathcal{L} = T$. That is, since we can apply T^{-1} with a sweep, it is preferable to modify the problem as so:

$$(1 - T^{-1}K)\psi = T^{-1}s \quad (3.1.22)$$

and so to form $T^{-1}K\psi$, one would first form the vector $K\psi$, then use a sweep to apply T^{-1} (with boundary condition always zero, since one is using the boundary condition of $T^{-1}K\psi$). This is advantageous because the linear system $1 - T^{-1}K$ will converge more quickly than $T - K$, since we have already done part of the work in inverting T [51, 66].

3.1.5 Approximate systems for acceleration

Consider the aforementioned error estimate in an SI iterate, $\varepsilon^p = \mathcal{L}^{-1}r^p$, as well as a pre-conditioned system $\mathcal{L}^{-1}L$ in GMRES. We will now discuss what kinds of \mathcal{L}^{-1} can be used.

First, it is possible to accelerate a slowly converging solution/discretization method with a coarse solve in a different solution/discretization method. This is described in tremendous depth in [66], involving both a description of the mathematical problem as well as thorough benchmarks with various combinations of acceleration methods and parameters in particular problems, carried out by the program SCEPTR. So suppose that applying \mathcal{L}^{-1} to some vector v were the operation of solving $L^{-1}v$ in a more coarsely discretized system, then refining the solution using something such as extrapolation. That is to say, the way to apply \mathcal{L}^{-1} to our (fine) vector v_f is:

$$\mathcal{L}^{-1}v_f = F(L_c^{-1}v_c) \quad (3.1.23)$$

where F is an operator which maps from a coarse system to a fine one. The vector v_c should

be the coarse system obtained from the fine v_f , say using an operator C . Thus, we can say:

$$\mathcal{L}^{-1}v_f = FL_c^{-1}Cv_f \quad (3.1.24)$$

Therefore:

$$\mathcal{L}^{-1} = FL_c^{-1}C \quad (3.1.25)$$

In other words, to apply \mathcal{L}^{-1} to a fine vector, take the fine vector and map it to a coarse vector, then apply the coarse matrix L_c^{-1} using any desired solution method, then map the result to a fine vector.

To determine the operators F and C in S_N angular discretization, say we consider a fine system to have $N_{\Omega,f}$, while a coarse system has $N_{\Omega,c}$. One method of extrapolation is to use (preferably real) spherical harmonics, y_ℓ^m . That is, one can form the approximate spherical harmonic moments of any vector with angular indices s_i using angular quadrature, and use these as a continuous representation of s , then plug in the coarse or fine discrete ordinates. The general prescription is therefore:

$$s_{f,i} = \sum_{\ell=0}^{2(N+1)} \sum_{m=-\ell}^{\ell} \sum_{i'=1}^{N_{\Omega,c}} w_{i'} y_\ell^m(\hat{\mathbf{k}}_i) y_\ell^m(\hat{\mathbf{k}}_{i'}) s_{c,i'} \quad (3.1.26)$$

and vice versa for fine to coarse, as long as the correct quadrature and ordinates sets are used for the summation. In Legendre and Chebyshev quadrature, the spherical harmonics set must go up to order $2(N + 1)$, where N is the number of polar angles in the discrete ordinates set of the vector being integrated [66], in the above case, $N = N_{\Omega,c}$. In Lebedev quadrature, however, N must be the maximum order of spherical harmonics integrated by the number of points N_Ω .

By extension, one could use a solution discretized by spherical harmonics expansions (P_N , to be discussed in this document on a later update), with a solution discretized by S_N , and vice versa. This is an interesting subject that we can not discuss because we have not discussed more than one discretization method per coordinate, but the utility of such practices is very well discussed by [66] and the reader is recommended to this paper for more information.

We'll finally consider an older method which is well suited to SI for massive particles, such as electrons. This method initially rose to popularity in the context of neutron transport [68–70]. If electrons scatter very much, then instead of considering every individual scattering event in source iteration, it is interesting to suggest that the electrons diffuse inbetween scattering events. That is, in principle, the streaming operator $\hat{\mathbf{k}} \cdot \nabla$ describes straight-line, ray-like travel between scattering events. Instead, one can use the diffusion operator:

$$\hat{D}\psi = -\nabla \cdot [C(\mathbf{r}, E) \nabla \psi] \quad (3.1.27)$$

where $C(\mathbf{r}, E)$ is the mean free path of the particle of energy E in the material at \mathbf{r} . The mean free path is the inverse of the attenuation coefficient:

$$C(\mathbf{r}, E) = \frac{1}{\Sigma_t(\mathbf{r}, E)} \quad (3.1.28)$$

Then, \mathcal{L} could be:

$$\mathcal{L} = D - K \quad (3.1.29)$$

Notably, we have not discussed discretization of \hat{D} , and we will not do so. However, just like the matrix T , a discretized form of \hat{D} would not mix angular indices, and discretization follows from re-formulating the weak form and applying the finite element method again.

3.2 Further useful numerical approximations

We now discuss two numerical methods that are important in the case of electron transport. In fact, both of these methods are directly intended to alleviate trouble caused by the extremely small mean free path of keV - MeV electrons. The first method, the extended transport correction [30, 50, 71] is directly related to convergence of the iterative methods described above. The second is a quadrature method to construct volume integrals of the fluence $\varphi(\mathbf{r})$, which are absolutely required to accurately find the finite-element method's matrix elements \tilde{s}_k^e in the FCS. See the discussion surrounding (2.2.35).

3.2.1 The extended transport correction

The mean free path of electrons is known to be very small for keV - MeV electrons [3, 29, 30]. Because this means electrons tend to scatter a lot, this means that the scattering matrix K generally has elements that are dramatically larger than the transport matrix, and so clearly when we lag the scattering matrix K (i.e., in SI), or we pre-condition the system matrix with T^{-1} (i.e., in GMRES), we find poor convergence (although, it is a much bigger problem in SI). One major culprit for the large mean free paths is elastic scattering [30, 50, 71]. However, elastic scattering is extremely forward peaked. Quantitatively, in the Rutherford scattering model, 0.01/0.1/1.0 MeV electrons on average scatter with angle cosine approximately 0.9580/0.9960/0.9997 [71], noting that 1 corresponds to perfect forward scattering. The cross section of elastic scattering is still large, and so many forward scattering events will happen and will compound to a significant overall deflection even if each event only causes deflection with an angle cosine of 0.9997. However, a simpler treatment of these forward peaked scattering events should be possible.

This is the motivation for the extended transport correction (ETC). In the ETC one removes from Σ_t and Σ_s the most forward-peaked parts of elastic scattering. The approach is to split elastic scattering into a component which is perfectly forward peaked, and its remainder, like:

$$\Sigma_{\text{el}} \equiv \tilde{\Sigma}_{\text{el}} + \frac{1}{2\pi} C \delta(\mu_s - 1) \quad (3.2.1)$$

for some $C(E)$. This defines $\tilde{\Sigma}_{\text{el}}$, with C being a choice motivated by utility (which will soon be discussed). Now, this scattering mechanism yields the scattering operator:

$$\int d\Omega' \Sigma_{\text{el}} \psi(\hat{\mathbf{k}}') = \int d\Omega' \tilde{\Sigma}_{\text{el}} \psi(\hat{\mathbf{k}}') + C \psi(\hat{\mathbf{k}}) \quad (3.2.2)$$

Interestingly, it also yields the attenuation coefficient:

$$\Sigma_{t,\text{el}} = \int d\Omega' \Sigma_{\text{el}} = \int d\Omega' \tilde{\Sigma}_{\text{el}} + C \equiv \tilde{\Sigma}_{t,\text{el}} + C \quad (3.2.3)$$

Therefore, the transport operator:

$$\hat{T}\psi = \hat{\mathbf{k}} \cdot \nabla\psi + \tilde{\Sigma}_{t,\text{el}}\psi + C\psi \quad (3.2.4)$$

(neglecting all other scattering mechanisms momentarily). An interesting cancellation occurs in $\hat{T} - \hat{K}$. The terms $C\psi$ negate one another, and we have:

$$(\hat{T} - \hat{K})\psi = \hat{\mathbf{k}} \cdot \nabla\psi + \tilde{\Sigma}_{t,\text{el}}\psi - \int d\Omega' \tilde{\Sigma}_{\text{el}}\psi(\hat{\mathbf{k}}') \equiv (\hat{\mathcal{T}} - \hat{\mathcal{K}})\psi \quad (3.2.5)$$

with $\hat{\mathcal{T}} = \hat{\mathbf{k}} \cdot \nabla + \tilde{\Sigma}_{t,\text{el}}$ and $\hat{\mathcal{K}} = \int d\Omega' \tilde{\Sigma}_{\text{el}}$. Clearly, $\hat{T} \neq \hat{\mathcal{T}}$ and $\hat{K} \neq \hat{\mathcal{K}}$ unless $C = 0$. However, the problem of Boltzmann transport is equivalent with respect to Σ_{el} and $\tilde{\Sigma}_{\text{el}}$. The point is therefore that, with the removal of C from $\Sigma_{t,\text{el}}$ due to this cancellation, $\hat{\mathcal{T}}$ leverages an attenuation coefficient that is smaller, and thus, a mean free path that is larger, and matrix elements that are more competitive with those of $\hat{\mathcal{K}}$. Therefore, SI should converge more quickly with $\hat{\mathcal{T}}$, despite that $\hat{\mathcal{T}}$ is not truly the transport operator, and GMRES should be better pre-conditioned with $\hat{\mathcal{T}}^{-1}$.

Now, the rationale for the choice of C is generally made to provide a ‘free’ Legendre moment. That is, if we were to choose that $\tilde{\Sigma}_{\text{el},L+1} = 0$, then:

$$C = \Sigma_{\text{el},L+1} \quad (3.2.6)$$

and thus:

$$\tilde{\Sigma}_{\text{el},\ell} = \Sigma_{\text{el},\ell} - \Sigma_{\text{el},L+1} \quad (3.2.7)$$

With this choice of C , we have:

$$\tilde{\Sigma}_{\text{el},t} = \Sigma_{\text{el},0} - \Sigma_{\text{el},L+1} \quad (3.2.8)$$

where we also recognize that $\Sigma_{\text{el},0} = \Sigma_{\text{el},t}$.

Briefly note that the above discussion is also implicated in the FCS. That is, in the FCS, it becomes useful to once again re-define the uncollided particles as per:

$$\hat{\mathcal{T}}\tilde{\psi}^0 = s \quad (3.2.9)$$

which only means that the attenuation coefficient used for the optical path length now uses $\tilde{\Sigma}_{\text{el},t}$ instead of $\Sigma_{\text{el},t}$. Thus, the exponentially-decaying-with-depth $\tilde{\varphi}^0$ does not fall off quite as quickly anymore [50]. However, it still generally decays on a spatial scale much smaller than the size of a finite element, and so one may still not approximate $\tilde{s}_k^e \approx \tilde{s}(\mathbf{r}_k^e)$.

3.2.2 Integration of uncollided fluence

Here, we discuss the formation of \tilde{s}_k^e as mentioned in Section 2.2.3.

First, we defined much earlier:

$$\tilde{s}_k^e \equiv \sum_{k'=1}^{N_K^e} (I_1^{-1})_{kk'}^e \int_{V^e} d^3\mathbf{r} u_{k'}^e(\mathbf{r}) \tilde{s}(\mathbf{r}) \quad (3.2.10)$$

We saw that we can relate the above directly to what we will now define as:

$$\begin{aligned} F_{\ell k}^{me} &\equiv \sum_{k'=1}^{N_K^e} (I_1^{-1})_{kk'}^e \int_{V^e} d^3\mathbf{r} u_{k'}^e(\mathbf{r}) Y_{\ell}^{m*}[\hat{\mathbf{k}}_0(\mathbf{r})] \tilde{\varphi}^0(\mathbf{r}) \\ &\equiv \sum_{k'=1}^{N_K^e} (I_1^{-1})_{kk'}^e \int_{V^e} d^3\mathbf{r} u_{k'}^e(\mathbf{r}) F_{\ell}^m(\mathbf{r}) \end{aligned} \quad (3.2.11)$$

Notably, the spherical harmonic $Y_{\ell}^{m*}[\hat{\mathbf{k}}_0(\mathbf{r})]$ is lumped into the integral. If the spherical harmonics have been replaced by Legendre polynomials, the functions $F_{\ell}^m(\mathbf{r})$ can be swapped out with the new expression which would be derived from applying (2.3.10) to (2.4.16). Note also, if $Y_{\ell}^{m*}[\hat{\mathbf{k}}_0(\mathbf{r})]$ is approximately constant within the entire given element, then in principle it could be pulled out of the integral and k' sum as $Y_{\ell}^{m*}[\hat{\mathbf{k}}_0(\mathbf{r}_k^e)]$. This means that if the points in the mesh \mathbf{r} are far from the beam source, or the source is planar (in which case $\hat{\mathbf{k}}_0$ is a constant), then the volume integrals in \tilde{s}_k^e can be done on $\tilde{\varphi}^0$ alone, with no (ℓ, m) dependence.

Now, the problem is to we perform the integrals $F_{\ell k}^{me}$ efficiently using only values of $\tilde{\varphi}^0(\mathbf{r})$ at a finite set of pre-determined points. We can turn to quadrature [36]. Specifically, within a linear tetrahedron, we can perform ‘ N –point’ quadrature to yield exact solutions to 3D polynomials of a particular order, similar to 1D Gauss-Legendre quadrature. For instance, a four-point quadrature rule yields exact integration to polynomials of order up to 3 [36]. This makes a far better approximation of \tilde{s}_k^e than $\tilde{s}(\mathbf{r}_k^e)$ given that $\tilde{s}(\mathbf{r})$ is generally not approximately linear in the element e .

We will describe quadrature for a linear tetrahedron, but this discussion can be generalized easily. Let the nodes for such a quadrature rule be expressed in the linear tetrahedron as \mathbf{c}_k . Let the weights be w_k . We then transform our integral to the linear tetrahedron using:

$$\int_{V^e} d^3\mathbf{r} u_k^e(\mathbf{r}) F_{\ell}^m(\mathbf{r}) = 6\tau^e \int_{\text{lin-tet}} d^3\mathbf{r}' u_k(\mathbf{r}') F_{\ell}^m[\mathbf{r}^e(\mathbf{r}')] \quad (3.2.12)$$

which follows directly from Section 2.2.4, using notation from there as well. It is most important to restate:

$$\mathbf{r}^e(\mathbf{r}') = \sum_{k=1}^{N_K^e} u_k(\mathbf{r}') \mathbf{r}_k^e \quad (3.2.13)$$

which is, of course, valid within the tetrahedron in question e . Now, the integral in the linear tetrahedron follows from quadrature:

$$\int_{\text{lin-tet}} d^3\mathbf{r}' u_k(\mathbf{r}') F_{\ell}^m[\mathbf{r}^e(\mathbf{r}')] \approx \sum_{p=1}^N w_p u_k(\mathbf{c}_p) F_{\ell}^m[\mathbf{r}^e(\mathbf{c}_p)] \quad (3.2.14)$$

In matrix multiplication form, we can write:

$$T_{kp} \equiv w_p u_k(\mathbf{c}_p) \quad (3.2.15)$$

$$f_{\ell p}^{me} \equiv F_{\ell}^m [\mathbf{r}^e(\mathbf{c}_p)] \quad (3.2.16)$$

then:

$$\int_{\text{lin-tet}} d^3 \mathbf{r}' u_k(\mathbf{r}') F_{\ell}^m [\mathbf{r}^e(\mathbf{r}')] \approx \sum_{p=1}^N T_{kp} \Phi_{\ell p}^{me} \quad (3.2.17)$$

where we emphasize that the elements T_{pk} have no dependence on any specified element, making this a computationally useful expression. Note also that the quantities $f_{\ell p}^{me}$ are relatively easy to obtain once one decides on the entire set of points $\mathbf{r}(\mathbf{c}_p)$ at which one wishes to evaluate $\tilde{\varphi}^0$. That is, as discussed previously, ray-tracing [37] is used in general to determine optical path lengths from a source to any point of interest. Once these points are known, $\tilde{\varphi}^0$ can be constructed at any point of interest. Nevertheless, the final vector element we obtain is:

$$F_{\ell k}^{me} = 6\tau^e \sum_{k'=1}^{N_K^e} (I_1^{-1})_{kk'}^e \sum_{p=1}^N T_{k'p} f_{\ell p}^{me} \quad (3.2.18)$$

Now, the above is straightforward, but can still be computationally expensive if every element is integrated. Yet, it is hardly necessary for every element. It is only worthwhile for elements that are both large and shallow, i.e., close to the surface facing the source. Only in such elements is the exponential decay in $\tilde{\varphi}$ not closely linear.

3.3 Workflow of wiscobolt

Having detailed the discretization and solution of the Boltzmann transport equation, wiscobolt's structure is summarized by the workflow in Figure 8.

A Angular inner products

During the P_N discretization method (to be discussed in this document on a later update), it is important to express sets of angular inner products:

This section will soon be split into a subsection wherein we describe the *analytical* solutions to the integrals with which we are dealing, as well as one wherein we describe the *numerical* solutions, i.e., via quadrature. The analytical solutions are a bit complicated but nonetheless fascinating, and one would hope, can be implemented optimally to make the construction of the relevant arrays during implementation rather fast (despite how many quantities must be constructed – a lot, so many that storage is a significant issue here). As of this version of wiscobolt, however, the quadrature solutions are much faster (and, frankly, the analytical solutions have not been validated at all, so take their derivation with a mountain of salt). They are still rather slow. So, implementation of these angular inner products is very much a work-in-progress.

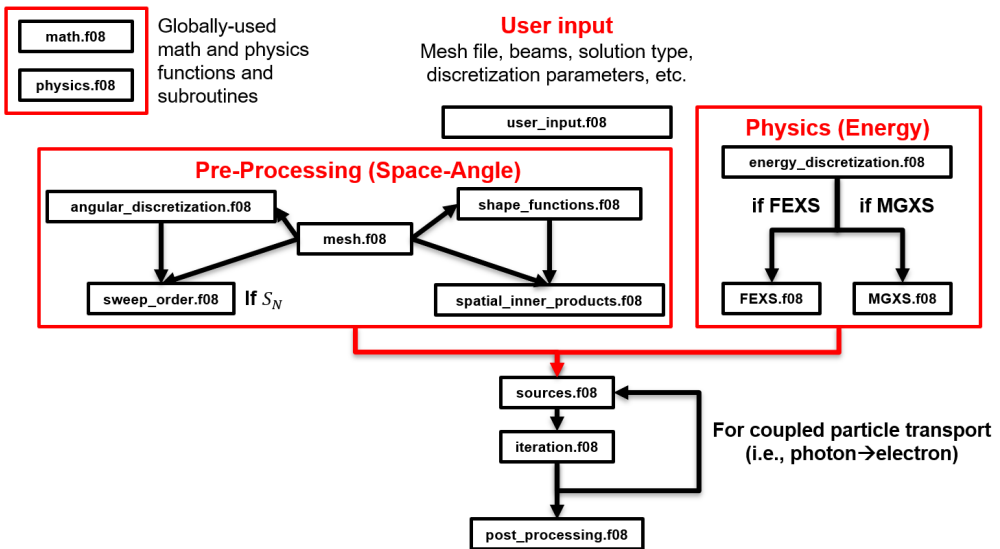


Figure 8: The workflow of wiscobolt. Global math and physics modules house frequently used math and physics functions. User input defines the problem and discretization coarseness. Then, a large pre-processing procedure determines all quantities of interest in relation to space-angle discretization. Next, physics modules perform energy discretization and then construct cross sections (which was not discussed in this document). Finally, source arrays are created, and a solution is obtained by iterating on these arrays. Optionally, a post-processing step produces quantities of interest, such as fluence maps, energy/angular distributions, deposition maps, etc.

Nevertheless, both the analytical and numerical solutions follow from a common, simpler analytical derivation. First, note that each integral will have an integrand involving:

$$k_x y_\ell^m y_{\ell'}^{m'} = \cos \phi \sqrt{1 - \mu^2} y_\ell^m y_{\ell'}^{m'} \quad (\text{A.0.1})$$

$$k_y y_\ell^m y_{\ell'}^{m'} = \sin \phi \sqrt{1 - \mu^2} y_\ell^m y_{\ell'}^{m'} \quad (\text{A.0.2})$$

$$k_z y_\ell^m y_{\ell'}^{m'} = \mu y_\ell^m y_{\ell'}^{m'} \quad (\text{A.0.3})$$

Our approach will be to express a given $k_i y_\ell^m$ in terms of a superposition of other y_k^n . Analytically, this is the first step to a solution, but numerically, this allows us to drastically reduce the number of integrals we are really performing. Additionally, it can be done rather simply.

Now, we will first suppose that we have found the expansion coefficients, i.e., we have found:

$$k_i y_\ell^m = \sum_{\ell'=0}^{\infty} \sum_{m'=-\ell'}^{\ell'} \kappa_{i,\ell\ell'}^{mm'} y_{\ell'}^{m'} \quad (\text{A.0.4})$$

Then, if we attempt to form the whole-sphere inner products $\mathbf{A}_{\ell\ell'}^{mm'}$ immediately by multiplying through with $y_{\ell'}^{m'}$ and integrating, we have:

$$A_{i,\ell\ell'}^{mm'} = \sum_{\ell'',m''} \kappa_{i,\ell\ell''}^{mm''} \int d\Omega y_{\ell'}^{m'} y_{\ell''}^{m''} = \kappa_{i,\ell\ell'}^{mm'} \quad (\text{A.0.5})$$

Therefore, the expansion coefficients *are* our whole-sphere inner products. That is to say:

$$\hat{\mathbf{k}} y_\ell^m = \sum_{\ell',m'} \mathbf{A}_{\ell\ell'}^{mm'} y_{\ell'}^{m'} \quad (\text{A.0.6})$$

This expansion will be used to simplify determination of the half-sphere integrals shortly. First, we'll determine $\mathbf{A}_{\ell\ell'}^{mm'}$.

To begin, we will first return to the definition:

$$y_\ell^m(\mu, \phi) = C_\ell^m S^m(\phi) P_\ell^m(\mu) \quad (\text{A.0.7})$$

We recognize that we can actually express terms like $\cos \phi S^m(\phi)$ and $\sin \phi S^m(\phi)$ in terms of a superposition of $S^n(\phi)$. We can *also* express $\sqrt{1 - \mu^2} P_\ell^m$ and μP_ℓ^m in terms of superpositions of P_k^n using recursion relations. Then, we will be able to match up terms in the product of these expansions and relate them to distinct y_k^n . Following that, we can exploit orthonormality and other properties of the spherical harmonics in order to perform the necessary integrals. The associated Legendre polynomial recursion relations we will need are [58]:

$$\mu P_\ell^m = \frac{1}{2\ell + 1} [(\ell - m + 1) P_{\ell+1}^m + (\ell + m) P_{\ell-1}^m] \quad (\text{A.0.8})$$

$$\sqrt{1 - \mu^2} P_\ell^m = \frac{1}{2\ell + 1} [(\ell - m + 1)(\ell - m + 2) P_{\ell+1}^{m-1} - (\ell + m - 1)(\ell + m) P_{\ell-1}^{m-1}] \quad (\text{A.0.9})$$

$$\sqrt{1 - \mu^2} P_\ell^m = \frac{1}{2\ell + 1} (P_{\ell-1}^{m+1} - P_{\ell+1}^{m+1}) \quad (\text{A.0.10})$$

It goes without saying that you should only use valid pairs of (ℓ, m) , but if one puts some (ℓ, m) that invokes a polynomial with an invalid pair (ℓ, m) , that polynomial just goes to zero. Notice as well that the first relation relates polynomials of the same m and some ℓ to $\ell \pm 1$, while the second relates polynomials of some m and ℓ to those with $m - 1$ and $\ell \pm 1$, and the last relates polynomials of some m and ℓ to those with $m + 1$ and $\ell \pm 1$. Now, we must express $\cos \phi S^m(\phi)$ as a sum of $S^k(\phi)$. Let's look for:

$$\cos \phi S^m(\phi) = \sum_{k=-\infty}^{\infty} c_{mk} S^k(\phi) \quad (\text{A.0.11})$$

and similarly for $\sin \phi S^m(\phi)$. How do we find an expression for c_{mk} ? One may suggest approaching this like a Fourier expansion or other basis expansion, where if we can find a convenient function with which to integrate both sides, we can express c_{mk} easily, then sum over $c_{mk} S^k$ for a convenient expression for $\cos \phi S^m$. And, we could do a similar thing with $\sin \phi S^m$. We'll first check if $S^n(\phi)$ itself permits a convenient expansion:

$$\int_0^{2\pi} d\phi S^n(\phi) S^k(\phi) = \pi(1 + \delta_{n0}) \delta_{nk} \quad (\text{A.0.12})$$

which is convenient enough that we can then say:

$$c_{mn} = \frac{1}{\pi(1 + \delta_{n0})} \int_0^{2\pi} d\phi S^n(\phi) \cos \phi S^m(\phi) \quad (\text{A.0.13})$$

So what is the integral on the RHS? We can find:

$$\int_0^{2\pi} d\phi S^n(\phi) \cos \phi S^m(\phi) = \begin{cases} \frac{1}{2} \pi \delta_{|n-m|,1} (1 + \delta_{|n+m|,1}), & \text{sign}(n) = \text{sign}(m), \\ 0, & \text{else} \end{cases} \quad (\text{A.0.14})$$

so finally:

$$c_{mn} = \begin{cases} \frac{1}{2} \delta_{|n-m|,1} \frac{1 + \delta_{|n+m|,1}}{1 + \delta_{n0}}, & \text{sign}(n) = \text{sign}(m), \\ 0, & \text{else} \end{cases} \quad (\text{A.0.15})$$

It can be (tediously) demonstrated that this is equivalent to a simpler expression:

$$c_{mn} = \frac{1}{2} (1 + \delta_{m0} - \delta_{m,-1}) \delta_{n,m+1} + \frac{1}{2} (1 - \delta_{m0}) \delta_{n,m-1} \quad (\text{A.0.16})$$

which can be found by supposing that one can write c_{mn} in the form $a_m \delta_{n,m+1} + b_m \delta_{n,m-1}$, an intuition gained from the presence of $\delta_{|n \pm m|,1}$. Nevertheless, we are left with:

$$\cos \phi S^m = \frac{1}{2} (1 + \delta_{m0} - \delta_{m,-1}) S^{m+1} + \frac{1}{2} (1 - \delta_{m0}) S^{m-1} \quad (\text{A.0.17})$$

Now, the case of $\sin \phi S^m$ is almost as tedious, except for the ability to use integration by parts to get the integral of $S^n \sin \phi S^m$ from our result for the integral of $S^n \cos \phi S^m$. Nevertheless, the result will simply be provided:

$$\sin \phi S^m = \frac{1}{2} (1 + \delta_{m0}) S^{-(m+1)} - \frac{1}{2} (1 - \delta_{m0} - \delta_{m1}) S^{-(m-1)} \quad (\text{A.0.18})$$

We will define:

$$\begin{aligned}
A_{c,m} &\equiv \frac{1}{2}(1 + \delta_{m0} - \delta_{m,-1}) \\
B_{c,m} &\equiv \frac{1}{2}(1 - \delta_{m0}) \\
A_{s,m} &\equiv \frac{1}{2}(1 + \delta_{m0}) \\
B_{s,m} &\equiv -\frac{1}{2}(1 - \delta_{m0} - \delta_{m1})
\end{aligned} \tag{A.0.19}$$

Let's see how to use these results. We will expand each $k_i y_\ell^m$ and evaluate its whole-sphere integral immediately, then later return and discuss the half-sphere integrals. We'll start trying to work on the x -component. We first consider:

$$\cos \phi \sqrt{1 - \mu^2} y_\ell^m = C_\ell^m \sqrt{1 - \mu^2} P_\ell^m (A_{c,m} S^{m+1} + B_{c,m} S^{m-1}) \tag{A.0.20}$$

For the term $\sqrt{1 - \mu^2} P_\ell^m S^{m+1}$, we use the recursion relation which involves $P_{\ell \pm 1}^{m+1}$, i.e., (A.0.10). That is to say, we take:

$$\sqrt{1 - \mu^2} P_\ell^m S^{m+1} = \frac{1}{2\ell + 1} (P_{\ell-1}^{m+1} S^{m+1} - P_{\ell+1}^{m+1} S^{m+1}) \tag{A.0.21}$$

and for the term $\sqrt{1 - \mu^2} P_\ell^m S^{m-1}$, we use (A.0.9):

$$\begin{aligned}
\sqrt{1 - \mu^2} P_\ell^m S^{m-1} &= \frac{1}{2\ell + 1} [(\ell - m + 1)(\ell - m + 2) P_{\ell+1}^{m-1} S^{m-1} \\
&\quad - (\ell + m - 1)(\ell + m) P_{\ell-1}^{m-1} S^{m-1}]
\end{aligned} \tag{A.0.22}$$

We then leverage:

$$P_k^n S^n = \frac{y_k^n}{C_k^n} \tag{A.0.23}$$

so that we can finally write:

$$\begin{aligned}
\cos \phi \sqrt{1 - \mu^2} y_\ell^m &= \frac{C_\ell^m}{2\ell + 1} \left[\frac{A_{c,m}}{C_{\ell-1}^{m+1}} y_{\ell-1}^{m+1} \right. \\
&\quad - \frac{A_{c,m}}{C_{\ell+1}^{m+1}} y_{\ell+1}^{m+1} \\
&\quad + \frac{B_{c,m}}{C_{\ell+1}^{m-1}} (\ell - m + 1)(\ell - m + 2) y_{\ell+1}^{m-1} \\
&\quad \left. - \frac{B_{c,m}}{C_{\ell-1}^{m-1}} (\ell + m - 1)(\ell + m) y_{\ell-1}^{m-1} \right]
\end{aligned} \tag{A.0.24}$$

For the integral over the whole sphere, we go to integrate this with $y_{\ell'}^{m'}$, then we utilize the

orthonormality relationship for the real spherical harmonics. Then:

$$\begin{aligned}
A_{\ell\ell',x}^{mm'} = & \frac{C_\ell^m}{2\ell+1} \left[\frac{A_{c,m}}{C_{\ell-1}^{m+1}} \delta_{\ell-1,\ell'}^{m+1,m'} \right. \\
& - \frac{A_{c,m}}{C_{\ell+1}^{m+1}} \delta_{\ell+1,\ell'}^{m+1,m'} \\
& + \frac{B_{c,m}}{C_{\ell+1}^{m-1}} (\ell-m+1)(\ell-m+2) \delta_{\ell+1,\ell'}^{m-1,m'} \\
& \left. - \frac{B_{c,m}}{C_{\ell-1}^{m-1}} (\ell+m-1)(\ell+m) \delta_{\ell-1,\ell'}^{m-1,m'} \right]
\end{aligned} \tag{A.0.25}$$

Which is quite sparse. Now, the y -component is just a bit more difficult. We have in the integrand:

$$\sin \phi \sqrt{1-\mu^2} y_\ell^m = C_\ell^m \sqrt{1-\mu^2} P_\ell^m [A_{s,m} S^{-(m+1)} + B_{s,m} S^{-(m-1)}] \tag{A.0.26}$$

Now, the term with, for instance, $S^{-(m-1)}$ gets what recursion relation? We will use the relation with $P_{\ell\pm 1}^{m-1}$, but, we will relate $P_{\ell\pm 1}^{m-1}$ to $P_{\ell\pm 1}^{-(m-1)}$. The relationship we need is:

$$P_\ell^m = (-1)^m \frac{(\ell+m)!}{(\ell-m)!} P_\ell^{-m} \tag{A.0.27}$$

Now first take $m \rightarrow m-1$ and $\ell \rightarrow \ell \pm 1$:

$$P_{\ell\pm 1}^{m-1} = (-1)^{m-1} \frac{(\ell \pm 1 + m - 1)!}{(\ell \pm 1 - m + 1)!} P_{\ell\pm 1}^{-(m-1)} \tag{A.0.28}$$

so what we are saying is:

$$\begin{aligned}
\sqrt{1-\mu^2} P_\ell^m S^{-(m-1)} = & \frac{(-1)^{m-1}}{2\ell+1} \left[\frac{(\ell-m+1)(\ell-m+2)(\ell+m)!}{(\ell-m+2)!} P_{\ell+1}^{-(m-1)} S^{-(m-1)} \right. \\
& \left. - \frac{(\ell+m-1)(\ell+m)(\ell+m-2)!}{(\ell-m)!} P_{\ell-1}^{-(m-1)} S^{-(m-1)} \right]
\end{aligned} \tag{A.0.29}$$

Then the $S^{-(m+1)}$ term needs us to know:

$$P_{\ell\pm 1}^{m+1} = (-1)^{m-1} \frac{(\ell \pm 1 + m + 1)!}{(\ell \pm 1 - m - 1)!} P_{\ell\pm 1}^{-(m+1)} \tag{A.0.30}$$

And then:

$$\begin{aligned}
\sqrt{1-\mu^2} P_\ell^m S^{-(m+1)} = & \frac{(-1)^{m-1}}{2\ell+1} \left[\frac{(\ell+m)!}{(\ell-m-2)!} P_{\ell-1}^{-(m+1)} S^{-(m+1)} \right. \\
& \left. - \frac{(\ell+m+2)!}{(\ell-m)!} P_{\ell+1}^{-(m+1)} S^{-(m+1)} \right]
\end{aligned} \tag{A.0.31}$$

We could then put these together to have:

$$\begin{aligned} \sin \phi \sqrt{1 - \mu^2} y_\ell^m &= \frac{(-1)^{m-1} C_\ell^m}{2\ell + 1} \left[\frac{A_{s,m}}{C_{\ell-1}^{-(m+1)}} \frac{(\ell + m)!}{(\ell - m - 2)!} y_{\ell-1}^{-(m+1)} \right. \\ &\quad - \frac{A_{s,m}}{C_{\ell+1}^{-(m+1)}} \frac{(\ell + m + 2)!}{(\ell - m)!} y_{\ell+1}^{-(m+1)} \\ &\quad + \frac{B_{s,m}}{C_{\ell+1}^{-(m-1)}} \frac{(\ell - m + 1)(\ell - m + 2)(\ell + m)!}{(\ell - m + 2)!} y_{\ell+1}^{-(m-1)} \\ &\quad \left. - \frac{B_{s,m}}{C_{\ell-1}^{-(m-1)}} \frac{(\ell + m - 1)(\ell + m)(\ell + m - 2)!}{(\ell - m)!} y_{\ell-1}^{-(m-1)} \right] \end{aligned} \quad (\text{A.0.32})$$

which integrates to:

$$\begin{aligned} A_{\ell\ell',y}^{mm'} &= \frac{(-1)^{m-1} C_\ell^m}{2\ell + 1} \left[\frac{A_{s,m}}{C_{\ell-1}^{-(m+1)}} \frac{(\ell + m)!}{(\ell - m - 2)!} \delta_{\ell-1,\ell'}^{-(m+1),m'} \right. \\ &\quad - \frac{A_{s,m}}{C_{\ell+1}^{-(m+1)}} \frac{(\ell + m + 2)!}{(\ell - m)!} \delta_{\ell+1,\ell'}^{-(m+1),m'} \\ &\quad + \frac{B_{s,m}}{C_{\ell+1}^{-(m-1)}} \frac{(\ell - m + 1)(\ell - m + 2)(\ell + m)!}{(\ell - m + 2)!} \delta_{\ell+1,\ell'}^{-(m-1),m'} \\ &\quad \left. - \frac{B_{s,m}}{C_{\ell-1}^{-(m-1)}} \frac{(\ell + m - 1)(\ell + m)(\ell + m - 2)!}{(\ell - m)!} \delta_{\ell-1,\ell'}^{-(m-1),m'} \right] \end{aligned} \quad (\text{A.0.33})$$

The easiest is done last. $A_{\ell\ell',z}^{mm'}$ does not involve shifting m values. So we just have:

$$\mu y_\ell^m = \frac{C_\ell^m}{2\ell + 1} \left(\frac{\ell - m + 1}{C_{\ell+1}^m} y_{\ell+1}^m + \frac{\ell + m}{C_{\ell-1}^m} y_{\ell-1}^m \right) \quad (\text{A.0.34})$$

Then:

$$A_{\ell\ell',z}^{mm'} = \frac{C_\ell^m}{2\ell + 1} \left(\frac{\ell - m + 1}{C_{\ell+1}^m} \delta_{\ell+1,\ell'}^{mm'} + \frac{\ell + m}{C_{\ell-1}^m} \delta_{\ell-1,\ell'}^{mm'} \right) \quad (\text{A.0.35})$$

So, we are done with the whole-sphere integrals.

How would we treat the half-sphere integrals? Notice that each integral has been fully reduced to:

$$\int_{\pm \hat{\mathbf{k}} \cdot \hat{\mathbf{n}} > 0} d\Omega k_i y_\ell^m y_{\ell'}^{m'} = \sum_{n,k} A_{i,\ell k}^{mn} \int_{\pm \hat{\mathbf{k}} \cdot \hat{\mathbf{n}} > 0} d\Omega y_k^n y_{\ell'}^{m'} \quad (\text{A.0.36})$$

We are therefore only concerned with integrating $y_k^n y_\ell^m$ over the half-spheres. We are going to distinguish the set of integrals we must evaluate into four categories:

$$\mathcal{I}_{k\ell,\pm}^{nm}(\hat{\mathbf{n}}) \equiv \int_{\pm \hat{\mathbf{k}} \cdot \hat{\mathbf{n}} > 0} d\Omega y_k^n(\hat{\mathbf{k}}) y_\ell^m(\hat{\mathbf{k}}) \quad (\text{A.0.37})$$

1. Integral over $\hat{\mathbf{k}} \cdot \hat{\mathbf{n}} > 0$, $k + \ell$ is even.

2. Integral over $\hat{\mathbf{k}} \cdot \hat{\mathbf{n}} < 0$, $k + \ell$ is even.
3. Integral over $\hat{\mathbf{k}} \cdot \hat{\mathbf{n}} > 0$, $k + \ell$ is odd.
4. Integral over $\hat{\mathbf{k}} \cdot \hat{\mathbf{n}} < 0$, $k + \ell$ is odd.

We can evaluate some of these outright utilizing the parity of these harmonics. In particular, we first note that:

$$\int_{\hat{\mathbf{k}} \cdot \hat{\mathbf{n}} > 0} d\Omega y_k^n(\hat{\mathbf{k}}) y_\ell^m(\hat{\mathbf{k}}) = \int_{-\hat{\mathbf{k}} \cdot \hat{\mathbf{n}} > 0} d\Omega y_k^n(-\hat{\mathbf{k}}) y_\ell^m(-\hat{\mathbf{k}}) \quad (\text{A.0.38})$$

We are saying that integrating $f(\hat{\mathbf{k}})$ over some half-sphere is identical to integrating $f(-\hat{\mathbf{k}})$ over the opposite side of the sphere. However, we have a special $f(-\hat{\mathbf{k}})$, i.e., we can relate the two sides of the equation above in another manner:

$$y_k^n(\hat{\mathbf{k}}) y_\ell^m(\hat{\mathbf{k}}) = (-1)^{k+\ell} y_k^n(-\hat{\mathbf{k}}) y_\ell^m(-\hat{\mathbf{k}}) \quad (\text{A.0.39})$$

Thus:

$$\int_{\hat{\mathbf{k}} \cdot \hat{\mathbf{n}} > 0} d\Omega y_k^n(\hat{\mathbf{k}}) y_\ell^m(\hat{\mathbf{k}}) = (-1)^{k+\ell} \int_{-\hat{\mathbf{k}} \cdot \hat{\mathbf{n}} > 0} d\Omega y_k^n(\hat{\mathbf{k}}) y_\ell^m(\hat{\mathbf{k}}) \quad (\text{A.0.40})$$

Thus, the half integral for $\hat{\mathbf{k}} \cdot \hat{\mathbf{n}} > 0$ is equal to that over $\hat{\mathbf{k}} \cdot \hat{\mathbf{n}} < 0$ up to a factor of $(-1)^{k+\ell}$. This is useful when considering the orthonormality of the whole-sphere integrals of $y_k^n y_\ell^m$, written as:

$$\int_{\hat{\mathbf{k}} \cdot \hat{\mathbf{n}} > 0} d\Omega y_k^n(\hat{\mathbf{k}}) y_\ell^m(\hat{\mathbf{k}}) + \int_{-\hat{\mathbf{k}} \cdot \hat{\mathbf{n}} > 0} d\Omega y_k^n(\hat{\mathbf{k}}) y_\ell^m(\hat{\mathbf{k}}) = \delta_{k\ell}^{nm} \quad (\text{A.0.41})$$

Suppose that $k + \ell$ is even. Then, the two integrals are identical, and because of the orthonormality condition, they are equal to:

$$\int_{\pm \hat{\mathbf{k}} \cdot \hat{\mathbf{n}} > 0} d\Omega y_k^n(\hat{\mathbf{k}}) y_\ell^m(\hat{\mathbf{k}}) = \frac{1}{2} \delta_{k\ell}^{nm}, \quad k + \ell = \text{even} \quad (\text{A.0.42})$$

Thus, we have completely evaluated categories 1 and 2. If, however, $k + \ell$ is odd, then the two integrals are of opposite sign. Since odd $k + \ell$ means $k \neq \ell$, we have $\delta_{k\ell} = 0$ according to the orthonormality condition. But this provides no new information. Thus, we can not immediately state the result of either integral. All we know is that they sum to zero. We can therefore only yet say:

$$\int_{\hat{\mathbf{k}} \cdot \hat{\mathbf{n}} > 0} d\Omega y_k^n(\hat{\mathbf{k}}) y_\ell^m(\hat{\mathbf{k}}) = - \int_{-\hat{\mathbf{k}} \cdot \hat{\mathbf{n}} > 0} d\Omega y_k^n(\hat{\mathbf{k}}) y_\ell^m(\hat{\mathbf{k}}), \quad k + \ell = \text{odd} \quad (\text{A.0.43})$$

But, knowing this, we can seek to integrate either term above given $\hat{\mathbf{n}}$. Thus, if we know category 3, we know category 4, and vice versa. None of this actually simplifies the *general* case that we will ultimately be able to know how to solve, however, it's stated because the process of actually solving these integrals is computationally expensive, and this discussion allows us to minimize the actual number of integrals we eventually calculate to only those with $\hat{\mathbf{k}} \cdot \hat{\mathbf{n}} > 0$ and $\ell + k = \text{even}$.

A.1 Analytical solution

What follows is a method that I have yet to implement, and a derivation which I have not seen elsewhere. For this reason, the derivation should be taken with a grain of salt. However, if validated and implemented, it may serve as a far more efficient method of generating angular inner products than the quadrature solution we will discuss in the following section.

Let's pick the $\hat{\mathbf{k}} \cdot \hat{\mathbf{n}} > 0$ term to solve (category 3). Our rationale will be as follows: we don't wish to perform an entire integral for every normal vector in our mesh. Instead, we will transform our integrals to run exclusively over the northern hemisphere, over which we can analytically integrate the real spherical harmonics. Now, rotation of complex spherical harmonics is well understood. Thus, we will prefer to perform the angular inner products in terms of complex spherical harmonics, then perform a change of basis to the real spherical harmonics. That is, both the complex and real spherical harmonics span the unit sphere. They are related as:

$$y_\ell^m(\hat{\mathbf{k}}) = \sum_{m'=-m,0,m} \chi_{mm'}^\ell Y_\ell^{m'}(\hat{\mathbf{k}}) \quad (\text{A.1.1})$$

for the set of complex coefficients $\chi_{mm'}^\ell$ given by direct comparison of y_ℓ^m and Y_ℓ^m . That is:

$$\chi_{mm'} = \begin{cases} \frac{1}{\sqrt{2}} [\delta_{m',-m} + (-1)^m \delta_{m'm}], & m > 0 \\ \delta_{m'0}, & m = 0 \\ \frac{i}{\sqrt{2}} [\delta_{m'm} - (-1)^m \delta_{m',-m}], & m < 0 \end{cases} \quad (\text{A.1.2})$$

Thus, the problem can be phrased in terms of complex spherical harmonics, using:

$$\int_{\hat{\mathbf{k}} \cdot \hat{\mathbf{n}} > 0} d\Omega y_k^n(\hat{\mathbf{k}}) y_\ell^m(\hat{\mathbf{k}}) = \sum_{m'=-m,0,m} \sum_{n'=-n,0,n} \chi_{nn'}^k \chi_{mm'}^\ell \int_{\hat{\mathbf{k}} \cdot \hat{\mathbf{n}} > 0} d\Omega Y_k^{n'*}(\hat{\mathbf{k}}) Y_\ell^{m'}(\hat{\mathbf{k}}) \quad (\text{A.1.3})$$

where we've conventionally chosen to take the complex conjugate of one of the real spherical harmonics (since y_k^n is real, this is fine, but produces complex conjugated coefficients $\chi_{nn'}^k$ and complex spherical harmonics $Y_k^{n'}$). Now, the problem is phrased in terms of integrals of complex spherical harmonics. We wish to rotate these. First, we must describe conventions we are using. We decide that the matrix R will rotate the normal vector $\hat{\mathbf{n}}$ to $\hat{\mathbf{z}}$:

$$R\hat{\mathbf{n}} = \hat{\mathbf{z}} \quad (\text{A.1.4})$$

We are integrating over vectors $\hat{\mathbf{k}}$ which are pointing in a hemisphere (particularly, $\hat{\mathbf{k}} \cdot \hat{\mathbf{n}} > 0$) about $\hat{\mathbf{n}}$, but when we apply R , these vectors are all rotated to the northern hemisphere. So we will define:

$$R\hat{\mathbf{k}} \equiv \hat{\mathbf{k}}' \quad (\text{A.1.5})$$

so that our integrals transform like:

$$\int_{\hat{\mathbf{k}} \cdot \hat{\mathbf{n}} > 0} d\Omega f(\hat{\mathbf{k}}) = \int_0^{2\pi} d\phi' \int_0^1 d\mu' f(R^{-1}\hat{\mathbf{k}}') \quad (\text{A.1.6})$$

(The determinant of the Jacobian of a rotation is one). So now we briefly ask, what is $Y_\ell^m(R^{-1}\hat{\mathbf{k}}')$? It can be demonstrated [72] that these can be expanded in terms of spherical harmonics of the same order ℓ , with the so-called **Wigner D-matrix** elements as the coefficients:

$$Y_\ell^m(R^{-1}\hat{\mathbf{k}}') = \sum_{m'=-\ell}^{\ell} D_{m'm}^\ell(R) Y_\ell^{m'}(\hat{\mathbf{k}}') \quad (\text{A.1.7})$$

where $R(\hat{\mathbf{n}})$ is determined as the rotation required to bring $\hat{\mathbf{n}}$ to $\hat{\mathbf{z}}$, and $D_{m'm}^\ell(R)$ is the corresponding set of Wigner D-matrix elements. We will discuss their construction in explicit terms of $\hat{\mathbf{n}}$ later. First, recognize that our problem now comes down to:

$$\int_{\hat{\mathbf{k}} \cdot \hat{\mathbf{n}} > 0} d\Omega Y_k^{n*}(\hat{\mathbf{k}}) Y_\ell^m(\hat{\mathbf{k}}) = \sum_{n'=-k}^k \sum_{m'=-\ell}^{\ell} D_{n'n}^{k*} D_{m'm}^\ell \int_0^{2\pi} d\phi \int_0^1 d\mu Y_k^{n'*}(\hat{\mathbf{k}}) Y_\ell^{m'}(\hat{\mathbf{k}}) \quad (\text{A.1.8})$$

so we have kicked the can down the road until finally, we need only to evaluate the integrals:

$$Q_{k\ell}^{nm} \equiv \int_0^{2\pi} d\phi \int_0^1 d\mu Y_k^{n*}(\hat{\mathbf{k}}) Y_\ell^m(\hat{\mathbf{k}}) \quad (\text{A.1.9})$$

This is a very doable task. The ϕ integral, which can be separated, simplifies the problem substantially:

$$\int_0^{2\pi} d\phi e^{-in\phi} e^{im\phi} = \int_0^{2\pi} d\phi e^{i(m-n)\phi} \quad (\text{A.1.10})$$

Recognize that if $m - n$ is zero, this is just 2π . However, if $m - n$ is anything but zero, this integral corresponds to summing together all vectors lying on a unit circle, or asking the center of ‘mass’ or a circle, which is zero. Thus:

$$\int_0^{2\pi} d\phi e^{i(m-n)\phi} = 2\pi \delta_{mn} \quad (\text{A.1.11})$$

This is great, because now we need only to evaluate the μ integral when $m = n$. Now, these integrals are known for μ spanning from -1 to 1 :

$$\int_{-1}^1 d\mu P_\ell^m(\mu) P_k^m(\mu) = \frac{2(\ell+m)!}{(2\ell+1)(\ell-m)!} \delta_{k,\ell}, \quad m \geq 0 \quad (\text{A.1.12})$$

The case for $m < 0$ is doable using the identity relating P_ℓ^{-m} to P_ℓ^m , which we wrote in (A.0.27). What can we say for this integral with our bounds? First, recognize that if $\ell + k$ is an even number, then the integrand is even over μ , and we would have the integral be half of the above:

$$\int_0^1 d\mu P_\ell^m(\mu) P_k^m(\mu) = \frac{(\ell+m)!}{(2\ell+1)(\ell-m)!} \delta_{k,\ell}, \quad \ell + k = \text{even} \quad (\text{A.1.13})$$

Note that, while we are only looking for $\mathcal{I}_{k\ell,+}^{nm}$ for $\ell + k = \text{even}$, we need the integrals above for the general case, by virtue of the many expansions we made. The case for $\ell + k = \text{odd}$ is not too difficult. Let’s again focus on $m \geq 0$, which can be generalized later.

There could be a better way to do this, but the best way I can come up with is to expand $P_\ell^m P_k^m$ as a polynomial. We know we *can* expand it as a polynomial, despite that P_ℓ^m and P_k^m are themselves not generally polynomials. Specifically, write:

$$P_\ell^m(\mu) = (-1)^m 2^\ell (1 - \mu^2)^{m/2} \sum_{\ell'=m}^{\ell} \binom{\ell}{\ell'} \binom{(\ell + \ell' - 1)/2}{\ell} \frac{\ell'!}{(\ell' - m)!} \mu^{\ell' - m} \quad (\text{A.1.14})$$

Due to the factor $(1 - \mu^2)^{m/2}$, this is not a polynomial for odd m . However, we can now write:

$$\begin{aligned} P_k^m(\mu) P_\ell^m(\mu) &= 2^\ell (1 - \mu^2)^m \sum_{\ell'=m}^{\ell} \sum_{k'=m}^k \times \\ &\quad \binom{\ell}{\ell'} \binom{(\ell + \ell' - 1)/2}{\ell} \binom{k}{k'} \binom{(k + k' - 1)/2}{k} \frac{k'!}{(k' - m)!} \mu^{\ell' - m + k' - m} \end{aligned} \quad (\text{A.1.15})$$

which, with another cumbersome expansion of $(1 - \mu^2)^m$, is always a polynomial. We use the binomial theorem:

$$(1 - \mu^2)^m = \sum_{m'=0}^m \binom{m}{m'} (-1)^{m'} \mu^{2m'} \quad (\text{A.1.16})$$

Thus, in total, we have:

$$\begin{aligned} P_k^m(\mu) P_\ell^m(\mu) &= 2^\ell \sum_{m'=0}^m \sum_{\ell'=m}^{\ell} \sum_{k'=m}^k \times \\ &\quad (-1)^{m'} \binom{m}{m'} \binom{\ell}{\ell'} \binom{(\ell + \ell' - 1)/2}{\ell} \binom{k}{k'} \binom{(k + k' - 1)/2}{k} \frac{k'!}{(k' - m)!} \mu^{\ell' + k' - 2m + 2m'} \end{aligned} \quad (\text{A.1.17})$$

which, of course, can be analytically integrated.

$$\begin{aligned} \int_0^1 d\mu P_k^m(\mu) P_\ell^m(\mu) &= 2^\ell \sum_{m'=0}^m \sum_{\ell'=m}^{\ell} \sum_{k'=m}^k \times \\ &\quad \frac{(-1)^{m'}}{\ell' + k' - 2m + 2m' + 1} \binom{m}{m'} \binom{\ell}{\ell'} \binom{(\ell + \ell' - 1)/2}{\ell} \binom{k}{k'} \binom{(k + k' - 1)/2}{k} \frac{k'!}{(k' - m)!} \end{aligned} \quad (\text{A.1.18})$$

It's a big, ugly, inefficient equation, but since this needs to be calculated only once, this is fine.

Thus, we have, for $m \geq 0$, and $\ell + k = \text{even}$:

$$\int_0^1 d\mu P_\ell^m(\mu) P_k^m(\mu) = \frac{(\ell + m)!}{(2\ell + 1)(\ell - m)!} \delta_{k,\ell} \quad (\text{A.1.19})$$

and for $m \geq 0$, $\ell + k = \text{odd}$:

$$\int_0^1 d\mu P_k^m(\mu) P_\ell^m = 2^\ell \sum_{m'=0}^m \sum_{\ell'=m}^{\ell} \sum_{k'=m}^k \times \frac{(-1)^{m'}}{\ell' + k' - 2m + 2m' + 1} \binom{m}{m'} \binom{\ell}{\ell'} \binom{(\ell + \ell' - 1)/2}{\ell} \binom{k}{k'} \binom{(k + k' - 1)/2}{k} \frac{k'!}{(k' - m)!} \quad (\text{A.1.20})$$

As for $m < 0$, we use (A.0.27) with $m \rightarrow |m|$. Since $P_\ell^{|m|}$ satisfies $|m| > 0$, we can use the previous results. Thus, if $m < 0$, we perform the integral with $|m|$ and apply a factor:

$$F_{k\ell}^m \equiv \frac{(\ell - |m|)!}{(\ell + |m|)!} \frac{(k - |m|)!}{(k + |m|)!} \quad (\text{A.1.21})$$

Now that the integrals $Q_{k\ell}^{nm}$ are determined, we just need to discuss the Wigner D-matrix elements. Written exactly like (A.1.7), we can multiply both sides by $Y_\ell^{m'*}(\hat{\mathbf{k}}')$ and integrate, yielding:

$$D_{m'm}^\ell(R) = \int d\Omega' Y_\ell^{m'*}(\hat{\mathbf{k}}') Y_\ell^m(R^{-1}\hat{\mathbf{k}}') \quad (\text{A.1.22})$$

We will provide $D_{m'm}^\ell$ without derivation, given some rotation, after we describe the rotation R in terms of the normal vector we are evaluating. Let's define an operator $\mathcal{D}(R)$ which rotates functions in the manner we desire. We will find this easiest to understand by looking at a simpler problem similar to ours. Say we have some polar plot $f(\theta)$, which we want to integrate over the semicircle whose north pole is θ_0 . If the unit vector describing the north pole of the semicircle is $(\cos \theta_0, \sin \theta_0) \equiv \hat{\mathbf{n}}$, then we want a rotation by angle α such that:

$$R(\alpha)\hat{\mathbf{n}} = \hat{\mathbf{y}} \quad (\text{A.1.23})$$

So then, if one evaluates $f(\mathbf{r})$, they will find it identical to $f(R^{-1}\mathbf{r}')$, and in the new coordinate system, one can integrate over $[0, \pi]$. We can easily see that, since $\hat{\mathbf{r}} = (\cos \theta, \sin \theta)$, the desired rotation angle leads us to perform:

$$R(\alpha)(\cos \theta, \sin \theta) = (\cos(\theta + \alpha), \sin(\theta + \alpha)) \equiv (\cos \theta', \sin \theta') \quad (\text{A.1.24})$$

This means that the relationship between the new system θ' and the old system θ is $\theta = \theta' - \alpha$. But, in this approach, we are looking at a rotation as a coordinate transformation. If we want to *actively* rotate $f(\theta)$ and let it sit in the same coordinate system, then we define a rotation *operator*, which does not leave an equality like the above, but instead:

$$\mathcal{D}[R(\alpha)]f(\theta) = f(\theta - \alpha) \quad (\text{A.1.25})$$

where we recognize that taking $\theta - \alpha$ is like applying $R^{-1}\hat{\mathbf{r}}$, since $R\hat{\mathbf{r}}$ moves θ to $\theta + \alpha$. We generalize now:

$$\mathcal{D}(R)f(\hat{\mathbf{k}}) \equiv f(R^{-1}\hat{\mathbf{k}}) \quad (\text{A.1.26})$$

Thus:

$$D_{m'm}^\ell(R) = \int d\Omega' Y_\ell^{m'*}(\hat{\mathbf{k}}') \mathcal{D}(R) Y_\ell^m(\hat{\mathbf{k}}') \quad (\text{A.1.27})$$

So, the Wigner D-matrix is the matrix formed by the matrix elements of the rotation operator. The purpose of this discussion is so that we can have the exact same convention for \mathcal{D} and R that is frequently used in the literature to define the Wigner D-matrix elements $D_{m'm}^\ell$. It is too involved for us to describe the form of the rotation operator $\mathcal{D}(R)$, but it must be noted that R is typically written with respect to **Euler angles** (α, β, γ) in the *xyz*-convention. This is useful because the effect of a polar rotation, such as that implemented by some $\mathcal{D}(\alpha, 0, 0)$ or $\mathcal{D}(0, 0, \gamma)$, on a spherical harmonic is well-known to only affect the phase $e^{im\phi}$. If these angles are successfully determined by that rotation which maps $\hat{\mathbf{n}}$ to $\hat{\mathbf{z}}$, then one can write the Wigner D-matrices as:

$$D_{m'm}^\ell(R) = e^{-im'\alpha} d_{m'm}^\ell(\beta) e^{-im\gamma} \quad (\text{A.1.28})$$

where $d_{m'm}^\ell(\beta)$ are the elements of the **Wigner d-matrix**, which can be given by:

$$d_{m'm}^\ell(\beta) = \sqrt{(\ell + m')!(\ell - m')!(\ell + m)!(\ell - m)!} \times \sum_{s=s_{\min}}^{s_{\max}} \frac{(-1)^{m'-m+s} \cos(\beta/2)^{2\ell+m-m'-2s} \sin(\beta/2)^{m'-m+2s}}{(\ell + m - s)!s!(m' - m + s)!(\ell - m' - s)!} \quad (\text{A.1.29})$$

where $s_{\min} = \max[0, m - m']$ and $s_{\max} = \min[\ell + m, \ell - m']$.

How do we determine *xyz* Euler angles for the rotation $R\hat{\mathbf{n}} = \hat{\mathbf{z}}$? This can be tricky to think through, so we will first outline the operation(s) we mean to perform, then discuss a geometrically simple way to perform this. Our rotation matrix is of the form:

$$R(\alpha, \beta, \gamma) = R_z(\alpha)R_y(\beta)R_z(\gamma) \quad (\text{A.1.30})$$

Where:

$$R_z(x) = \begin{pmatrix} \cos x & -\sin x & 0 \\ \sin x & \cos x & 0 \\ 0 & 0 & 1 \end{pmatrix} \quad (\text{A.1.31})$$

$$R_y(x) = \begin{pmatrix} \cos x & 0 & \sin x \\ 0 & 1 & 0 \\ -\sin x & 0 & \cos x \end{pmatrix} \quad (\text{A.1.32})$$

It is not trivial that these are Euler rotations, because they appear to be a somewhat mundane sequence of rotations. However, a deep discussion on Euler angles is not warranted here, and we will work with these. These matrices perform counterclockwise rotations about the given axis of the vector to which they are applied, with ‘counterclockwise’ defined via the right hand rule. Now, how do we determine α , β , and γ ? We can consider $R_z(\gamma)$ to bring the vector $\hat{\mathbf{n}}$ to, say, the *xz*-plane, i.e., to have $\phi = 0$. Thus, it is just:

$$\gamma(\hat{\mathbf{n}}) \equiv -\phi_0(\hat{\mathbf{n}}) = -\text{atan2}(n_y, n_x) \quad (\text{A.1.33})$$

where $\text{atan2}(y, x)$ is a special function given in certain programming languages, that returns $\phi_0 \in [-\pi, \pi)$ given the y -component and x -component of a vector. It is fine to use this range of ϕ_0 because, to transform it to our customary range $\phi \in [0, 2\pi)$, we would simply add 2π to any angles that are negative. Doing so leaves $\sin \phi$, $\cos \phi$, and $e^{i\phi}$, the only arguments

with which we are right now concerned, completely unchanged. We can then consider $R_y(\beta)$ to bring the resulting vector to $\hat{\mathbf{z}}$. Thus, it is just:

$$\beta(\hat{\mathbf{n}}) \equiv -\theta_0(\hat{\mathbf{n}}) = -\cos(n_z) \quad (\text{A.1.34})$$

and we then take $\alpha = 0$ as a matter of convenience.

A.1.1 Summary

We now summarize the results of this section. What we ultimately have is a sequence of matrix multiplications, with only one set of matrices being dependent on the mesh normal vectors. We have broken the problem down as follows:

$$\mathcal{I}_{k\ell,+}^{nm} = \sum_{m'=-m,0,m} \sum_{n'=-n,0,n} \chi_{nn'}^{k*} \chi_{mm'}^{\ell} I_{k\ell}^{n'm'} \quad (\text{A.1.35})$$

where:

$$\chi_{mm'} = \begin{cases} \frac{1}{\sqrt{2}} [\delta_{m',-m} + (-1)^m \delta_{m'm}], & m > 0 \\ \delta_{m'0}, & m = 0 \\ \frac{i}{\sqrt{2}} [\delta_{m'm} - (-1)^m \delta_{m',-m}], & m < 0 \end{cases} \quad (\text{A.1.36})$$

and the integrals $I_{k\ell}^{nm}$ are given by:

$$I_{k\ell}^{nm} = \sum_{m'=-\ell}^{\ell} \sum_{n'=-k}^k D_{n'n}^{k*}(\hat{\mathbf{n}}) D_{m'm}^{\ell}(\hat{\mathbf{n}}) Q_{k\ell}^{n'm'} \quad (\text{A.1.37})$$

where:

$$D_{m'm}^{\ell}(\hat{\mathbf{n}}) = e^{-im'\alpha} d_{m'm}^{\ell}(\beta) e^{-im\gamma} \quad (\text{A.1.38})$$

$$\alpha(\hat{\mathbf{n}}) = 0$$

$$\beta(\hat{\mathbf{n}}) = -\cos(n_z) \quad (\text{A.1.39})$$

$$\gamma(\hat{\mathbf{n}}) = -\text{atan2}(n_y, n_x)$$

$$d_{m'm}^{\ell}(\beta) = \sqrt{(\ell+m')!(\ell-m')!(\ell+m)!(\ell-m)!} \times \sum_{s=s_{\min}}^{s_{\max}} \frac{(-1)^{m'-m+s} \cos(\beta/2)^{2\ell+m-m'-2s} \sin(\beta/2)^{m'-m+2s}}{(\ell+m-s)!s!(m'-m+s)!(\ell-m'-s)!} \quad (\text{A.1.40})$$

where $s_{\min} = \max[0, m - m']$ and $s_{\max} = \min[\ell + m, \ell - m']$. Then, the integrals $Q_{k\ell}^{nm}$ are given by:

$$Q_{k\ell}^{nm} = 2\pi \delta_{mn} \begin{cases} \mathcal{Q}_{k\ell}^m, & m \geq 0 \\ F_{k\ell}^m \mathcal{Q}_{k\ell}^{|m|}, & m < 0 \end{cases} \quad (\text{A.1.41})$$

where:

$$F_{k\ell}^m = \frac{(\ell - |m|)!}{(\ell + |m|)!} \frac{(k - |m|)!}{(k + |m|)!} \quad (\text{A.1.42})$$

and:

$$\mathcal{Q}_{k\ell}^m = \frac{(\ell + m)!}{(2\ell + 1)(\ell - m)!} \delta_{k,\ell} \quad (\text{A.1.43})$$

if $\ell + k$ is even and:

$$\mathcal{Q}_{k\ell}^m = 2^\ell \sum_{m'=0}^m \sum_{\ell'=m}^{\ell} \sum_{k'=m}^k \times \frac{(-1)^{m'}}{\ell' + k' - 2m + 2m' + 1} \binom{m}{m'} \binom{\ell}{\ell'} \binom{(\ell + \ell' - 1)/2}{\ell} \binom{k}{k'} \binom{(k + k' - 1)/2}{k} \frac{k'!}{(k' - m)!} \quad (\text{A.1.44})$$

if $\ell + k$ is odd. The relationship of the integrals $\mathcal{I}_{k\ell,+}^{nm}$ to the integrals $\mathbf{A}_{\uparrow,\ell\ell'}^{mm'}$ and $\mathbf{A}_{\downarrow,\ell\ell'}^{mm'}$ was described in the previous section, of course. The integrals $\mathcal{I}_{k\ell,+}^{nm}$ need only be evaluated this way when $\ell + k$ is odd. Otherwise, they are simply $\delta_{k\ell}^{nm}/2$. Note also that we can make use of more identities, for instance that \mathcal{I} is symmetric when one swaps (k, n) with (m, ℓ) , etc.

A.2 Quadrature solution

An alternative is to formulate the integral problems $\mathcal{I}_{k\ell,+}^{nm}(\hat{\mathbf{n}})$ by precisely expressing the domain given by $\hat{\mathbf{k}} \cdot \hat{\mathbf{n}} > 0$. We know that this is a hemisphere whose pole is $\hat{\mathbf{n}}$. So, how do we specify the μ and ϕ ranges that allow us to integrate over this hemisphere? Consider that, at each polar angle θ , the hemisphere can be travelled along ϕ with a certain range, corresponding to a slice at the z -value given by θ . This is demonstrated in **Figure 9**. For a given μ and $\hat{\mathbf{n}}$, we will call the minimal ϕ value $\alpha(\mu, \hat{\mathbf{n}})$, and the maximal ϕ value $\beta(\mu, \hat{\mathbf{n}})$. Surprisingly simple trigonometry can lead to the following complicated expressions:

$$\alpha(\mu, \hat{\mathbf{n}}) = \begin{cases} \phi_0(\hat{\mathbf{n}}) - \frac{\pi}{2} + \text{sign}(n_z)\frac{\pi}{2}, & -1 \leq \mu \leq -\sqrt{1 - n_z^2} \\ \phi_0(\hat{\mathbf{n}}) - \frac{\pi}{2} - \text{asin}\left[\frac{\mu n_z}{\sqrt{(1-\mu^2)(1-n_z^2)}}\right], & -\sqrt{1 - n_z^2} < \mu < \sqrt{1 - n_z^2} \\ \phi_0(\hat{\mathbf{n}}) - \frac{\pi}{2} - \text{sign}(n_z)\frac{\pi}{2}, & \sqrt{1 - n_z^2} \leq \mu \leq 1 \end{cases} \quad (\text{A.2.1})$$

$$\beta(\mu, \hat{\mathbf{n}}) = \begin{cases} \phi_0(\hat{\mathbf{n}}) + \frac{\pi}{2} - \text{sign}(n_z)\frac{\pi}{2}, & -1 \leq \mu \leq -\sqrt{1 - n_z^2} \\ \phi_0(\hat{\mathbf{n}}) + \frac{\pi}{2} + \text{asin}\left[\frac{\mu n_z}{\sqrt{(1-\mu^2)(1-n_z^2)}}\right], & -\sqrt{1 - n_z^2} \leq \mu \leq \sqrt{1 - n_z^2} \\ \phi_0(\hat{\mathbf{n}}) + \frac{\pi}{2} + \text{sign}(n_z)\frac{\pi}{2}, & \sqrt{1 - n_z^2} \leq \mu \leq 1 \end{cases}$$

which you can verify graphically if you wish. With these in hand, we can write our integrals as:

$$\mathcal{I}_{k\ell,+}^{nm}(\hat{\mathbf{n}}) = \int_{-1}^1 d\mu \int_{\alpha(\mu, \hat{\mathbf{n}})}^{\beta(\mu, \hat{\mathbf{n}})} d\phi y_k^n(\hat{\mathbf{k}}) y_\ell^m(\hat{\mathbf{k}}) \quad (\text{A.2.2})$$

Here, quadrature could be performed somewhat conveniently. The scheme is:

$$\phi(\mu, v, \hat{\mathbf{n}}) \equiv \frac{1}{2} [\beta(\mu, \hat{\mathbf{n}}) - \alpha(\mu, \hat{\mathbf{n}})] v + \frac{1}{2} [\beta(\mu, \hat{\mathbf{n}}) + \alpha(\mu, \hat{\mathbf{n}})] \quad (\text{A.2.3})$$

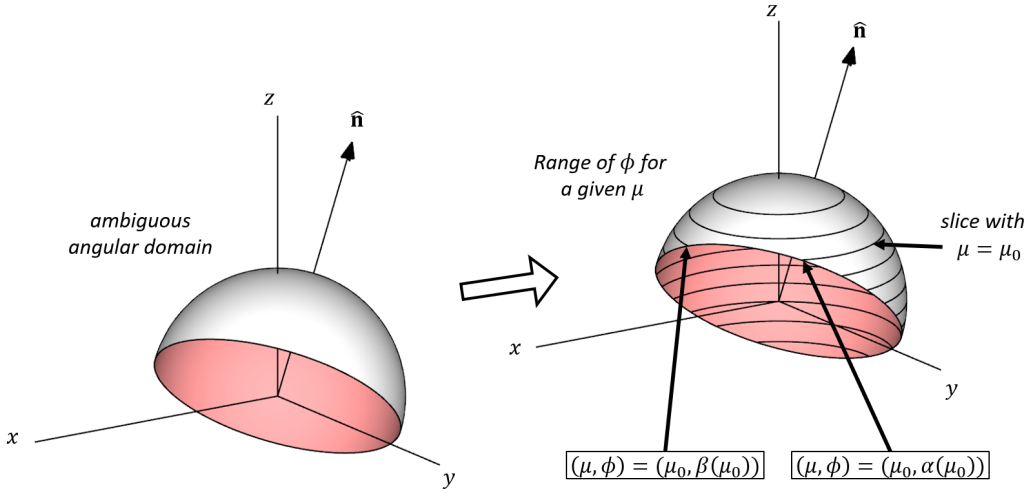


Figure 9: One method to treat integrals over an angular domain such as $\hat{\mathbf{k}} \cdot \hat{\mathbf{n}} > 0$. Slice the region at an arbitrary value of μ , and consider ϕ to range from $\alpha(\mu)$ to $\beta(\mu)$. Then, integrate over these ϕ , and finally integrate over μ .

Therefore:

$$\boxed{\mathcal{I}_{k\ell+}^{nm}(\hat{\mathbf{n}}) = \frac{1}{2} C_k^n C_\ell^m \times \int_{-1}^1 d\mu P_k^n(\mu) P_\ell^m(\mu) [\beta(\mu, \hat{\mathbf{n}}) - \alpha(\mu, \hat{\mathbf{n}})] \int_{-1}^1 dv S^n[\phi(\mu, v, \hat{\mathbf{n}})] S^m[\phi(\mu, v, \hat{\mathbf{n}})]}$$

(A.2.4)

While this approach may be conceptually more simple, quadrature is only approximate, and rather slow. One may suspect that the exact formulation can be implemented to be dramatically faster. That said, storage of the necessary quantities $\hat{\mathbf{n}} \cdot \mathbf{A}_{\uparrow,qq'}$ and $\hat{\mathbf{n}} \cdot \mathbf{A}_{\downarrow,qq'}$ represents a bit of a problem. It is described in the **wiscobolt implementation** document how wiscobolt creates and stores these arrays in order to lessen the burden of storage. Briefly, it is recommended that they are stored as constructed for ‘global’ faces. That is, every face in the interior of the mesh actually corresponds to two faces; one owned by each of the two elements that share the face. The normal vectors of these faces have opposite sign. Thus, one can say that \mathbf{A}_\uparrow of the face referenced in element e is identical to \mathbf{A}_\downarrow of the face referenced in $e'(e, f)$. If the ‘right’ sign can be stored separately, then one can get by with only storing either \mathbf{A}_\uparrow or \mathbf{A}_\downarrow , and only for the global faces. This lessens the burden of storage by almost a factor of 4 (I find it’s closer to 3, it depends on how many boundary faces there are). A factor of two is due to only carrying either \mathbf{A}_\uparrow or \mathbf{A}_\downarrow , a factor of almost 2 is due to only carrying one element per global face. Finally, wiscobolt carries $\hat{\mathbf{n}} \cdot \mathbf{A}_\uparrow$ instead of just \mathbf{A}_\uparrow , for a few reasons. First, that is how it is needed everywhere in the problem. Second, the scalar product will reduce the number of entries required by a factor of three.

Third, it will prevent the need to form the scalar product during iteration, which is very wasteful. At the same time, $\hat{\mathbf{n}}$ is indexed by face, so the quantity $\hat{\mathbf{n}} \cdot \mathbf{A}_\uparrow$ does not pickup any more indices in comparison to \mathbf{A}_\uparrow .

Future updates of wiscobolt will hopefully involve better strategies.

References

- [1] F. H. Attix, *Introduction to radiological physics and radiation dosimetry* (Wiley-VCH, 1986).
- [2] J. Battista, *Introduction to megavoltage x-ray dose computation algorithms* (CRC Press, 2019).
- [3] N. Carron, *An introduction to the passage of energetic particles through matter* (CRC Press, 2007).
- [4] H. Cember and T. E. Johnson, *Introduction to health physics* (McGraw Hill Education, 2017).
- [5] D. E. Bartine, “Low-energy electron transport by the method of discrete ordinates”, PhD thesis (Missouri University of Science and Technology, 1971).
- [6] W. Dunn, A. Yacout, and F. O’Foghludha, *Boltzmann transport equation algorithms for infinite-slab buildup and albedo factors*, tech. rep. (Naval Surface Warfare Center, 1990).
- [7] W. W. Engle, *A users manual for ANISN: a one dimensional discrete ordinates transport code with anisotropic scattering*, tech. rep. (Oak Ridge National Laboratory, 1967).
- [8] W. W. Engle, M. A. Boling, and B. W. Colston, *DTF-II, a one-dimensional, multigroup neutron transport program*, tech. rep. (Atomics International, 1966).
- [9] C. Pao, “Numerical methods for the linear Boltzmann transport equation in slab geometry”, *Numerical Methods for Partial Differential Equations* **2**, 131 (2005).
- [10] G. J. Lockwood, L. E. Ruggles, G. H. Miller, and J. A. Halbeib, *Calorimetric measurement of electron energy deposition in extended media – theory vs experiment*, tech. rep. (Sandia National Laboratories, 1980).
- [11] M. B. Emmett, *The MORSE Monte Carlo radiation transport code system*, tech. rep. (Oak Ridge National Laboratory, 1984).
- [12] O. N. Vassiliev, *Monte Carlo methods for radiation transport* (Springer, 2017).
- [13] J. von Neumann and R. D. Richtmyer, *Statistical methods in neutron diffusion*, tech. rep. (Los Alamos National Laboratory, 1947).
- [14] K. A. Gifford, J. L. Horton, T. A. Wareing, G. Failla, and F. Mourtada, “Comparison of a finite-element multigroup discrete-ordinates code with Monte Carlo for radiotherapy calculations”, *Physics in Medicine and Biology* **51**, 2253 (2006).
- [15] O. N. Vassiliev, T. A. Wareing, I. M. Davis, J. McGhee, D. Barnett, J. L. Horton, K. Gifford, G. Failla, U. Titt, and F. Mourtada, “Feasibility of a multigroup deterministic solution method for three-dimensional radiotherapy dose calculations”, *International Journal of Radiation Oncology Biology Physics* **72**, 220 (2008).
- [16] O. N. Vassiliev, T. A. Wareing, J. McGhee, G. Failla, M. R. Salehpour, and F. Mourtada, “Validation of a new grid-based Boltzmann equation solver for dose calculation in radiotherapy with photon beams”, *Physics in Medicine and Biology* **55**, 581 (2010).

- [17] O. Zienkiewicz, R. Taylor, and J. Zhu, *The finite element method: its basis and fundamentals* (Elsevier, 2005).
- [18] P. Zygmanski and E. Sajo, “Nanoscale radiation transport and clinical beam modeling for gold nanoparticle dose enhanced radiotherapy (GNPT) using X-rays”, *British Journal of Radiology* **89**, 20150200 (2016).
- [19] L. Bourhrara, “A new numerical method for solving the Boltzmann transport equation using the PN method and the discontinuous finite elements on unstructured and curved meshes”, *Journal of Computational Physics* **397**, 108801 (2019).
- [20] S. Pautz, W. Fan, W. Bohnhoff, C. Drumm, D. Bruss, and B. Campbell, *SCEPTRE v. 2.0 (Sandia Computational Engine for Particle Transport Radiation Effects)*, tech. rep. (US Department of Energy, 2018).
- [21] J. L. Bedford, “Calculation of absorbed dose in radiotherapy by solution of the linear Boltzmann transport equations”, *Physics in Medicine and Biology* **64**, 02TR01 (2019).
- [22] S. J. McMahon, “The linear quadratic model: usage, interpretation and challenges”, *Physics in Medicine and Biology* **61**, 01TR01 (2019).
- [23] M. Scholz, A. M. Kellerer, W. Kraft-Weyrather, and G. Kraft, “Computation of cell survival in heavy ion beams for therapy. the model and its approximation”, *Radiation and Environmental Biophysics* **36**, 59 (1997).
- [24] T. Elsasser and M. Scholz, “Cluster effects within the local effect model”, *Radiation Research* **167**, 319 (2007).
- [25] S. J. McMahon, H. Paganetti, and K. M. Prise, “Optimising element choice for nanoparticle radiosensitisers”, *Nanoscale* **8**, 581 (2016).
- [26] W. Sung and J. Schuemann, “Energy optimization in gold nanoparticle enhanced radiation therapy”, *Physics in Medicine and Biology* **63**, 135001 (2018).
- [27] A. Meghzifene, D. R. Dance, D. McLean, and H.-M. Kramer, “Dosimetry in diagnostic radiology”, *European Journal of Radiology* **76**, 11 (2010).
- [28] A. Wang, A. Maslowski, T. Wareing, J. Star-Lack, and T. G. Schmidt, “A fast, linear boltzmann transport equation solver for computed tomography dose calculation (Acuros CTD)”, *Medical Physics* **46**, 925 (2019).
- [29] F. Salvat, in *PENELOPE-2018: a code system for Monte Carlo simulation of electron and photon transport* (2019).
- [30] L. Lorence, J. Morel, and G. Valdez, *Physics guide to CEPXS: a multigroup coupled electron-photon cross-section generating code*, tech. rep. (Sandia National Laboratories, 1989).
- [31] R. Otazo, P. Lambin, J.-P. Pignol, M. E. Ladd, H.-P. Schlemer, M. Baumann, and H. Hricak, “MRI-guided radiation therapy: an emerging paradigm in adaptive radiation oncology”, *Radiology* **298**, 248 (2020).
- [32] A. Gayol, J. Vedelago, and M. Valente, “MRI-LINAC dosimetry approach by Monte Carlo codes coupling charged particle radiation transport with strong magnetic fields”, *Radiation Physics and Chemistry* **200**, 110171 (2022).

- [33] A. R. Chaudhuri, *The physics of fluids and plasmas: an introduction for astrophysicists* (Cambridge University Press, 2012).
- [34] C. Drumm, *Spherical harmonics (PN) methods in the SCEPTR_E radiation transport code*, tech. rep. (Sandia National Laboratories, 2015).
- [35] K. D. Lathrop, “Ray effects in discrete ordinates equations”, Nuclear Science and Engineering **32**, 357 (1968).
- [36] T. Wareing, J. Morel, and D. Parsons, *A first collision source method for ATTILA, an unstructured tetrahedral mesh discrete ordinates code*, tech. rep. (Los Alamos National Lab, 1998).
- [37] T. Möller and B. Trumbore, “Fast, minimum storage ray/triangle intersection”, Journal of Graphics Tools **2**, 21 (1997).
- [38] E. B. Podgorsak, *Radiation physics for medical physicists* (Springer, 2010).
- [39] S. Perkins, D. Cullen, M. Chen, J. Hubbell, J. Rathkopf, and J. Scofield, *Tables and graphs of atomic subshell and relaxation data derived from the LLNL Evaluated Atomic Data Library (EADL), Z = 1-100*, tech. rep. (Lawrence Livermore National Laboratory, 1991).
- [40] X. Llovet, C. J. Powell, F. Salvat, and A. Jablonski, “Cross sections for inner-shell ionization by electron impact”, Journal of Physical and Chemical Reference Data **43**, 013102 (2014).
- [41] C. Drumm and R. P. Kensek, *Scattering cross sections for electron transport using energy-finite-element weighting*, tech. rep. (Sandia National Laboratories, 2017).
- [42] T. Haut, P. Maginot, V. Tomov, B. Southworth, T. Brunner, and T. Bailey, “An efficient sweep-based solver for the SN equations on high-order meshes”, Nuclear Science and Engineering **193**, 746 (2019).
- [43] J. Jarrell, “An adaptive angular discretization method for neutral-particle transport in three-dimensional geometries”, PhD thesis (Texas A&M University, 2012).
- [44] C. Fang, H. Wu, L. Cao, Y. Li, and J. Miao, “Modified least-squares finite element method for solving the boltzmann transport equation with spherical harmonic angular approximation”, Annals of Nuclear Energy **140**, 107126 (2020).
- [45] D. E. Bruss, C. R. Drumm, W. C. Fan, and S. D. Pautz, *SCEPTR_E 2.2 quick start guide*, tech. rep. (Sandia National Laboratories, 2021).
- [46] A. Naceur, A. Hebert, P. Romano, B. Forget, C. Chilian, and J.-F. Carrier, “Feasibility of a multigroup Boltzmann–Fokker–Planck solution for electron beam dose calculations”, Nature Scientific Reports **13**, 1310 (2023).
- [47] A. Hébert, “DRAGON5 and DONJON5, the contribution of école Polytechnique de Montréal to the SALOME platform”, Annals of Nuclear Energy **87**, 12 (2016).
- [48] S. A. Zein, M. Bordage, Z. Francis, G. Macetti, A. Genoni, C. Dal Cappello, W. Shin, and S. Incerti, “Electron transport in DNA bases: An extension of the Geant4-DNA Monte Carlo toolkit”, Nuclear Instruments and Methods in Physics Research Section B: Beam Interactions with Materials and Atoms **488**, 70 (2021).

- [49] J. Morel, “Fokker-Planck calculations using standard discrete ordinates transport codes”, Nuclear Science and Engineering **79**, 340 (1981).
- [50] C. R. Drumm, W. C. Fan, L. Lorence, and J. Liscum-Powell, “An analysis of the extended-transport correction with application to electron beam transport”, Nuclear Science and Engineering **155**, 355 (2007).
- [51] L. N. Trefethen and D. Bau, *Numerical linear algebra* (Society for Industrial and Applied Mathematics, 1997).
- [52] D. Badouel, in *Graphics gems i*, edited by A. S. Glassner (Academic Press Inc., 1993) Chap. VII.3, pp. 390–393.
- [53] R. J. Segura and F. R. Feito, “Algorithms to test ray-triangle intersection. Comparative study”, Journal of WSCG **9**, 76 (2001).
- [54] T. A. Wareing, J. M. McGhee, J. E. Morel, and S. D. Pautz, “Discontinuous finite element SN methods on three-dimensional unstructured grids”, Nuclear Science and Engineering **138**, 256 (2001).
- [55] C. Geuzaine and J. Remacle, “Gmsh: a three-dimensional finite element mesh generator with built-in pre- and post-processing facilities.”, International Journal for Numerical Methods in Engineering **79**, 1309 (2009).
- [56] M. Berger, J. Hubbell, S. Seltzer, J. Chang, J. Coursey, R. Sukumar, D. Zucker, and K. Olsen, *XCOM: Photon cross sections database*, tech. rep. (National Institute of Standards and Technology, 2010).
- [57] *Nist digital library of mathematical functions*, <https://dlmf.nist.gov/>, Release 1.2.0 of 2024-03-15, F. W. J. Olver, A. B. Olde Daalhuis, D. W. Lozier, B. I. Schneider, R. F. Boisvert, C. W. Clark, B. R. Miller, B. V. Saunders, H. S. Cohl, and M. A. McClain, eds.
- [58] M. L. Boas, *Mathematical methods in the physical sciences* (Wiley, 2006).
- [59] J. Morel, “A hybrid collocation-Galerkin-SN method for solving the Boltzmann transport equation”, Nuclear Science and Engineering **101**, 72 (1989).
- [60] V. I. Lebedev, “Quadratures on a sphere”, USSR Computational Mathematics and Mathematical Physics **16**, 10 (1976).
- [61] V. I. Lebedev and D. Laikov, “A quadrature formula for the sphere of the 131st algebraic order of accuracy”, Doklady Mathematics **366**, 741 (1999).
- [62] N. Jeevanjee, *An introduction to tensors and group theory for physicists* (Birkhäuser, 2015).
- [63] D. E. Bruss, C. R. Drumm, W. C. Fan, and S. D. Pautz, *SCEPTRE 2.2 angular quadrature sets*, tech. rep. (Sandia National Laboratories, 2021).
- [64] S. Pautz, B. Bohnhoff, C. Drumm, and W. Fan, *Parallel discrete ordinates methods in the SCEPTRE project*, tech. rep. (Sandia National Laboratories, 2009).
- [65] J. Patel, L. Moraes, R. Vasques, and R. Barros, “Transport synthetic acceleration for the solution of one-speed nonclassical spectral SN equations in slab geometry”, Journal of Computational and Applied Mathematics **401**, 113768 (2022).

- [66] C. Drumm and W. Fan, “Multi-level acceleration of scattering-source iterations with application to electron transport”, Nuclear Engineering and Technology **49**, 1114 (2017).
- [67] Y. Saad and M. H. Schultz, “GMRES: a generalized minimal residual algorithm for solving nonsymmetric linear systems”, SIAM Journal on Scientific Computing **7**, 856 (1986).
- [68] C. Demazière, *Modelling of nuclear reactor multi-physics* (Academic Press, 2020).
- [69] E. W. Larsen, “Diffusion-synthetic acceleration methods for discrete-ordinates problems”, Transport Theory and Statistical Physics **13**, 107 (1984).
- [70] R. S. Modak, A. Gupta, V. Kumar, and S. V. G. Menon, *Transport synthetic acceleration scheme for multi-dimensional neutron transport problems*, tech. rep. (Bhabha Atomic Research Center, 2005).
- [71] J. Morel, “On the validity of the extended transport cross-section correction for low-energy electron transport”, Nuclear Science and Engineering **71**, 64 (1979).
- [72] J. Sakurai and J. Napolitano, *Modern quantum mechanics* (Cambridge University Press, 2021).